University of Nebraska - Lincoln

DigitalCommons@University of Nebraska - Lincoln

Spring 2024

Ecological Dynamics of Cenozoic North American Mammals

Alexandria Brandis Shupinski
University of Nebraska-Lincoln

Follow this and additional works at: https://digitalcommons.unl.edu/dissunl

ECOLOGICAL DYNAMICS OF NORTH AMERICAN CENOZOIC MAMMALS

by

Alexandria Brandis Shupinski

A DISSERTATION

Presented to the Faculty of

The Graduate College at the University of Nebraska

In Partial Fulfillment of Requirements

For the Degree of Doctor of Philosophy

Major: Biological Sciences

(Ecology, Evolution, and Behavior)

Under the Supervision of Professor S. Kathleen Lyons

Lincoln, Nebraska

May, 2024

ECOLOGICAL DYNAMICS OF NORTH AMERICAN CENOZOIC MAMMALS

Alexandria Brandis Shupinski, Ph.D.

University of Nebraska, 2024

Adviser: S. Kathleen Lyons

Understanding how community structure is affected by various ecological, climatic, and environmental changes is a long-standing goal in ecology. However, disentangling human impacts from these other variables is difficult when using short modern timescales and anthropogenically altered communities. The fossil record provides a means to investigate community structure dynamics across critical intervals, excluding humans as a variable. Here, in three studies, I assess changes in North American mammal paleocommunity structure across the last 66 million years (Ma) at multiple temporal and spatial scales. In Chapter 1, I identify changes in mammal functional diversity (FD) locally and continentally, using three independent metrics: functional richness, functional evenness, and functional divergence. I find that the metrics were disassociated within and across spatial scales throughout the Cenozoic, except for the Paleocene when they were changing synchronously. This suggests unique dynamics in community structure, likely due to early Cenozoic mammal radiation. In Chapter 2, I quantify spatial variation in Cenozoic mammal paleocommunities using taxonomic beta diversity and functional beta diversity. I use 5-million-year time slices to assess changes in spatial distributions of taxa

and traits and the relationship between taxonomic and functional beta diversity. I find that taxonomic and functional beta diversity are highly correlated, and peak during grassland expansion, likely a result of increased habitat heterogeneity. In my third chapter, I investigate the co-occurrence structure of western North American mammal across the Plio-Pleistocene transition (3-2.5 ma) during the Great Biotic Interchange. By combining co-occurrence analysis with functional diversity, I calculate how the influence of functional roles on patterns of genus associations changed across the transition. Although the functional distance between significantly associated genus pairs decreased and new mammals formed the associations, there was no significant shift in the overall co-occurrence structure. My dissertation deepens our understanding of how ecological, climatic, and environmental events impact the community structure of mammals, providing a baseline for ecological dynamics without anthropogenic influences.

Dedication

I want to dedicate my dissertation to my Mom and Dad.

Acknowledgements

My years at the University of Nebraska-Lincoln have been some of the best days of my life. I have also had some of the most exhausting and stressful days during this process. But I am so thankful to all the people in my life that helped me get to this point, because the roller coaster ride of graduate school has helped me grow as a scientist, a teacher and a person.

I am overwhelmed with gratitude to my parents, Wendy and Doug Shupinski. You both always nurtured my passions and encouraged me to find a career that involved them. You never focused on money or being the best but instead focused on me being happy. Through the many years of schooling, you cheered me on and were my foundation of support. I especially appreciate your support in moving halfway across the country to finalize my graduate school career here in Lincoln. I know it was and continues to be hard living at such a distance. But I hope you know that I am so happy with my everyday life and this career I've chosen. Through it all, you have helped me manage the roller coaster ride of my PhD. College has been a long road, and I couldn't have done it without you. I also want to make a special shout out to my Mom for always being on the other end of the phone when I needed you or was just bored and wanted company. You are my best friend and I know that I am never alone.

I also want to thank the members of the Lyons-Wagner lab. Our lab was a supportive environment filled with encouragement. Everyone was always willing to dedicate their time and efforts to help each other grow and improve their skills in writing and presenting. It was such a great group of people that I thoroughly enjoyed my time and experiences with. Thank you all for your collaboration and feedback over the years. Lastly, I want to express my never-ending gratitude to my incredible advisor, Kate Lyons. You took a chance on me and gave me the opportunity to live my dream. You've built an amazing lab that encourages the growth and development of researchers. Through knowing you as a mentor, a scientist, and a person, I have developed the utmost respect for you. You are always open and honest with the highest level of integrity. You always expected the best and never let me take the easier route. To help me through graduate school and the many ups and downs, you were always willing to share your academic wisdom and provide advice. You have provided me with so many opportunities to grow as a scientist. You helped me challenge myself, demonstrate my skills and build my confidence in an academic setting by including me in your research collaborations. It was truly an honor to be your PhD student and I hope that we continue to collaborate throughout my scientific career.

Lincoln, Nebraska will always hold a special place in my heart, and I will always look back fondly on my time here.

Table of Contents

CHAPTER 1: UNIQUE FUNCTIONAL DIVERSITY DURING EARLY CENOZOIC

MAMMAL RADIATION OF NORTH AMERICAN

Supplementary Material

List of Tables

List of Figures

List of Appendices

Preface

Chapter 1 is currently in review at Proceedings of the Royal Society B. Chapter 2 is in the editing stage with coauthors and I plan to submit to the Journal of Global Ecology and Biogeography. Chapter 3 is currently in review in the Journal of Paleobiology.

Introduction

The composition and ecological roles of taxa in mammal communities directly influence the processes that maintain ecosystem function (Larsen, Williams, and Kremen 2005; Caswell 1976). Major perturbations, such as invasion, climate change and anthropogenic activity can significantly modify community structure, altering processes (Doherty, Hays, and Driscoll 2021; Carrillo et al. 2020; Clyde and Gingerich 1998; Cooke et al. 2022). Furthermore, the effects of ecological, climatic, and environmental events can differ across temporal and spatial scales, contributing to its complexity. This is because the effect of ecological and environmental mechanisms varies across scale (Bernhardt-Römermann et al. 2015; Siefert et al. 2012; González-Maya et al. 2016; Arellano et al. 2016). For example, global meta-analysis of vegetation distributions demonstrates that local community compositions are more dependent on edaphic factors such as soil composition, while compositions across larger spatial extents are more determined by climatic factors (Siefert et al. 2012). Thus, investigating the effects of biotic and abiotic factors on ecological communities has become a principal goal in mammal conservation, yet the relationship between these factors and changes in community structure is poorly understood. Disentangling the role of scales, biotic and abiotic factors using modern data has proven problematic for several reasons: 1) the lack of non-anthropogenically altered communities that may be more or less resilient to disturbance, 2) the inability to completely remove human impacts to better understand the effects of non-human factors, and 3) shorter scales that often fail to show the before,

during and after effect of major perturbations, as well as long term evolutionary consequences.

The record of past life on this planet provides an extraordinary opportunity to analyze ecological dynamics prior to human influence. Using the fossil record provides the advantage of multiple temporal and spatial scales across major ecological, climatic, and environmental transitions. With a paleoecological approach we can extract and compare the long-term consequences of major perturbations on community structure. In particular, the North American mammalian fossil record is well-studied, providing a robust timeline and wide geographic spread of communities over the last 66 million years. It is worth noting that the data quantity and quality vary over time because of biases in the fossil record (Díaz and Cabido 2001). However, these biases vary in nature and often contribute noise rather than systematic biases. Furthermore, the biases in paleoecology are well studied by taphonomists and can be addressed using a variety of sensitivity analyses (Behrensmeyer, Kidwell, and Gastaldo 2000; Behrensmeyer 1982). Moreover, with the recent rise in collaborative activities (cites), development of large databases ("The Paleobiology Database," n.d.; Community 2020)and improved computing power, we have the capability to investigate broad, evolutionary patterns in mammalian community structure while still accounting for biases in the record. Community structure is a term that can be quantified by many different metrics. Taxonomic richness, abundance and diversity are traditional approaches (Caswell 1976). However, extrapolating ecosystem services from taxonomic composition is difficult. Taxonomic approaches can fail to capture critical information about community structure

(Díaz and Cabido 2001). For example, two communities can have the same richness and abundance, but the ecological roles of the constituent species may be very different. Functional diversity (trait composition) has become a widely used concept in ecology due to its strong link to ecosystem function (Díaz and Cabido 2001; Villéger, Mason, and Mouillot 2008; Cadotte, Carscadden, and Mirotchnick 2011). The ecological role and biological associations of an organism are heavily influenced by the combination of functional traits it possesses, therefore, determining the ecosystem services that it provides and causing not all species to be created equal in ecological importance (Mouchet et al. 2010). Conservation aims to maintain ecosystem functioning and services. By evaluating the ecological role of species, as well as the redundancy of those roles, preservation efforts can better target critical species. Therefore, combining taxonomic and functional methodologies can deepen our understanding of biotic and abiotic impacts on community structure, relationships between taxa and traits, and help inform conservation strategies.

In Chapter 1, I examine changes in alpha and gamma functional diversity of North American mammals over the last 66 Ma. My aim is to identify major shifts in functional diversity and associated ecological, environmental, and climatic events. In addition, I examine changes in functional diversity at the continental and community scales to assess the effect of spatial scale on the underlying processes. To analyze the broad, evolutionary changes in alpha and gamma functional diversity, I compiled a database of 264 mammal paleocommunities that includes 2,465 species and four functional traits: body mass, life habit, locomotion, and diet. Functional diversity was dissected into three independent

components that quantify the changes in the distribution of species throughout trait space: functional evenness, functional richness and functional divergence (Villéger et al. 2008). These metrics were calculated for each paleocommunity to assess local changes and in 1-million-year time bins to explore continental variation. I then used a breakpoint analysis to identify the timing of significant shifts in all three functional diversity metrics of North American mammals across the Cenozoic.

I find that the three components of functional diversity are disassociated in the timing and direction of change throughout the Cenozoic. Furthermore, the metrics are also uncoupled between spatial scales. The majority of significant shifts in local functional diversity occur during the early or late Cenozoic, while continental functional diversity primarily shifts during the middle Cenozoic. Fascinatingly, the only period when all metrics and both spatial scales are transitioning in synchrony, is during the first 10 million years of the Cenozoic, a period called the Paleocene. This epoch follows the K-Pg mass extinction and encompasses the rapid radiation of mammals (Alroy 1999; Lyson et al. 2019). These results suggest that the radiation event was the only environmental, ecological, or climatic transition with a magnitude great enough to have a similar impact at all spatial scales assessed in this study. I hypothesize that the ecological dynamics of mammals during the Paleocene were unique compared to the following ~56 Ma because of the rapid diversification occurring at this time. The overall findings of chapter 1 demonstrate that components of functional diversity are impacted differently by ecological processes. Furthermore, the role of driving processes varies depending on spatial scale. As a result, I advocate for the examination of multiple spatial scales and

functional diversity metrics to better understand temporal changes in functional diversity of organisms.

Chapter 2 investigates temporal changes in beta diversity of Cenozoic North American mammals to build upon my findings concerning alpha and gamma diversity from Chapter 1. Here, I aim to assess how the distributions of mammal taxa and traits across space were altered across major climatic, ecological and environmental events. In addition, I evaluate the relationship between taxonomic and functional trait distributions on an evolutionary timescale. I use the same database of 264 paleocommunities to analyze taxonomic and functional beta diversity across the Cenozoic, in 5-million year sliding window bins. The dimensions of beta diversity were calculated at the genus-level due to the temporal extent of the time bins. The relationship between taxonomic and functional beta diversity was quantified using a linear regression.

I find that taxonomic and functional beta diversity are strongly correlated across the Cenozoic. This suggests that changes in the distribution of taxa and traits respond similarly. Moreover, the periods of highest taxonomic and functional beta diversity overlap with the development of grasslands during the late Eocene to early Oligocene and the expansion of grasslands during the early Miocene (Janis, Damuth, and Theodor 2002). I show that habitat heterogeneity is a major influence in determining the beta diversity of mammals and that taxa and traits respond similarly to widespread, vegetative changes across long timescales. Therefore, I highlight the importance of investigating evolutionary timelines. Indeed, examining shorter temporal scales may fail to capture the analogous response across dimensions of beta diversity due to differences in timing.

In Chapter 3, I examine changes in the co-occurrence structure of western North American mammals across the onset of glaciation and the corresponding intensification of the Great American Biotic Interchange at the Plio-Pleistocene transition (~3-2.5 Ma) (Bartoli et al. 2005; Bacon et al. 2016). I evaluate how the strengths and types of mammal associations (aggregated: appearing together more often than expected, segregated: appearing together less often than expected) are altered by the climate transition and the influx of South American mammals into North America (Bacon et al. 2016; Woodburne 2010). Moreover, I use functional traits to examine the effect of ecological roles in determining taxonomic associations. For this analysis, I compiled a database of Plio-Pleistocene mammal paleocommunities from western North America. The paleocommunities were divided into two equal time bins, late Pliocene (4-2.5 Ma) and the early Pleistocene (2.5-1 Ma). I calculated co-occurrence at the genus-level for both time bins and compared the distribution of genus pair strengths. Furthermore, I ordinated each genus in trait space using a PCoA of body mass, life habitat, diet and locomotion.   Finally, I quantified the functional distance between each pair of genera to evaluate the relationship between functional distance and association strength and type. I find that regardless of the climatic shift and immigration of new mammals into North America, co-occurrence structure of mammals does not change. The distribution of pair types and strengths is not significantly different before and after the Plio-Pleistocene transition, even though the genera forming the pairs have changed. The number of North American mammalian genera forming pairs decreases and a greater number of genus pairs includes at least one South American genus. However, the functional distance

between the genus pairs does significantly change. Specifically, the functional distance between associating pairs becomes shorter, meaning they are more functionally similar after the transition. This is likely because South American genera occupy a very small area in the middle of functional trait space, while North American genera are more widely distributed. The significant associations of North American genera to South American genera could result in overall shorter functional distances due to South American genera plotting in the center of trait space. Remarkably, the co-occurrence structure of mammals is similar across this period of major ecological, environmental, and climatic change, even with the loss of native genera and the arrival of immigrant genera altering the composition of the North American fauna. This may suggest that regardless of the taxonomic composition, mammals have a general way of assembling.

In summary, my dissertation provides a baseline for mammal responses to climatic, environmental and ecological events on long timelines and across multiple spatial scales. My research takes a macroecological approach using an extensive geographic and temporal perspective to evaluate broad patterns in mammal ecological dynamics. I quantify alpha, beta and gamma diversity and show that the impact of ecological processes varies among them, demonstrating the importance of incorporating multiple spatial scales to deepen our understanding of ecological dynamics. Furthermore, I demonstrate the importance of the combination of a taxonomic and functional approach as these dimensions of ecology can vary in the type and timing of response. Understanding the temporal dynamics of mammalian diversity is difficult because of the interplay of numerous factors, varying across temporal and spatial scales. These factors

are complicated by anthropogenically altered communities in the modern. Using the fossil record can remove the role of human activity to provide greater insight into mammalian dynamics over space and time.

References

Alroy, John. 1999. "The Fossil Record of North American Mammals: Evidence for a Paleocene Evolutionary Radiation." Systematic Biology 48 (1): 107–18.

Arellano, Gabriel, J. Sebastián Tello, Peter M. Jørgensen, Alfredo F. Fuentes, M. Isabel Loza, Vania Torrez, and Manuel J. Macía. 2016. "Disentangling Environmental and Spatial Processes of Community Assembly in Tropical Forests from Local to Regional Scales." Oikos 125 (3): 326–35. https://doi.org/10.1111/oik.02426.

Bacon, Christine D., Peter Molnar, Alexandre Antonelli, Andrew J. Crawford, Camilo Montes, and Maria Camila Vallejo-Pareja. 2016. "Quaternary Glaciation and the Great American Biotic Interchange." Geology 44 (5): 375–78. https://doi.org/10.1130/G37624.1.

Bartoli, G., M. Sarnthein, M. Weinelt, H. Erlenkeuser, D. Garbe-Schönberg, and D. W. Lea. 2005. "Final Closure of Panama and the Onset of Northern Hemisphere Glaciation." Earth and Planetary Science Letters 237 (1): 33–44. https://doi.org/10.1016/j.epsl.2005.06.020.

Behrensmeyer, Anna K. 1982. "Time Resolution in Fluvial Vertebrate Assemblages." Paleobiology 8 (3): 211–27. https://doi.org/10.1017/S0094837300006941.

Behrensmeyer, Anna K., Susan M. Kidwell, and Robert A. Gastaldo. 2000. "Taphonomy and Paleobiology." Paleobiology 26 (S4): 103–47. https://doi.org/10.1017/S0094837300026907.

Bernhardt-Römermann, Markus, Lander Baeten, Dylan Craven, Pieter De Frenne, Radim Hédl, Jonathan Lenoir, Didier Bert, et al. 2015. "Drivers of Temporal Changes in Temperate Forest Plant Diversity Vary across Spatial Scales." Global Change Biology 21 (10): 3726–37. https://doi.org/10.1111/gcb.12993.

Cadotte, Marc W., Kelly Carscadden, and Nicholas Mirotchnick. 2011. "Beyond Species: Functional Diversity and the Maintenance of Ecological Processes and Services." Journal of Applied Ecology 48 (5): 1079–87. https://doi.org/10.1111/j.1365-2664.2011.02048.x.

Carrillo, Juan D., Søren Faurby, Daniele Silvestro, Alexander Zizka, Carlos Jaramillo, Christine D. Bacon, and Alexandre Antonelli. 2020. "Disproportionate Extinction of South American Mammals Drove the Asymmetry of the Great American Biotic Interchange." Proceedings of the National Academy of Sciences 117 (42): 26281–87. https://doi.org/10.1073/pnas.2009397117.

Caswell, Hal. 1976. "Community Structure: A Neutral Model Analysis." Ecological Monographs 46 (3): 327–54. https://doi.org/10.2307/1942257.

Clyde, William C., and Philip D. Gingerich. 1998. "Mammalian Community Response to the Latest Paleocene Thermal Maximum: An Isotaphonomic Study in the Northern

Bighorn Basin, Wyoming." Geology 26 (11): 1011. https://doi.org/10.1130/0091-
7613(1998)026<1011:MCRTTL>2.3.CO;2.

Community, The NOW. 2020. "NOW — New and Old Worlds: Database of Fossil
Mammals," November. https://doi.org/10.5281/ZENODO.4268068.

Cooke, Rob, William Gearty, Abbie S. A. Chapman, Jillian Dunic, Graham J. Edgar,
Jonathan S. Lefcheck, Gil Rilov, et al. 2022. "Anthropogenic Disruptions to
Longstanding Patterns of Trophic-Size Structure in Vertebrates." Nature Ecology &
Evolution 6 (6): 684–92. https://doi.org/10.1038/s41559-022-01726-x.

Díaz, Sandra, and Marcelo Cabido. 2001. "Vive La Différence: Plant Functional
Diversity Matters to Ecosystem Processes." Trends in Ecology & Evolution 16 (11):
646–55. https://doi.org/10.1016/S0169-5347(01)02283-2.

Doherty, Tim S., Graeme C. Hays, and Don A. Driscoll. 2021. "Human Disturbance
Causes Widespread Disruption of Animal Movement." Nature Ecology & Evolution
5 (4): 513–19. https://doi.org/10.1038/s41559-020-01380-1.

González-Maya, José F., Luis R. Víquez-R, Andrés Arias-Alzate, Jerrold L. Belant, and
Gerardo Ceballos. 2016. "Spatial Patterns of Species Richness and Functional
Diversity in Costa Rican Terrestrial Mammals: Implications for Conservation."
Diversity and Distributions 22 (1): 43–56. https://doi.org/10.1111/ddi.12373.

Janis, Christine M., John Damuth, and Jessica M. Theodor. 2002. "The Origins and Evolution of the North American Grassland Biome: The Story from the Hoofed Mammals." Palaeogeography, Palaeoclimatology, Palaeoecology 177 (1–2): 183.

Larsen, Trond H., Neal M. Williams, and Claire Kremen. 2005. "Extinction Order and Altered Community Structure Rapidly Disrupt Ecosystem Functioning." Ecology Letters 8 (5): 538–47. https://doi.org/10.1111/j.1461-0248.2005.00749.x.

Lyson, T. R., I. M. Miller, A. D. Bercovici, K. Weissenburger, A. J. Fuentes, W. C. Clyde, J. W. Hagadorn, et al. 2019. "Exceptional Continental Record of Biotic Recovery after the Cretaceous–Paleogene Mass Extinction." Science 366 (6468): 977–83. https://doi.org/10.1126/science.aay2268.

Mouchet, Maud A., Sébastien Villéger, Norman W. H. Mason, and David Mouillot. 2010. "Functional Diversity Measures: An Overview of Their Redundancy and Their Ability to Discriminate Community Assembly Rules." Functional Ecology 24 (4): 867–76. https://doi.org/10.1111/j.1365-2435.2010.01695.x.

Siefert, Andrew, Catherine Ravenscroft, David Althoff, Juan C. Alvarez-Yépiz, Benjamin E. Carter, Kelsey L. Glennon, J. Mason Heberling, et al. 2012. "Scale Dependence of Vegetation–Environment Relationships: A Meta-Analysis of Multivariate Data." Journal of Vegetation Science 23 (5): 942–51. https://doi.org/10.1111/j.1654-1103.2012.01401.x.

"The Paleobiology Database." n.d. Accessed February 19, 2024.

    https://paleobiodb.org/#/.

Villéger, Sébastien, Norman W. H. Mason, and David Mouillot. 2008. "New

    Multidimensional Functional Diversity Indices for a Multifaceted Framework in

    Functional Ecology." Ecology 89 (8): 2290–2301. https://doi.org/10.1890/07-1206.1.

Woodburne, Michael O. 2010. "The Great American Biotic Interchange: Dispersals,

    Tectonics, Climate, Sea Level and Holding Pens." Journal of Mammalian Evolution

    17 (4): 245–64. https://doi.org/10.1007/s10914-010-9144-8.

CHAPTER 1

UNIQUE FUNCTIONAL DIVERSITY DURING THE EARLY CENOZOIC

MAMMAL RADIATION OF NORTH AMERICA

Abstract

Mammals influence nearly all aspects of energy flow and habitat structure in modern terrestrial ecosystems. However, anthropogenic effects likely have altered mammalian community structure, raising the question of how these alterations compare with past perturbations. We use functional diversity to describe how the structure of North American mammal paleocommunities changed over the past 66 Ma, an interval spanning the rapid radiation following the K/Pg and several subsequent environmental disruptions including the Paleocene-Eocene Thermal Maximum (PETM), the expansion of grassland, and the onset of Pleistocene glaciation. For 264 fossil communities, we examine three aspects of ecological function: functional evenness, functional richness and functional divergence. Shifts in functional diversity are significantly related to major ecological and environmental transitions. All three measures of functional diversity increase immediately following the extinction of the non-avian dinosaurs, suggesting that high degrees of ecological disturbance can lead to synchronous responses both locally and continentally. Otherwise, the components of functional diversity respond differently to environmental changes and are decoupled for the last ~56 million years.

Introduction

Understanding the consequences of major ecological disruptions on community structures represents an important intersection between macroecological and

macroevolutionary theory. Communities are dynamic entities whose membership is determined by community assembly processes that might both shape and be shaped by taxonomic and morphological evolution (1–3). However, ecological processes that govern the way species assemble differs across spatial scales, making it difficult to disentangle the role of individual processes (3–5). For example, local scale diversity reflects the level of resource distribution and can be affected by different intensities of competition and niche packing (6). In contrast, environmental variability and climate become increasingly important at larger spatial scales (6–8). Although identifying general rules in community assembly is complicated by the fact that these processes act on various scales across space and time (9), trying to do so is important both for understanding Phanerozoic history and because preserving ecosystem functions is increasingly recognized as an important goal of conservation efforts (10).

Previous work measured community responses to biotic and abiotic changes using taxonomic diversity (i.e., numbers of species or genera) and/or morphological disparity (e.g., range of anatomical types) (11, 12). Although we expect the diversity of ecological roles to increase as taxonomic diversity increases (13), this relationship can vary across space and time. Thus, taxonomic diversity does not always provide adequate information about community dynamics or function (14). An alternative approach to infer processes driving community structure uses functional diversity (15), a "taxon-free" method that ordinates species in multidimensional trait space. Evaluating changes in multidimensional trait space can be beneficial because the changes in community structure are more directly associated with ecosystem functioning (11–13, 15–17). Functional traits directly

correspond to that species' role in the community. The composition of functional traits within a community determines the ecological services it provides. Functional diversity not only allows functional trait distributions to be mapped in multidimensional space, but it also allows community structure to be disentangled into different structural components (functional richness (FRic), functional evenness (FEve) and functional divergence (FDiv)). Measuring changes across multiple indices will allow other affects to be captured that may not be detected using other methods. However, without a baseline understanding of mammal community dynamics, it is difficult to interpret changes in functional diversity, as current communities reflect thousands of years of anthropogenic manipulation, complicating our ability to discern the effects of human activity on community assembly processes.

The fossil record provides a history of how mammal community functional diversity was influenced by the biotic and abiotic environment prior to large-scale impacts by humans. For example, over the Cenozoic (66-0 Ma), mammals underwent major faunal transitions, immigration events and significant reorganizations of paleocommunities (9, 18), beginning with the diversification of mammals triggered by the extinction of non-avian dinosaurs (19, 20). Moreover, the Cenozoic (66-0 Ma) was also marked by a variety of climatic, and environmental changes (Fig. 1) (21, 22). While climate cooled overall during this period, this was interspersed with periods of rapid global warming, resulting in a transition from high latitude subtropical forests in North America at the Paleocene-Eocene boundary (~56 ma) (23) to cyclical glaciation periods by the Early-Middle Pleistocene (EMPT, ~800 ka) (24). The changing climate led to

more open habitats, and the expansion of grasslands; North America was dominated by grasslands by the middle to late Miocene (24). By 2.7 Ma the onset of glacial cycles in North America began (24), resulting in ice sheets and boreal forests. This combination of abiotic and biotic shifts over the Cenozoic provides the opportunity to evaluate the responses of mammal communities to both ecological and environmental change.

Here, we evaluate mammal community evolution across the last 66 Ma using functional diversity of North American mammals. We measure functional diversity on the local and continental scale to individually analyze the effect of ecological, environmental, and climatic shifts on each scale, and investigate the relationship between local and continental functional diversity. Furthermore, we assess the effect of multiple biotic and abiotic variables on functional diversity through time as North American mammals experience a plethora of ecological, environmental, and climatic events. Our approach provides a deeper understanding of how community structure changes across evolutionary timescales and the influence of spatial scale.

Materials and Methods

Functional diversity, a taxon-free approach that focuses on species traits, provides a quantitative framework to explore the relationship between species diversity and ecosystem functioning (28). Here, we assess changes in functional diversity of mammal paleocommunities across the Cenozoic. We used presence-absence data for 264 North American paleocommunities encompassing 2,462 species taken from the Paleobiology Database (PBDB; fig. S1) and vetted for taxonomic errors. A paleocommunity was defined as a single collected fossil locality. We applied a series of taphonomic filters to

reduce the effects of biases in the fossil record (see Supplementary Material).

Paleocommunities were only included if they contained a minimum of 15 species that

encompassed multiple orders and trophic levels. When possible, we refined PBDB

locality dates based on faunal zone and local stage names (see Supplementary Material).

Due to the geographic and temporal range of this study, we had to address multiple facets

of possible bias. Firstly, it is possible that the 264 paleocommunities vary in spatial

extent. Indeed, determining spatial extent or excavation extent of each locality is difficult

and often the information is not available. However, we suggest that this variability is not

driving our results. We would expect the random variation in spatial extent among

paleocommunities to create noise, minimizing patterns and the significance of functional

diversity shifts. In addition, larger spatial extents would be expected to result in higher

levels of species richness. We address the possible issue of variable species richness in

this study (see methods in Supplementary Material: Sensitivity Analyses). Secondly, the

number of paleocommunities changes over time. If a period with a smaller number of

paleocommunities did not appropriately represent the entire range of functional diversity

present at that time, it is possible that the variation in sampling of paleocommunities

could affect functional diversity estimates. To address this, we ran a sub-sampling routine

to determine if this drives our results (see Supplementary Material: Sensitivity Analyses).

We collected data on species traits that are commonly used in studies on extant

mammalian functional diversity (i.e., body mass, locomotion, diet and life habit) (29, 30)

from the primary literature and online databases (table S1), making our data directly

comparable. Diet categories were restricted to those that could most accurately be

distinguished in the fossil record. Some diet categories used in the databases were combined to limit diet uncertainties in earlier or rarer species (table S1); granivores were combined with frugivores and piscivores were considered carnivores. When body mass was not available, body mass was averaged at the lowest available taxonomic level (genus, family, order). In this study, we address possible concerns with calculating functional diversity using averaged body masses based on higher taxonomic levels and combining continuous and categorical variables (see Supplementary Materials: Sensitivity Analysis).

We calculate three functional diversity (FD) indices using the R package "FD" (31, 32): functional richness (FRic), functional divergence (FDiv), and functional evenness (FEve), chosen due to their independence from one another (table S2). Functional diversity was calculated for the whole North American fauna in one-million-year bins, and for each of our 264 communities (see Supplementary Materials). Functional richness is the volume of trait space occupied, functional evenness represents how evenly species occupy the trait space, and functional divergence measures the degree of divergence of species traits relative to the centroid of trait space. These metrics are largely independent of one another compared to other functional diversity metrics and demonstrate the possible variation in the extent and distribution of community functional space (17). However, functional richness is often highly correlated with species richness due to the greater likelihood that there will unique ecological roles with more species while functional evenness and functional divergence are not dependent on species richness (17). To determine whether the variability in species richness across

paleocommunities was altering our findings, we used linear regressions to identify the threshold at which species richness is no longer significantly associated with functional richness functional diversity across the Cenozoic (see Supplementary Material: Sensitivity Analyses).

To calculate functional diversity, we created a trait matrix that included species names and four traits (i.e., locomotion, body mass, life habit, diet). Previous studies suggest that combining categorical and numerical traits may impact results due to magnitude variation between trait types (33). We addressed this possible issue in our study (see Supplementary Material: Sensitivity Analyses). We converted the trait matrix into a distance matrix using Gower's dissimilarity metric (34) and then ordinated species in multidimensional space using principal coordinates analysis (PCoA) on the distance matrix, with a square root correction applied to our non-Euclidean data. We based convex hull volumes for each paleocommunity on the first five PCoA axes. We calculated functional diversity for each paleocommunity across the Cenozoic, and we also calculated functional diversity of the continental fauna in 1-million-year time bins. A breakpoint analysis was used to identify periods during the Cenozoic when the slope of functional diversity over time significantly shifted. A breakpoint represents the start or end of a decline or increase in functional diversity. We identified the location and number of significant shifts in each functional diversity metric using breakpoint analyses and AICc values (table S3-S8). AICc values were used to determine the best supported model regarding the maximum number of breakpoints for each functional diversity index (table S3 - S8).

We estimated extinction and origination rates in 1-million-year time bins using sampling + survivorship (sampling + reverse-survivorship or nascence for origination) analyses (35–37) that accommodates sampling heterogeneity among contemporaneous taxa (38). The procedure was the same for both origination and extinction rates, save that we estimated extinction based on taxa sampled in younger intervals and origination based on taxa sampled in older intervals (fig. S7; See Supplementary Materials). We ran generalized linear models to analyze the effect of biotic and abiotic factors (i.e., global climate, estimated species richness, the proportion of archaic mammals) against continental and local functional diversity metrics (see Supplementary Material, table S10). Because origination and extinction rates were used for estimating species richness, we chose not to include them in the generalized linear models. However, origination and extinction rates were analyzed independently against local and continental scale functional diversity metrics using generalized linear regression. The best generalized linear models to explain variance in each functional diversity metric were determined by the lowest AIC value (table S9).

To standardize the data for the generalized linear models, we analyzed the relationship between abiotic and biotic variables and functional diversity metrics in 1-million-year time bins. To evaluate local functional diversity, we averaged palaeocommunitiy metrics in 1-million-year time bins. To evaluate the potential relationship between global climate and local mammalian functional diversity, $\delta^{18}O$ values were gathered from the most recent compilation of mean global temperature through the Cenozoic (25). $\delta^{18}O$ measurements in deep-see benthic foraminifera (25, 39)

commonly are used as a proxy of temperature, with higher ratios of ^{18}O to ^{16}O, reflecting colder global temperatures and more glaciation (25, 39). The δ^{18}O values were averaged for each paleocommunity based on the age range of that locality. For example, if a locality has an estimated age between 50 and 48 million years, all δ^{18}O values within those two million years were averaged and assigned to that paleocommunity. For continental functional diversity we averaged the δ^{18}O in 1-million-year time bin. We evaluated the proportion of archaic orders versus modern orders in paleocommunities to determine if archaic mammals assembled differently than modern orders. Archaic orders were identified as any order of mammal that is no longer extant. We averaged the proportion of archaic orders found in all paleocommunities for each 1-million-year time bins. For the continental scale, we used the overall proportion of archaic orders to extant within each 1-million-year time bin. If they assembled differently than modern orders, we expected to see a shift in mammal paleocommunity structure during the gradual extinction of archaic orders. We used ordinary least square regressions to characterize the individual relationships of abiotic and biotic factors and the continental and local functional diversity of North American mammal paleocommunities.

Results

Functional Metrics

Functional Richness (FRic) – volume of trait space

Local Scale: For the first 10 million years of the Cenozoic, the volume of functional space of North American mammal paleocommunities rises continuously (Fig. 2). The first breakpoint occurs during the latest Paleocene to earliest Eocene (58.3±1.7

Ma) when functional richness peaks. The rise in functional richness from the early Paleocene to early Eocene is not driven by an increasing number of paleocommunities as demonstrated by a sub-sampling routine (see Supplementary Material, fig. S8). Following this peak is a long period of decline until the second and final breakpoint (20.6 ± 2.6 Ma) during the early Miocene. Functional richness rises again and continues to increase through the Pleistocene epoch (Fig. 2). Although there is a relationship between functional richness and species richness of paleocommunities, this relationship does not drive our results (see Supplementary Material; fig. S2-S4).

Continental Scale: Functional richness of the North American mammalian fauna has four breakpoints (Fig. 3). Three of the breakpoints occur in the middle of the Cenozoic within a relatively short period of time. The first breakpoint (64 ± 0.4) is in the early Paleocene as functional richness begins the initial rise to the second breakpoint in the middle Eocene (45.3 ± 0.7). This is followed by a brief decline of ~5 Ma before the third breakpoint (41.7 ± 0.6; Fig. 3), after which, it increases briefly until the last breakpoint (35 ± 1). After the shift in the latest Eocene/earliest Oligocene until the Pleistocene, functional richness remains relatively consistent.

Functional Divergence (FDiv) – variation of species traits relative to the centroid of trait space

Local Scale: Of all three metrics, functional divergence shows the largest increase during the Paleocene epoch (Fig. 2). This rise in functional divergence from the early Paleocene to early Eocene was not driven by an increasing number of paleocommunities (see Supplementary Material, fig. S10). Functional divergence begins the Cenozoic at its

lowest point and rapidly increases until the first of three breakpoints (57.3±0.7 Ma) at the Paleocene-Eocene transition. A sharp decline follows that ends in the middle Eocene at the second breakpoint (48.3±1.8 Ma). Throughout the mid-Cenozoic to the late Miocene there are no significant shifts as functional divergence remains relatively consistent. The last breakpoint occurs during the late Miocene when functional divergence drops (7.4±5.8 Ma). However, this breakpoint has a large confidence interval, making the timing of the shift difficult to pinpoint (Fig. 2).

Continental Scale: At the onset of the Cenozoic, functional divergence has an initial rise until reaching the first breakpoint (62±1.2; Fig. 3). It increases until the second breakpoint in the late Eocene (44.7±2.7) and then begins declining. The period of decline ends with the third and final breakpoint in the middle Oligocene (28±2.8). Functional divergence remains relatively constant for the rest of the Cenozoic (Fig. 3).

Functional Evenness (FEve) - the distribution of species across trait space

Local Scale: Functional evenness varies more than the other metrics with four significant shifts over the last 66 million years (Fig. 2). Like functional richness, it starts low in the earliest Paleocene but increases until reaching the first breakpoint at the Paleocene-Eocene boundary (56.3±1.2 Ma). The rise in functional evenness from the early Paleocene to early Eocene was not driven by an increasing number of paleocommunities (see Supplementary Material, fig. S11). As with other metrics, it declines to the second breakpoint in the middle Eocene (49.9±1.6 Ma). There is slight increase until the third breakpoint (28.1±3.1 Ma). It then enters a period of decline into the middle Miocene (16.5±1.7 Ma). After which, it rises into the Pleistocene (Fig. 2).

Continental Scale: Functional evenness has two significant shifts. Similar to regional functional richness, the shifts occur over a relatively short period of time during the middle Cenozoic (Fig. 3). Functional evenness increases starting in the early Paleocene until the middle Eocene (39.7 ± 1.7). There is a brief period of decline to the second breakpoint in the latest Eocene/earliest Oligocene (35 ± 2.1). Regional functional evenness changes little for the rest of the Cenozoic (Fig. 3).

Addressing Potential Biases Affecting Broad-Scale Patterns in Functional Diversity

Functional diversity metrics fluctuate frequently across the Cenozoic on both the continental and the local scale. Due to the geographic and temporal extent of our study, components of our data are potentially variable. To confirm the robustness of our results, we performed extensive sensitivity analyses to show that the functional diversity variability we identify through time is not a result of data biases (see methods in Supplementary Material: Sensitivity Analyses). All sensitivity analyses addressing individual functional diversity metrics or time periods are mentioned above.

First, we determined that averaging species body mass at higher taxonomic levels for species with missing body mass data did not alter the overall pattern (fig. S5; see methods in Supplementary Material: Sensitivity Analyses). Second, we use a combination of continuous and categorical variables to calculate functional diversity. Previous studies have demonstrated possible complications with this approach due to variation in the magnitude of traits (33). However, the exclusion of body mass from our functional diversity analysis does not alter the overall trends in functional diversity indices through time (fig. S6). In fact, this analysis demonstrates the strong influence of

body size on the variation of ecological roles in mammals. Because ecological traits in mammals are highly correlated with body size, the imprint of body size is still reflected in the 3 other traits we use. Third, we addressed the possible bias against small-bodied mammals, in that they are less likely to preserve and are more common in the most recent fossil localities. Many studies exclude mammals under 1kg to remove this issue. However, including small-bodied mammals is essential in gaining an accurate understanding of paleocommunity functional diversity. We find no relationship between time and the number of small-bodied mammals, suggesting variability in the preservation of mammalian body sizes did not drive our results (fig. S9).

Biotic and Abiotic Variables

Continental

Functional Richness (FRic) – The best generalized linear model indicates a significant relationship between functional richness and the proportion of archaic orders within the 1-million-year time bins (Fig. 4, table S9, Data S3; $R^2 = 0.11$, p = 0.0095). There is a weak, positive relationship between functional richness and the proportion of archaic orders. Furthermore, functional richness is significantly associated with origination rates, showing a positive relationship. However, the relationship is only driven by two time bins in the early Paleocene (fig. S23).

Functional Divergence (FDiv) - The best generalized linear model indicates a positive, significant relationship between functional divergence and $\delta^{18}O$ averaged values for the 1-million-year time bins across the Cenozoic (Fig. 4, table S9, Data S3; $R^2 = 0.32$, p = 78e-07).

Functional Evenness (FEve) – Based on the generalized linear models, no single biotic or abiotic variable or combination of variables had a significant relationship with continental functional evenness in this study (table S9, Data S3; fig. S20).

Local

Functional Richness (FRic) – There is no significant relationship between local functional richness and the biotic and abiotic variables tested in this study (table S9, Data S3).

Functional Divergence (FDiv) - The best generalized linear model indicates a positive, significant relationship between functional divergence and the proportion of archaic orders in 1-million-year time bins (Fig. 5, table S9, Data S3; $R2 = 0.15$, $p=0.0048$). However, functional divergence and the averaged proportion of archaic orders are weakly associated.

Functional Evenness (FEve) – The generalized linear models did not show a significant relationship between local functional evenness and the biotic and abiotic variables tested in this study (table S9, Data S3).

Discussion

North American mammalian functional diversity changes over evolutionary timescales. Individual metrics of functional diversity differ in the timing and direction of change suggesting that the influence differs among components of functional diversity. The decoupling of functional diversity metrics is found locally and regionally for most of the Cenozoic. The decoupling of functional diversity patterns through time is evident at

both the continental and local scales, the two spatial scales also differ in the timing and direction of change in each functional diversity metric. These results are consistent with modern studies that have shown significant change across habitats that vary in topography and vegetative cover across much smaller geographic regions, such as Costa Rica (37). Our study not only highlights the pronounced variation in functional diversity over time and space, but it also identifies a distinct period in the earliest Cenozoic when all functional diversity metrics at both spatial scales align.

Synchrony in the Paleocene

The Paleocene epoch (~66 - 56 ma) was a period of ecological change with mammals rapidly diversifying in response to an increase in unused resources following the K-Pg mass extinction (~66 ma) (10, 18, 19). This led to ~10 million years of unique mammalian dynamics in local and regional faunas. Mammals were expanding their niche occupancy, accumulating greater variation in ecological roles, and becoming more functionally distinct, while at the same time the distribution of ecological roles were becoming more even (Figs. 2, 4, fig. S12). On both local and continental scales. Mammalian diversity had a four-fold increase across this 10 Ma period (38, 39), with increasing body size and body size variation within ~300 ka following the mass extinction (40). Increasing body size was likely a major contributor to the expansion in ecological roles (11) as body size strongly influences mammal ecology (20, 40–43). The magnitude of this event and the recovery resulting in a unified change among community components, spanning all functional diversity metrics and spatial scales. The pronounced concurrence likely reflects the degree of filling of ecological niche space by mammals in

the ecosystem. However, this was a short-lived event. By the early Eocene, these metrics were largely decoupled.

Synchrony Ends: The Next 56 Ma

The latest Paleocene to earliest Eocene had a major immigration of cursorial and arboreal mammals from Asia and Europe (~56 Ma). This included the arrival of Primates, Perissodactyls and Artiodactyls (44). Around this time, the first disassociation in functional diversity patterns occur between local and continental scales. Meanwhile, metrics within spatial scales remain synchronous. The new mammal orders likely contributed to the rise in local functional diversity briefly; however, all local metrics entered a decline soon after (Fig. 2). The abrupt shift into a synchronous decline is unexpected, as mammals do not reach their maximum body size for another 15 Mya (~41 Ma) (20). In contrast, continental functional diversity continues to increase through the immigration event, only to decline approximately when maximum body size is reached (~41 Ma) (Fig. 3) (20). This suggests that the rate of niche saturation during ecological recovery is dependent on spatial scale. For instance, local communities saturate faster than regional or continental faunas. These results stress the importance of diverse spatial perspectives in understanding ecological recovery following a mass extinction.

The decline in local functional diversity metrics following the immigration event (~56 Ma) overlaps with a period of reorganization for the North American fauna, called the Bridgerian Crash; (50 – 47 Ma; (45, 46) (Fig. 1, 2). This event is marked by a cooling climate with increased seasonality and aridity, leading to the reduction of forests (46). The reduced forest cover caused the gradual loss of arboreal, archaic and medium-sized

mammals (Fig. 2, 4) (46, 47). Interestingly, functional diversity metrics of the continental fauna continues to increase. The rise in continental functional diversity may be partially due to increasing body size as landscapes opened. Specifically, we see higher concentrations of large-bodied browsers in trait space after the Bridgerian Crash (Fig. 4; Bridgerian Crash).

Shortly after the Bridgerian Crash, there was a major change in mammalian dynamics when all three functional diversity metrics became decoupled within the local and continental scales (Fig. 2, Fig. 3). Local niche differentiation and evenness of ecological roles increases after the Bridgerian Crash (46), while occupied trait space continues to shrink. The gradual reduction in trait space may partially be due to the continued loss of medium-sized and arboreal species with the opening of the landscape and expansion of grasslands into the Miocene (Fig. 2a). Meanwhile, niche differentiation enters a period of extensive consistency, lasting ~40 Myr (Fig. 2b). The long period of consistency suggests that the amount of variation among species traits does not change despite mammal taxonomic and functional turnover within North America during this time, even with the loss of archaic mammals and the development of grasslands (Fig. 4, fig. S12) (48). However, open-landscape species begin to increase in richness during the late Eocene to early Oligocene, and this created greater evenness in the dispersal of species throughout functional space (Fig. 2).

The Rise and Spread of North American Grasslands

During the middle Oligocene to middle Miocene, the widespread expansion of grasslands across the North American landscape led to a large degree of ecological

change. Ungulates and carnivores diversified, such as horses and canids (49, 50). For example, by the middle Oligocene there were over 25 species of canids present on the landscape (51, 52). The diversification of these two groups creates greater redundancy in functional space, causing a decline in local functional evenness (Fig. 2). Ungulates experienced rapid diversification until reaching their highest diversity around 16-14 Ma, at which, diversity declines and functional evenness begins to rise again (49). In addition to decreasing ungulate diversity during the middle to late Miocene, the richness of medium-sized mammals increased. This included more lagomorphs and burrowing rodents, as well as medium-sized carnivores like procyonids and mustelids (49, 52). During the latest Cenozoic, the richness of large-bodied mammals occupying niche space in the colder climate also increased (Fig. 4, fig. S12) (19, 49, 52, 53). These factors likely contributed to the shift in local functional richness during the early to middle Miocene when functional trait space begins increasing for the first time since the Eocene (Fig. 2, Fig.4). The expansion of functional space also coincides with the arrival of true felids (54) and proboscideans (55) into North America, resulting in unique large-bodied carnivores and herbivores. However, the level of local niche differentiation evinces a different response to these climatic and ecological changes and is the last of the local metrics to shift. Functional divergence transitions into a decline in the later Miocene. With a colder climate, species within paleocommunities are becoming more similar in overall functional traits. Specifically, medium-sized mammals and carnivores become more concentrated in trait space (Fig. 4, Plio-Pleistocene transition). However, the transition period of functional divergence has a large confidence interval, making it

difficult to infer influential abiotic and biotic factors (Fig. 2). Nonetheless, the confidence interval encompasses several major environmental changes, such as the C3/C4 photosynthesis transition in grasslands (48) and the expansion of continental glaciers in North America (24).

Continental functional divergence is the last of the spatial scale metrics to transition, shifting during the Oligocene to early Miocene. When the decline terminates and like continental functional evenness and richness, it remains relatively stable for the rest of the Cenozoic. The ~25 Mya of consistency within continental functional diversity metrics may suggest that functional diversity on larger spatial scales is more resistant to ecological and environmental events than local scale functional diversity. These results further highlight the differentiation in mammalian dynamics among spatial scales.

Biotic and Abiotic Factors – Local Functional Diversity

In our evaluation of abiotic and biotic factors on local scale functional diversity, we demonstrate that only functional divergence and the proportion of archaic orders in 1-million-year time bins have a significant, yet weak relationship (Fig. 5, fig. S13-17). As the average local proportion of archaic orders increases within 1-million-year time bins so does the average functional divergence of (~30 Ma). The weak, negative relationship is likely caused by the increasing diversity of ecological roles and body size following the Paleocene. In fact, the four points driving the relationship between local functional divergence and local proportion of archaic orders are all 1-million-year time bins from the Paleocene. This would explain why functional divergence is lower and the local proportion of archaic orders is higher. To ensure this relationship is not being driven by

the period of the Cenozoic when all archaic orders were extinct (<30 Ma), we also run local functional divergence against the average local proportion of archaic orders from 66-30 Ma (fig. S18). The relationship becomes only slightly stronger but remains weak (fig. S10). In contrast, there is no relationship between species richness or origination/extinction rates over time and local functional diversity (fig. S2-S4, S13-17, table S10). Nor did we find a relationship between local functional diversity and global temperature using $\delta^{18}O$ values as a global climate proxy (Fig. 5, fig. S15-17) (25). Studies have found local climate to influence functional diversity (59) but we could not analyze local climate for each paleocommunity, best suitable data are not available. Estimated origination and extinction rates did not exhibit any significant associations with local scale functional diversity (fig. S13-14).

Biotic and Abiotic Factors – Continental Functional Diversity

The relationship between continental functional diversity metrics and abiotic and biotic factors ($\delta^{18}O$, proportion of archaic orders, species richness, origination and extinction rates) (fig. S19-23). We only identify three significant relationships. Averaged $\delta^{18}O$ values for 1-million-year time bins has a significant relationship with continental functional divergence (Fig. 6). There is a trend of decreasing functional divergence across the Cenozoic, with lower $\delta^{18}O$ values during the Pleistocene (Fig. 6). This suggests that with a cooling climate, a fewer number of species have extreme traits and there are greater similarities among species within a paleocommunity (17). Similarly, we see a slight decline in functional divergence on the local scale (Fig. 2) during the Pleistocene. The Pleistocene decline could be explained by environmental filtering and increased

abiotic stresses (60). However, we would have expected higher continental functional

divergence during the middle Cenozoic with greater habitat heterogeneity. Notably,

variation in continental functional divergence across the Cenozoic is small and the

breakpoint analysis did not identify any significant shifts following the late Oligocene

and functional divergence remains relatively consistent. The response in continental scale

patterns in functional divergence would benefit from further investigation to illuminate

the possible biotic and abiotic drivers leading to the small decline. In our study, we also

find that the continental proportion of archaic orders has a relationship with continental

functional richness (Fig. 6, fig. S18). However, when we subset the data to only include

the period before archaic orders went extinct (66-30 Ma), there is no longer a significant

relationship (fig. S21). This suggests that the relationship is misleading only due to the

stability in continental functional richness in the later Cenozoic and the continued lack of

archaic orders following 30 Ma. Extinction and origination rates have little to no effect

on the variation we find in continental functional diversity metrics on evolutionary

timescales. Functional richness is positively associated with origination rates; however,

the association is solely driven by the two earliest time bins in the Paleocene which have

low functional richness (fig. S22-23). The higher origination rate is a reflection of the

rapid radiation of mammals during this period (11).

The lack of a straightforward relationship between these individual large-scale

abiotic and biotic factors despite the apparent changes in functional diversity around

major ecological and evolutionary transitions, suggests that long term variation in local

functional diversity is more likely a reflection of a complicated interplay between

ecological and evolutionary processes. It is possible that processes may vary in their influence on functional diversity metrics over time, and therefore a single process (or combination of processes) is not consistently driving functional diversity metrics or the same metric. Although investigating this concept is outside the scope of this paper, we suggest it would be beneficial to further explore if the effects of ecological processes changes through time. Understanding mechanistic drivers of functional diversity continues to prove difficult and complex but remains an important aim of ecology.

Conclusion

Mammal community structure can be highly variable temporally and across spatial scales. Moreover, spatial scales and functional diversity metrics are disassociated in the direction and timing of shifts. Functional diversity metrics of mammal paleocommunities do not synchronously change without an extreme degree of ecological disturbance. Our analysis finds regular variation in components of paleocommunity and the continental faunal structure. Functional diversity metrics were decoupled across evolutionary timescales and between spatial scales. Moreover, the Paleocene was unique in the 66 million years of North American mammal history, with extraordinary synchronicity across metrics and spatial scales. The differences in the trajectories of functional diversity metrics during the Paleocene and other intervals of significant environmental change suggests that Paleocene community dynamics were distinct from the rest of the Cenozoic. The magnitude of the radiation event was strong enough to link functional diversity metrics across spatial scale. Modern mammal communities are again experiencing extreme disturbance from multiple sources, including human impacts and

climate change, which are causing shifts in functional diversity (17). However, ignoring the variation in how these metrics change through time likely hides key information about the effects of these disturbances on a community's structure. By evaluating synchronous responses across metrics, we can identify communities that have been significantly disrupted and at highest risk for functional diversity loss.

References

1. H. V. Cornell, J. H. Lawton, Species Interactions, Local and Regional Processes, and Limits to the Richness of Ecological Communities: A Theoretical Perspective. J. Anim. Ecol. **61**, 1–12 (1992).

2. J.-P. Lessard, M. K. Borregaard, J. A. Fordyce, C. Rahbek, M. D. Weiser, R. R. Dunn, N. J. Sanders, Strong influence of regional species pools on continent-wide structuring of local communities. Proc. R. Soc. B Biol. Sci. **279**, 266–274 (2011).

3. N. J. Gotelli, A. M. Ellison, Assembly Rules for New England Ant Assemblages. Oikos **99**, 591–599 (2002).

4. A. H. Hurlbert, W. Jetz, Species richness, hotspots, and the scale dependence of range maps in ecology and conservation. Proc. Natl. Acad. Sci. **104**, 13384–13389 (2007).

5. Y. Liu, J. Bi, J. Lv, Z. Ma, C. Wang, Spatial multi-scale relationships of ecosystem services: A case study using a geostatistical methodology. Sci. Rep. **7**, 9486 (2017).

6. J. J. Sepkoski, Alpha, beta, or gamma: where does all the diversity go? Paleobiology **14**, 221–234 (1988).

7. G. Arellano, J. S. Tello, P. M. Jørgensen, A. F. Fuentes, M. I. Loza, V. Torrez, M. J. Macía, Disentangling environmental and spatial processes of community assembly in tropical forests from local to regional scales. Oikos **125**, 326–335 (2016).

8. A. Siefert, C. Ravenscroft, D. Althoff, J. C. Alvarez-Yépiz, B. E. Carter, K. L. Glennon, J. M. Heberling, I. S. Jo, A. Pontes, A. Sauer, A. Willis, J. D. Fridley, Scale dependence of vegetation–environment relationships: a meta-analysis of multivariate data. J. Veg. Sci. **23**, 942–951 (2012).

9. K. H. Bannar-Martin, Primate and Nonprimate Mammal Community Assembly: The Influence of Biogeographic Barriers and Spatial Scale. Int. J. Primatol. **35**, 1122–1142 (2014).

10. M. W. Cadotte, K. Carscadden, N. Mirotchnick, Beyond species: functional diversity and the maintenance of ecological processes and services. J. Appl. Ecol. **48**, 1079–1087 (2011).

11. J. Alroy, The Fossil Record of North American Mammals: Evidence for a Paleocene Evolutionary Radiation. Syst. Biol. **48**, 107–118 (1999).

12. T. J. D. Halliday, A. Goswami, Eutherian morphological disparity across the end-Cretaceous mass extinction. Biol. J. Linn. Soc. **118**, 152–168 (2016).

13. C. M. Tucker, T. J. Davies, M. W. Cadotte, W. D. Pearse, On the relationship between phylogenetic diversity and trait diversity. Ecology **99**, 1473–1479 (2018).

14. M. A. Jarzyna, W. Jetz, Taxonomic and functional diversity change is scale dependent. Nat. Commun. **9**, 2565 (2018).

15. S. Zhou, S. M. Edie, K. S. Collins, N. M. A. Crouch, D. Jablonski, Cambrian origin but no early burst in functional disparity for Class Bivalvia. Biol. Lett. **19**, 20230157 (2023).

16. S. Villéger, N. W. H. Mason, D. Mouillot, New Multidimensional Functional Diversity Indices for a Multifaceted Framework in Functional Ecology. Ecology **89**, 2290–2301 (2008).

17. D. W. Laméris, N. Tagg, J. K. Kuenbou, E. H. M. Sterck, J. Willie, Drivers affecting mammal community structure and functional diversity under varied conservation efforts in a tropical rainforest in Cameroon. Anim. Conserv. **23**, 182–191 (2020).

18. B. Figueirido, C. Janis, J. Pérez-Claros, M. De Renzi, P. Palmqvist, Cenozoic climate change influences mammalian evolutionary dynamics. Proc. Natl. Acad. Sci. U. S. A. **109**, 722–7 (2011).

19. J. Alroy, Cope's rule and the dynamics of body mass evolution in North American fossil mammals. Science **280**, 731–734 (1998).

20. F. A. Smith, A. G. Boyer, J. H. Brown, D. P. Costa, T. Dayan, S. K. M. Ernest, A. R. Evans, M. Fortelius, J. L. Gittleman, M. J. Hamilton, L. E. Harding, K. Lintulaakso, S. K. Lyons, C. McCain, J. G. Okie, J. J. Saarinen, R. M. Sibly, P. R. Stephens, J. Theodor, M. D. Uhen, The evolution of maximum body size of terrestrial mammals. Science **330**, 1216–1219 (2010).

21. J. C. Zachos, G. R. Dickens, R. E. Zeebe, An early Cenozoic perspective on greenhouse warming and carbon-cycle dynamics. Nature **451**, 279–283 (2008).

22. T. Westerhold, N. Marwan, A. J. Drury, D. Liebrand, C. Agnini, E. Anagnostou, J. S. K. Barnet, S. M. Bohaty, D. De Vleeschouwer, F. Florindo, T. Frederichs, D. A. Hodell, A. E. Holbourn, D. Kroon, V. Lauretano, K. Littler, L. J. Lourens, M. Lyle, H. Pälike, U. Röhl, J. Tian, R. H. Wilkens, P. A. Wilson, J. C. Zachos, An astronomically dated record of Earth's climate and its predictability over the last 66 million years. Science **369**, 1383–1387 (2020).

23. J. W. H. Weijers, S. Schouten, A. Sluijs, H. Brinkhuis, J. S. Sinninghe Damsté, Warm arctic continents during the Palaeocene–Eocene thermal maximum. Earth Planet. Sci. Lett. **261**, 230–238 (2007).

24. C. M. Brierley, A. V. Fedorov, Relative importance of meridional and zonal sea surface temperature gradients for the onset of the ice ages and Pliocene-Pleistocene climate evolution. Paleoceanography **25** (2010).

25. V. Gagic, I. Bartomeus, T. Jonsson, A. Taylor, C. Winqvist, C. Fischer, E. M. Slade, I. Steffan-Dewenter, M. Emmerson, S. G. Potts, T. Tscharntke, W. Weisser, R. Bommarco, Functional identity and diversity of animals predict ecosystem functioning better than species-based indices. Proc. R. Soc. B Biol. Sci. **282**, 20142620 (2015).

26. D. F. B. Flynn, M. Gogol-Prokurat, T. Nogeire, N. Molinari, B. T. Richers, B. B. Lin, N. Simpson, M. M. Mayfield, F. DeClerck, Loss of functional diversity under land use intensification across multiple taxa. Ecol. Lett. **12**, 22–33 (2009).

27. L. N. Weaver, D. M. Grossnickle, Functional diversity of small-mammal postcrania is linked to both substrate preference and body size. Curr. Zool. **66**, 539–553 (2020).

28. K. L. Voje, J. G. Saulsbury, J. Starrfelt, D. V. Latorre, A. Rojas, V. B. Kinneberg, L. H. Liow, C. J. Wilson, E. E. Saupe, M. Grabowski, Measurement theory and paleobiology. Trends Ecol. Evol. **38**, 1165–1176 (2023).

29. E. Laliberté, P. Legendre, B. Shipley, FD: Measuring functional diversity from multiple traits, and other tools for functional ecology. R Package Version **1**, 0–12 (2014).

30. E. Laliberté, P. Legendre, A distance-based framework for measuring functional diversity from multiple traits. Ecology **91**, 299–305 (2010).

31. J. C. Gower, A General Coefficient of Similarity and Some of Its Properties. Biometrics **27**, 857–871 (1971).

32. M. Foote, Inferring temporal patterns of preservation, origination, and extinction from taxonomic survivorship analysis. Paleobiology **27**, 602–630 (2001).

33. M. Foote, Origination and Extinction through the Phanerozoic: A New Approach. J. Geol. **111**, 125–148 (2003).

34. J. Alroy, Dynamics of origination and extinction in the marine fossil record. Proc. Natl. Acad. Sci. **105**, 11536–11542 (2008).

35. C. R. Congreve, M. E. Patzkowsky, P. J. Wagner, An early burst in brachiopod evolution corresponding with significant climatic shifts during the Great Ordovician Biodiversification Event. Proc. R. Soc. B Biol. Sci. **288**, 20211450.

36. J. D. Wright, "Global Climate Change in Marine Stable Isotope Records" in AGU Reference Shelf, J. S. Noller, J. M. Sowers, W. R. Lettis, Eds. (American Geophysical Union, Washington, D. C., 2013; http://doi.wiley.com/10.1029/RF004p0427), pp. 427–433.

37. J. F. González-Maya, L. R. Víquez-R, A. Arias-Alzate, J. L. Belant, G. Ceballos, Spatial patterns of species richness and functional diversity in Costa Rican terrestrial mammals: implications for conservation. Divers. Distrib. **22**, 43–56 (2016).

38. G. L. Benevento, R. B. J. Benson, R. A. Close, R. J. Butler, Early Cenozoic increases in mammal diversity cannot be explained solely by expansion into larger body sizes. Palaeontology **66**, e12653 (2023).

39. D. M. Grossnickle, E. Newham, Therian mammals experience an ecomorphological radiation during the Late Cretaceous and selective extinction at the K–Pg boundary. Proc. R. Soc. B Biol. Sci. **283**, 20160256 (2016).

40. T. R. Lyson, I. M. Miller, A. D. Bercovici, K. Weissenburger, A. J. Fuentes, W. C. Clyde, J. W. Hagadorn, M. J. Butrim, K. R. Johnson, R. F. Fleming, R. S. Barclay, S. A. Maccracken, B. Lloyd, G. P. Wilson, D. W. Krause, S. G. B. Chester, Exceptional continental record of biotic recovery after the Cretaceous–Paleogene mass extinction. Science **366**, 977–983 (2019).

41. S. Lyons, F. Smith, "Macroecological Patterns of Body Size in Mammals across Time and Space" (2013), pp. 114–142.

42. J. H. Brown, P. A. Marquet, M. L. Taper, Evolution of Body Size: Consequences of an Energetic Definition of Fitness. Am. Nat. **142**, 573–584 (1993).

43. S. Pineda-Munoz, A. R. Evans, J. Alroy, The relationship between diet and body mass in terrestrial mammals. Paleobiology **42**, 659–669 (2016).

44. B. H. Tiffney, "An Estimate of the Early Tertiary Paleoclimate of the Southern Arctic" in Cenozoic Plants and Climates of the Arctic, M. C. Boulter, H. C. Fisher, Eds. (Springer Berlin Heidelberg, Berlin, Heidelberg, 1994; http://link.springer.com/10.1007/978-3-642-79378-3_19), pp. 267–295.

45. P. Gingerich, Mammalian responses to climate change at the Paleocene-Eocene boundary: Polecat Bench record in the northern Bighorn Basin, Wyoming. Geol Soc Am Spec Pap **369** (2003).

46. M. O. Woodburne, G. F. Gunnell, R. K. Stucky, Climate directly influences Eocene mammal faunal dynamics in North America. Proc. Natl. Acad. Sci. **106**, 13399–13403 (2009).

47. P. D. Smits, Expected time-invariant effects of biological traits on mammal species duration. Proc. Natl. Acad. Sci. U. S. A. **112**, 13015–13020 (2015).

48. C. A. E. Strömberg, Evolution of Grasses and Grassland Ecosystems. Annu. Rev. Earth Planet. Sci. **39**, 517–544 (2011).

49. C. M. Janis, J. Damuth, J. M. Theodor, The origins and evolution of the North American grassland biome: the story from the hoofed mammals. Palaeogeogr. Palaeoclimatol. Palaeoecol. **177**, 183 (2002).

50. G. D. Wesley-Hunt, The morphological diversification of carnivores in North America. 21.

51. X. Wang, R. H. Tedford, B. E. Taylor, Phylogenetic Systematics of the Borophaginae (Carnivora: Canidae).

52. B. Van Valkenburgh, Deja vu: the evolution of feeding morphologies in the Carnivora. Integr. Comp. Biol. **47**, 147–163 (2007).

53. S. G. Lucas, W. Yuan, L. Min, The palaeobiogeography of South American gomphotheres. J. Palaeogeogr. **2**, 19–40 (2013).

54. T. Rothwell, A Partial Skeleton of Pseudaelurus (Carnivora: Felidae) from the Nambé Member of the Tesuque Formation, Española Basin, New Mexico. Am. Mus. Novit. **2001**, 1–31 (2001).

55. O. J. Schmitz, Haynes, G. 1991. Mammoths, mastodants and elephants: biology, behavior and the fossil record. Cambridge University Press, Cambridge. 413 p. ISBN:0-521-38435-4. J. Evol. Biol. **6**, 147–148 (1993).

56. M. A. Tsianou, M. Lazarina, D.-E. Michailidou, A. Andrikou-Charitidou, S. P. Sgardelis, A. S. Kallimanis, The Effect of Climate and Human Pressures on Functional Diversity and Species Richness Patterns of Amphibians, Reptiles and Mammals in Europe. Diversity **13**, 275 (2021).

57. M. J. Spasojevic, K. N. Suding, Inferring community assembly mechanisms from functional diversity patterns: the importance of multiple assembly processes. J. Ecol. **100**, 652–661 (2012).

Tables and Figures
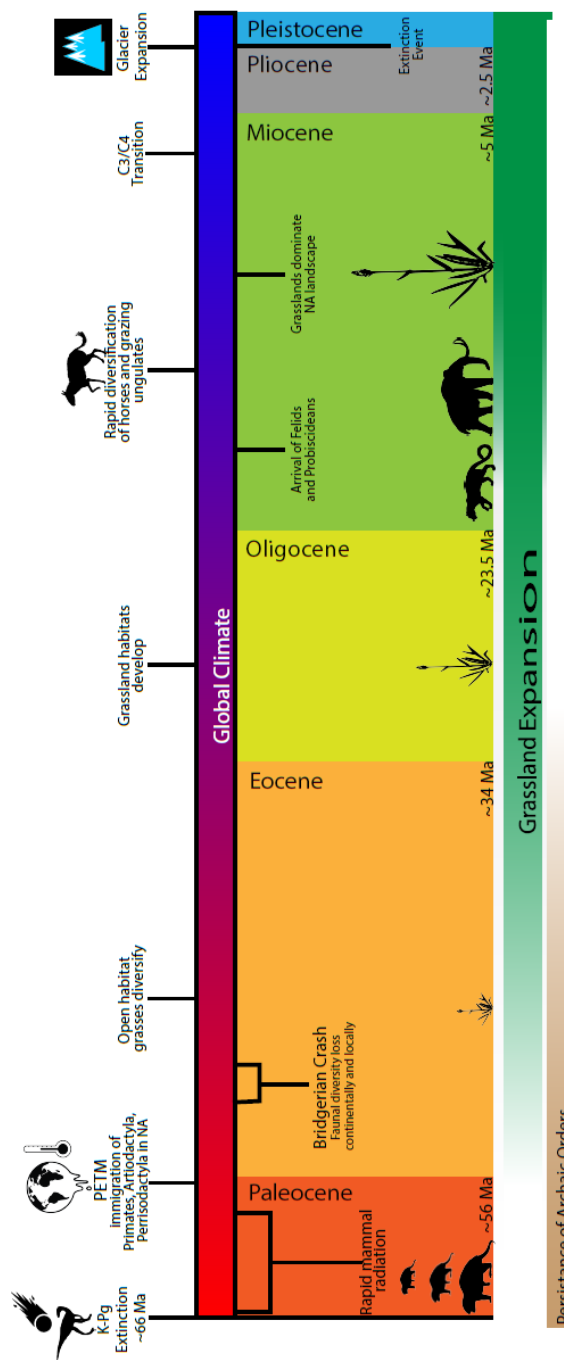
Figure 1. **Cenozoic timeline of abiotic and biotic factors influencing North American mammal paleocommunity structure.**
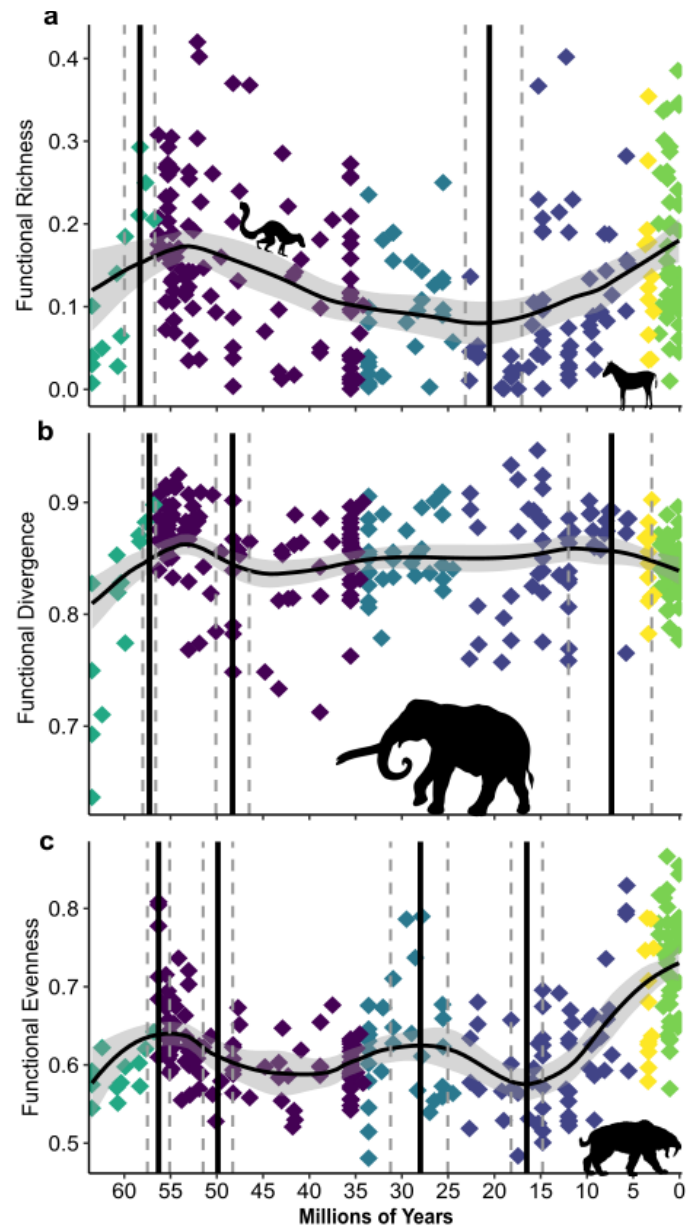
Figure 2. **Loess regressions of functional diversity indices through the Cenozoic (a) Functional Richness (b) Functional Divergence (c) Functional Evenness.** Loess regressions are a nonparametric method of fitting a smooth curve to data. Each datum represents a paleocommunity, which are color-coded by epoch. Dotted lines indicate confidence intervals, solid lines represent breakpoint.
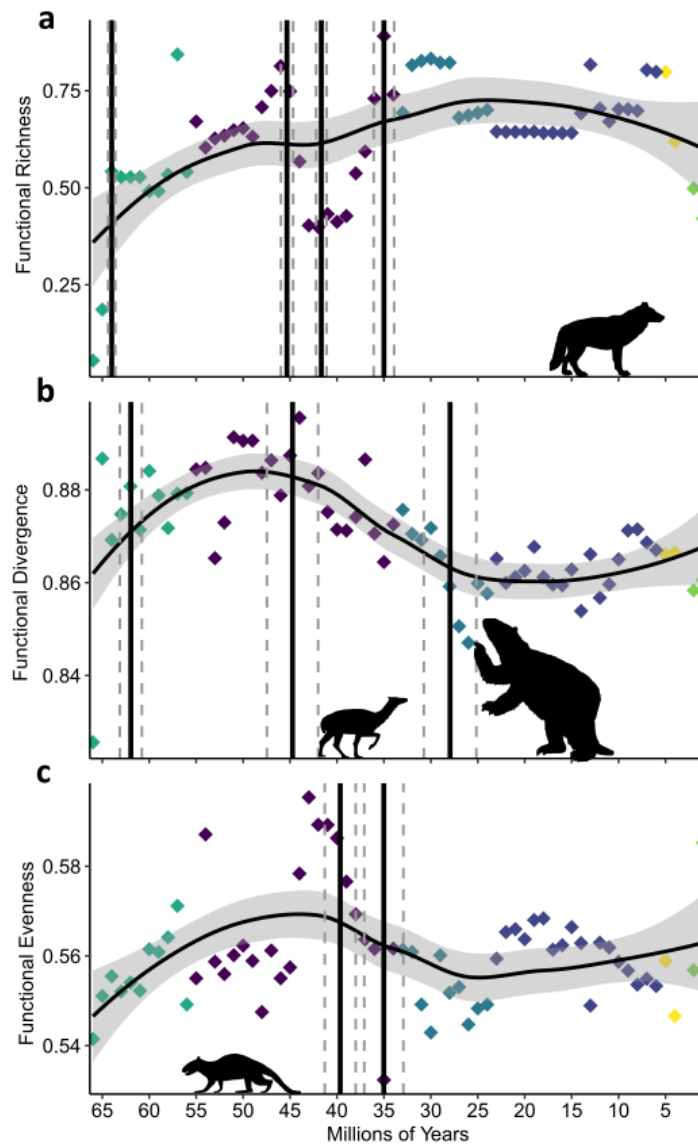
Figure 3. **Loess regressions for functional diversity indices of the North American mammal continental fauna in one-million-year time bins. (a) Functional Richness, (b) Functional Divergence (c) Functional Evenness.** Loess regressions are a nonparametric method of fitting a smooth curve to data. Each datum represents a paleocommunity, which are color-coded by epoch. Dotted lines indicate confidence intervals, solid lines represent breakpoint.
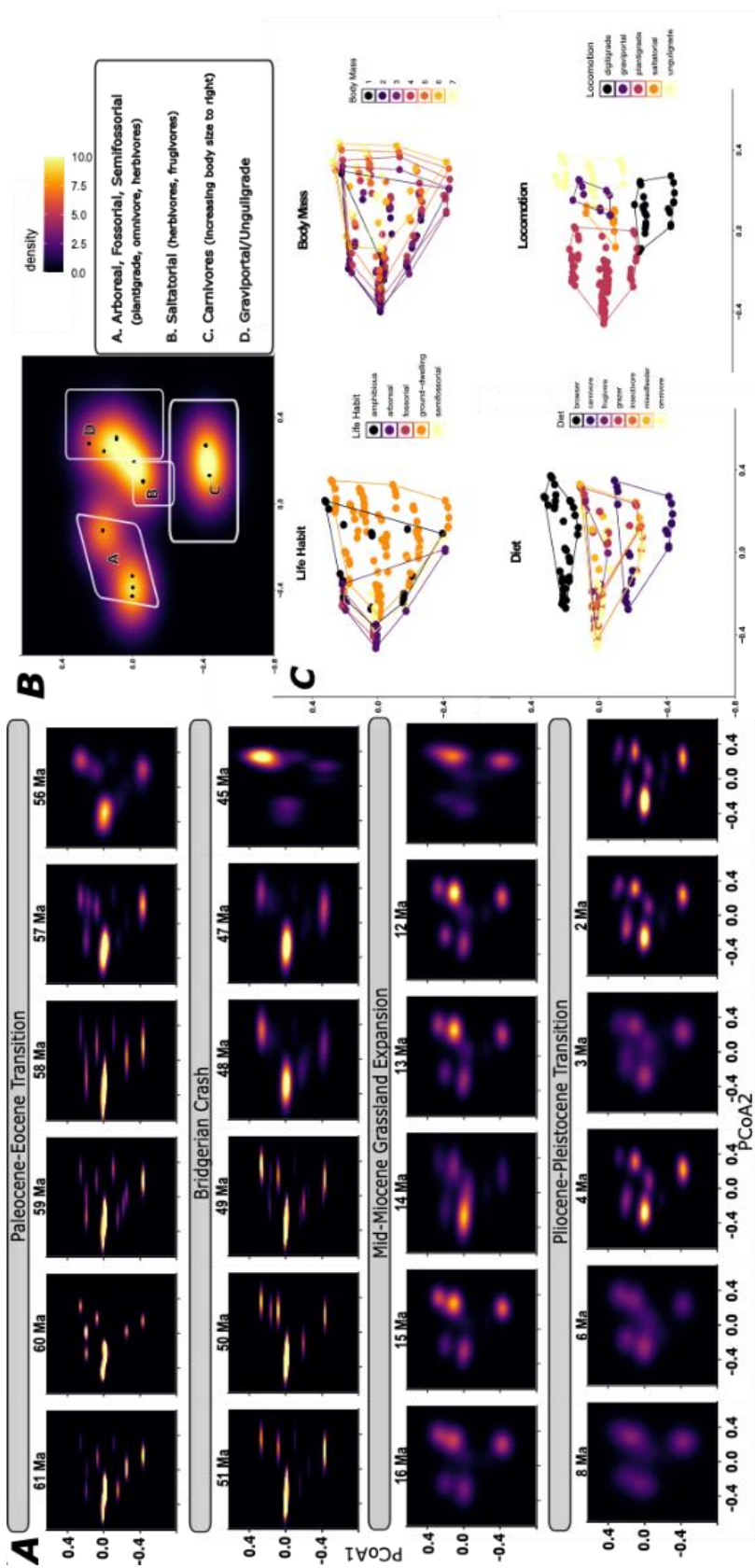
Figure 4. **The trait space density of North American mammals. A) Species were divided into 1-million-year time bins and species PCoA axes used to ordinate in multidimensional space.** Each time bin included all paleocommunities that fell within the date range. Titles indicate major events within the included time. B) an example paleocommunity made from a combination of paleocommunities in the dataset to display the full range of niches occupied by mammals across the Cenozoic. Boxes are used to identify the location of key niches discussed in our study (e.g. large carnivores, medium-sized mammals, etc.). This example paleocommunity can be used as a general reference to better understand what structural components of mammal paleocommunities are changing in section A. C) The location of each trait category and the range of multidimensional space occupied by each trait enclosed by convex hulls. Each point represents a unique combination of traits occupied by a species in the database (see Supplementary Material).
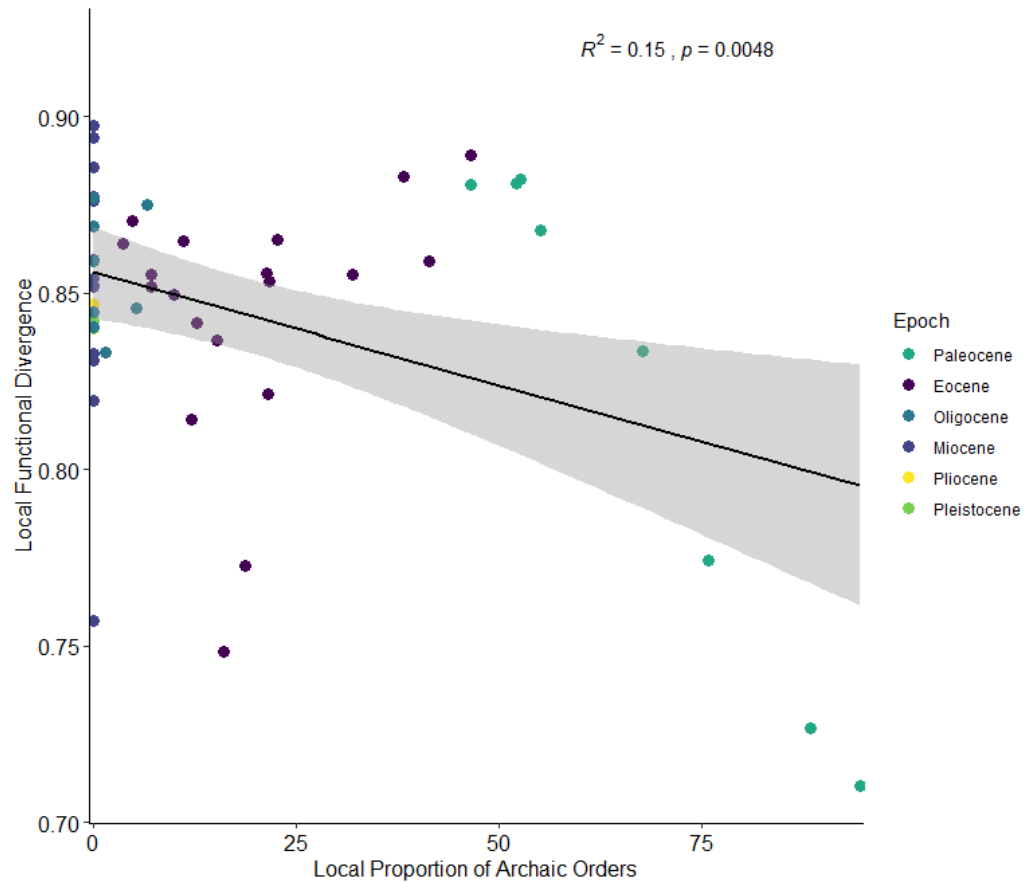
Figure 5. **Regression of local functional divergence against the local proportion of archaic orders.** Local proportion of archaic orders is the mean of all paleocommunities within 1-million-year time bins against the average functional divergence of all paleocommunities in each 1-million year time bins. It is the only abiotic or biotic variable that had a significant relationship with a functional diversity index ($R^2 = 0.15$, p=0.0048).
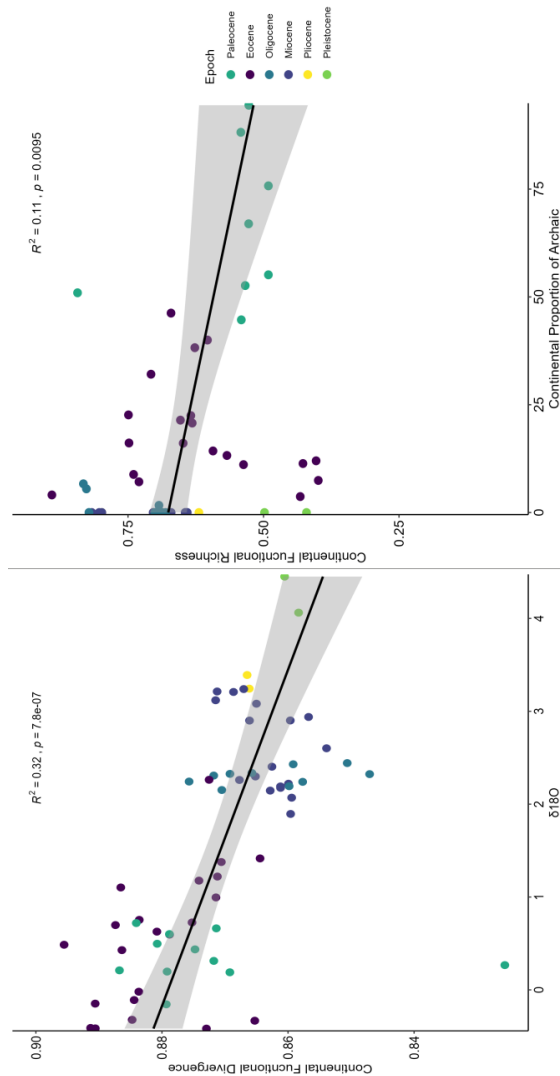
Figure 6. **Regressions of the biotic and abiotic variables that have a significant relationship with a continental functional divergence index.** $\delta^{18}O$ values were averaged for each 1-million year time bin and run against the functional divergence of the continental fauna for each 1-million year time bin (R2 = 0.32, p = 78e-07). The continental proportion of archaic orders had a significant relationship with functional richness. The continental proportion of archaic orders represents the proportion of archaic verses extant orders within each 1-million year time bin ($R^2 = 0.11$, p = 0.0095)
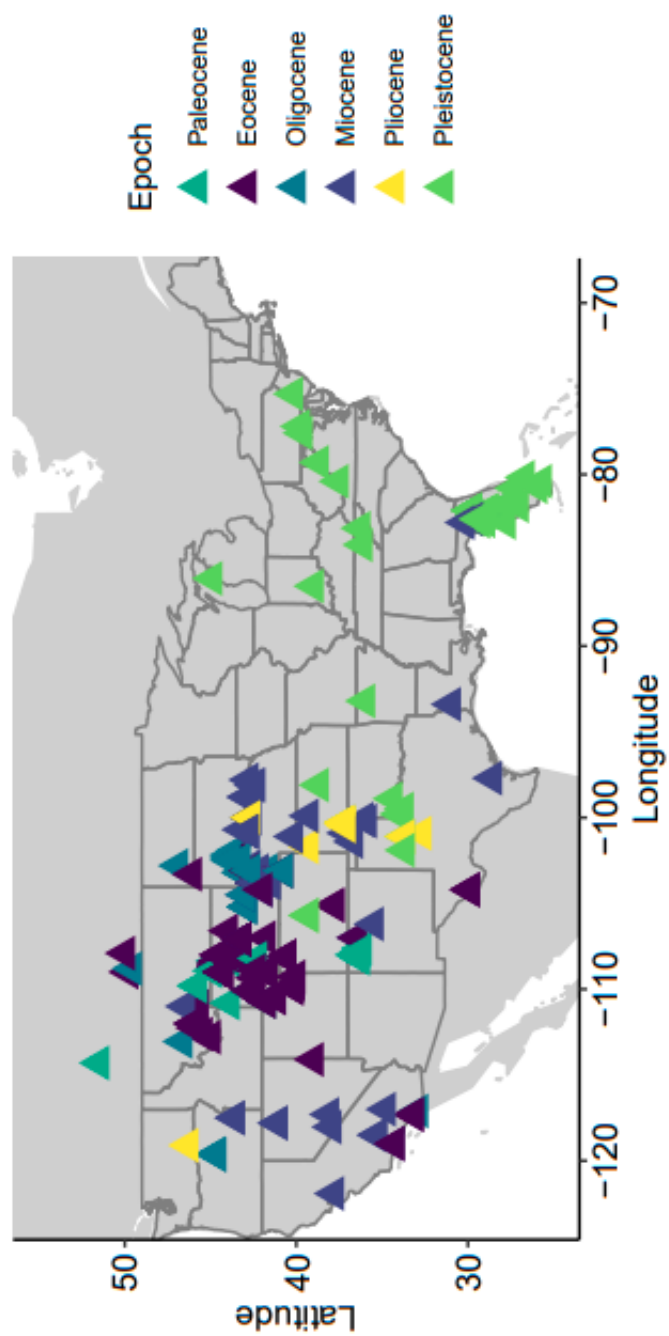
Figure S1. **Map of geographic locations of paleocommunities included in this study.**

Paleocommunities are color-coded by epoch.
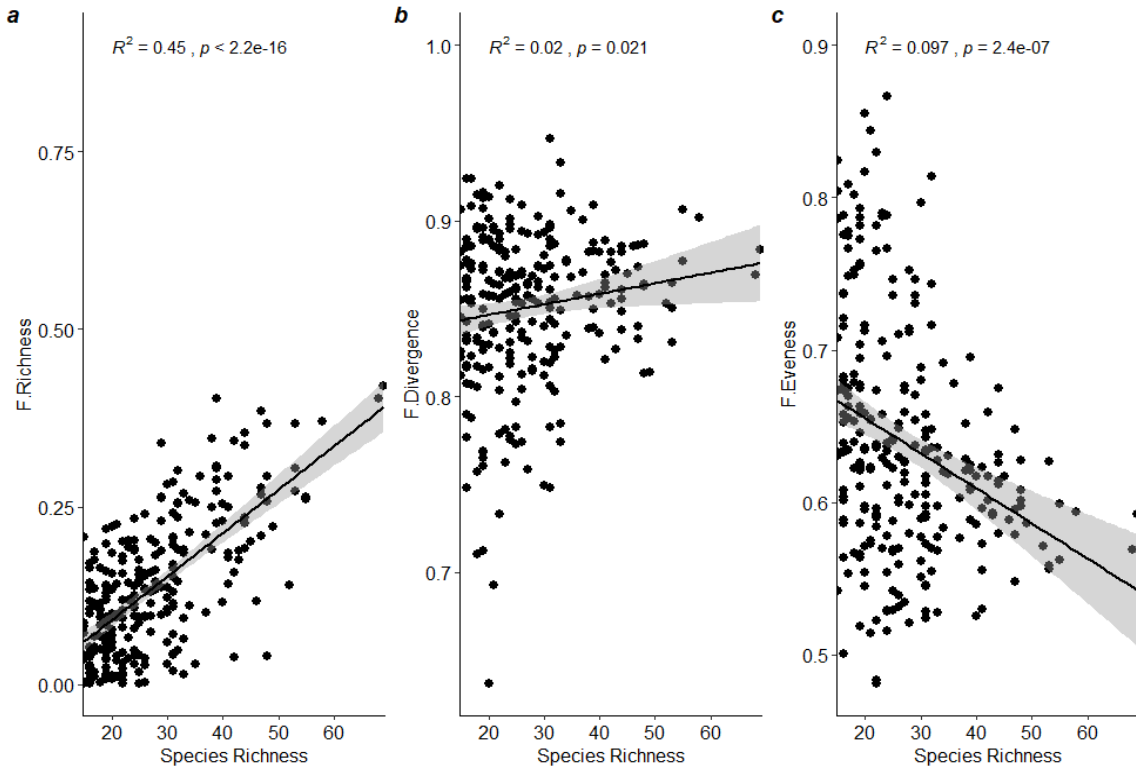
Figure S2. **Regressions showing the relationship between each functional diversity index and paleocommunity species richness.** As expected, FRic has a positive relationship with species richness.

Functional Richness

Species Richness of Palaeocommunities

54
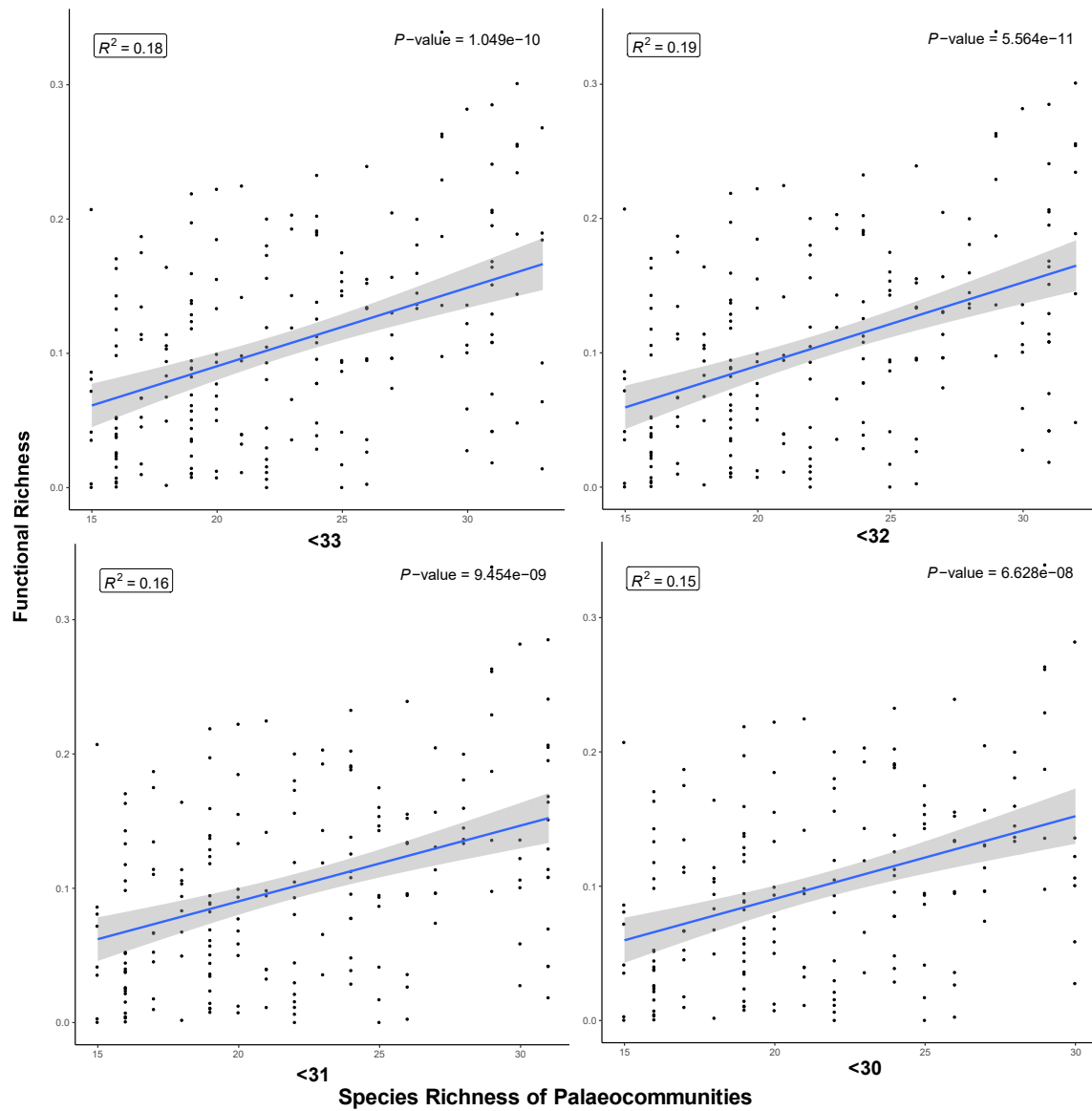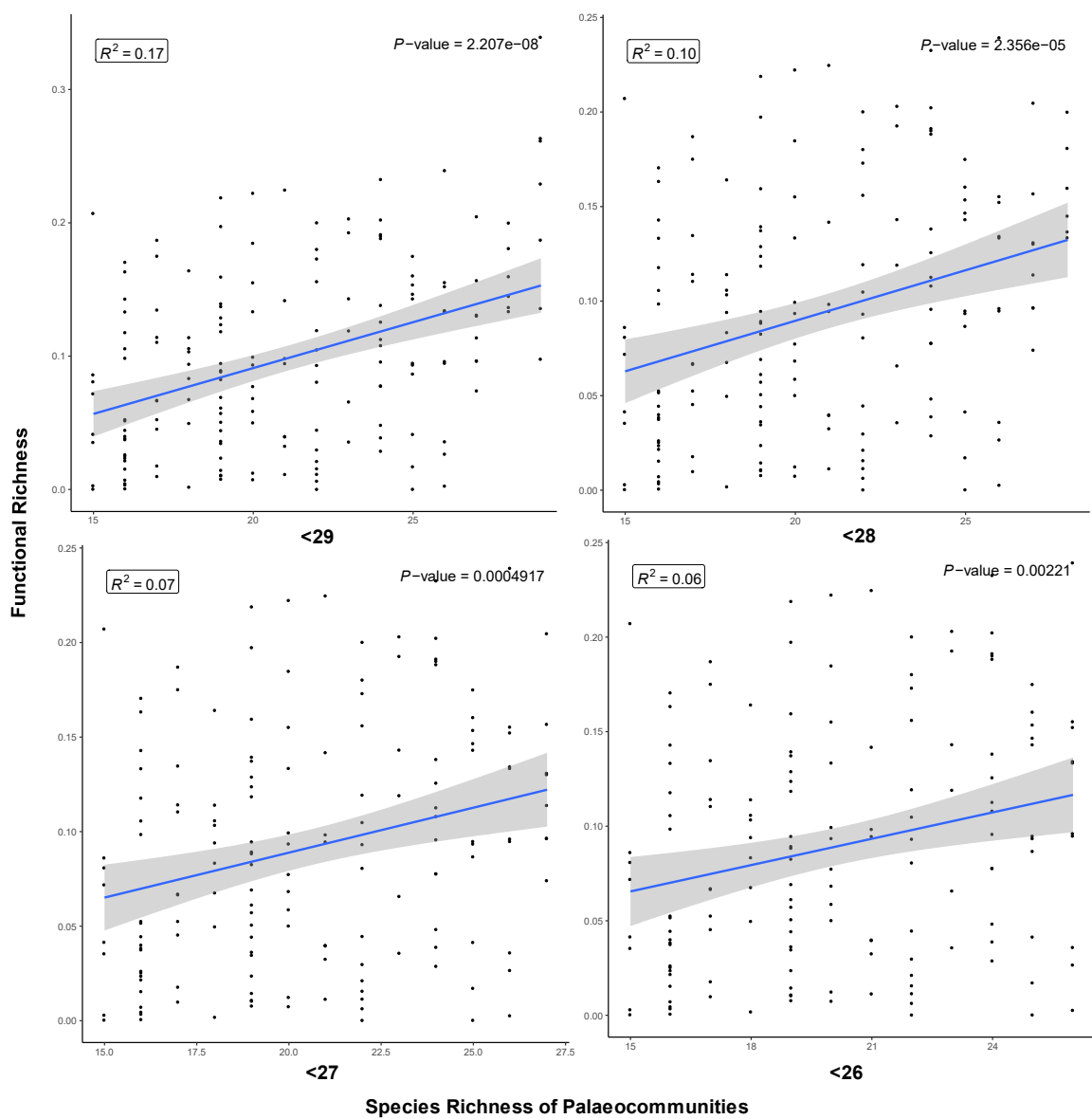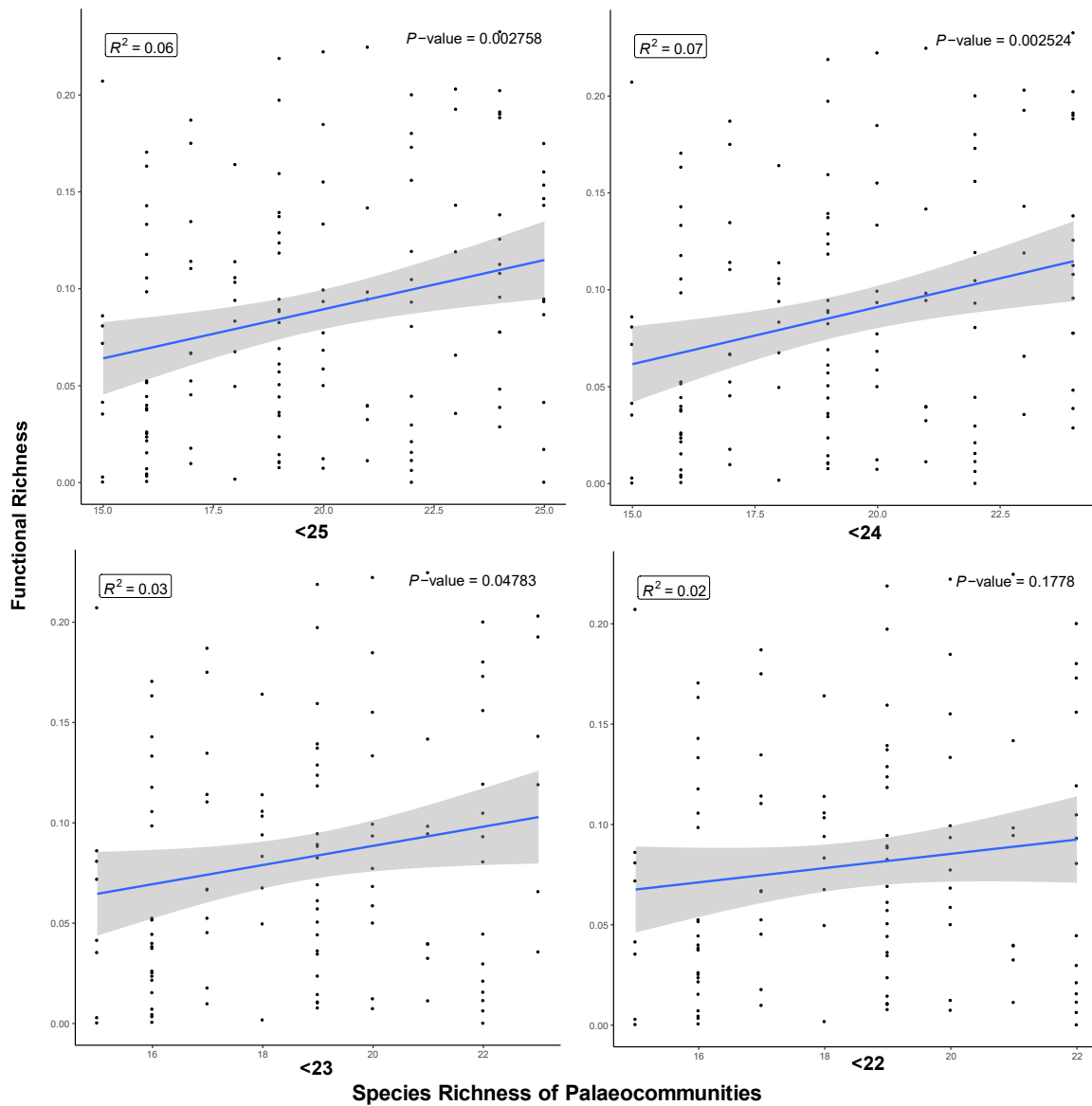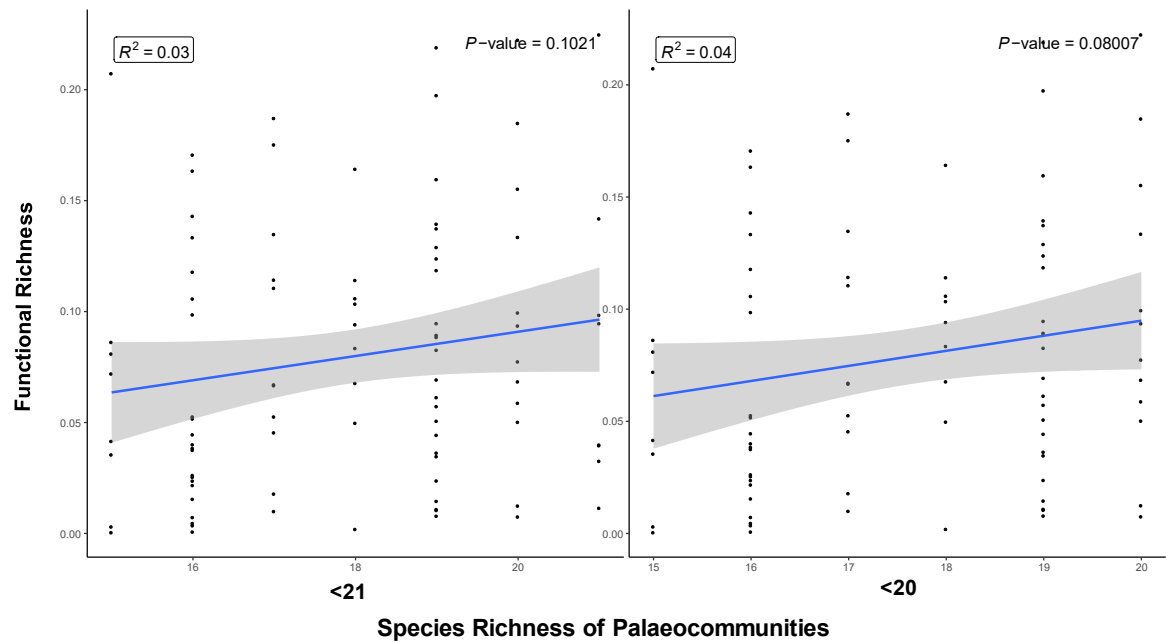
Figure S3. **Regressions demonstrating the relationship between functional richness and the species richness of paleocommunities.** The relationship remains weak but does become non-significant when restricting the analysis only including paleocommunities with 23 species or less. To determine if the significance of the relationship between species richness and functional richness drives our results, I plotted paleocommunities with 23 species or less in Figure S7.
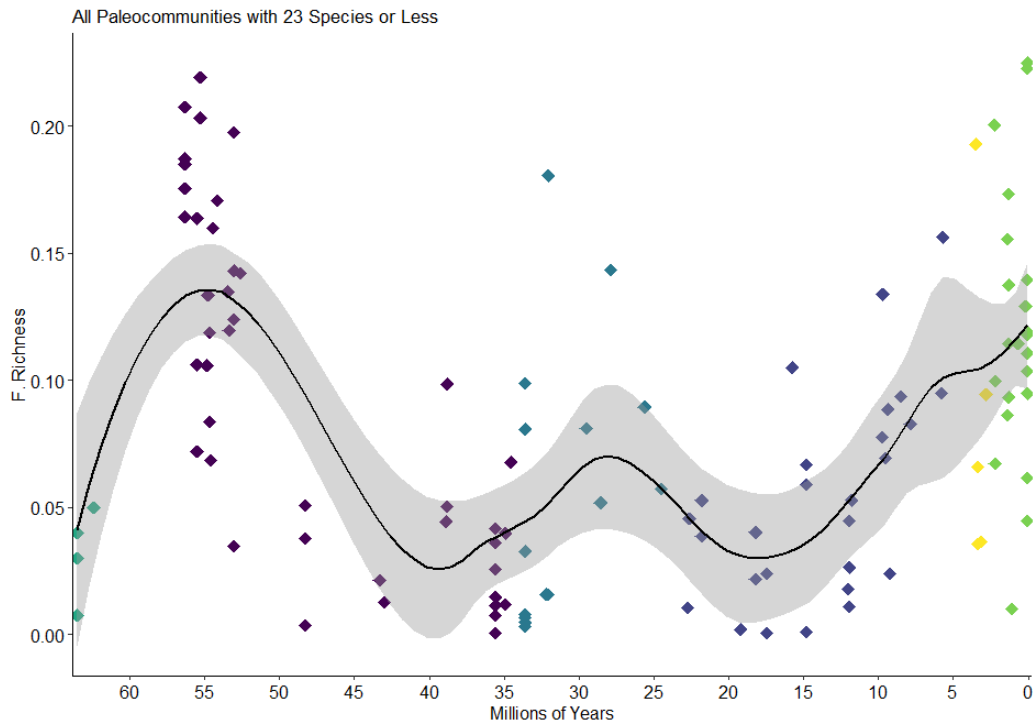
Figure S4. **Functional richness replotted following the removal of all paleocommunities with less than 23 species.** We found that under 23 species, the relationship between species richness and FRic is no longer significant as can be seen in Figure S6.
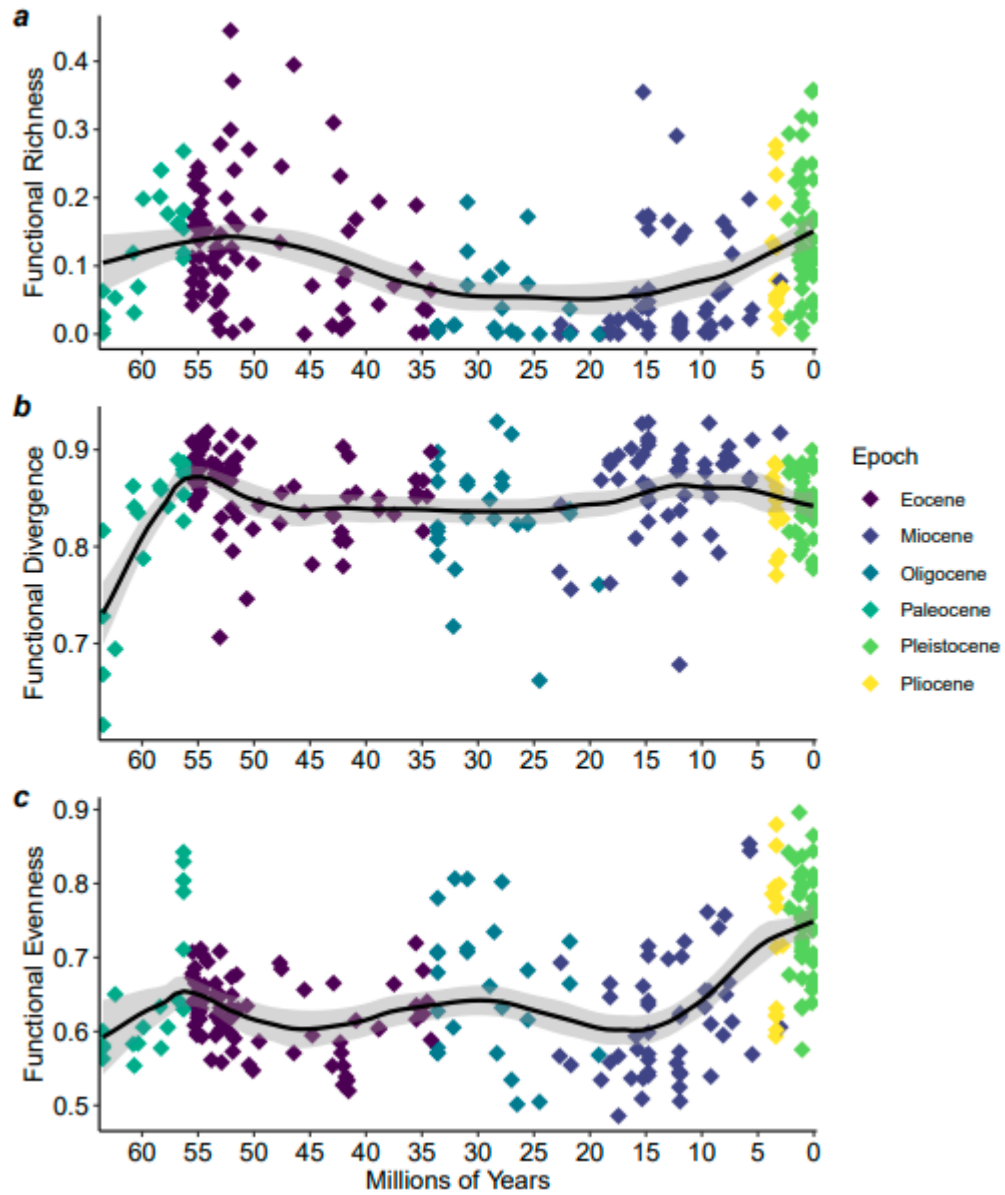
Figure S5. **Recalculated functional diversity indices excluding all species that body mass was averaged from genus or family to determine if averaged body mass drove our results**. These results suggest that the overall pattern in functional diversity indices across time are not being driven by the averaging of body mass.
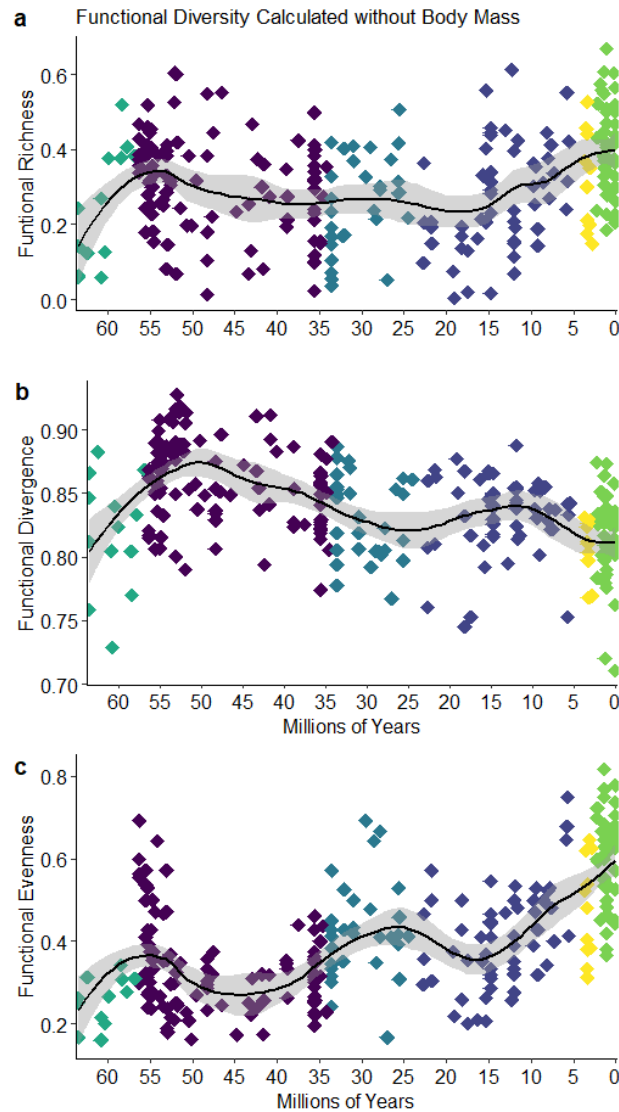
Figure S6. **Functional diversity was recalculated for each paleocommunity excluding body mass as a trait for mammalian species and plotted against time.** This analysis is used to evaluate the possible effects of combining categorical and numerical variables in functional diversity. However, the overall trends and patterns of each functional diversity index is consistent with original results found in Figure 2 of the main manuscript. Furthermore, these results demonstrate the strong influence that body mass has on ecological role variation.
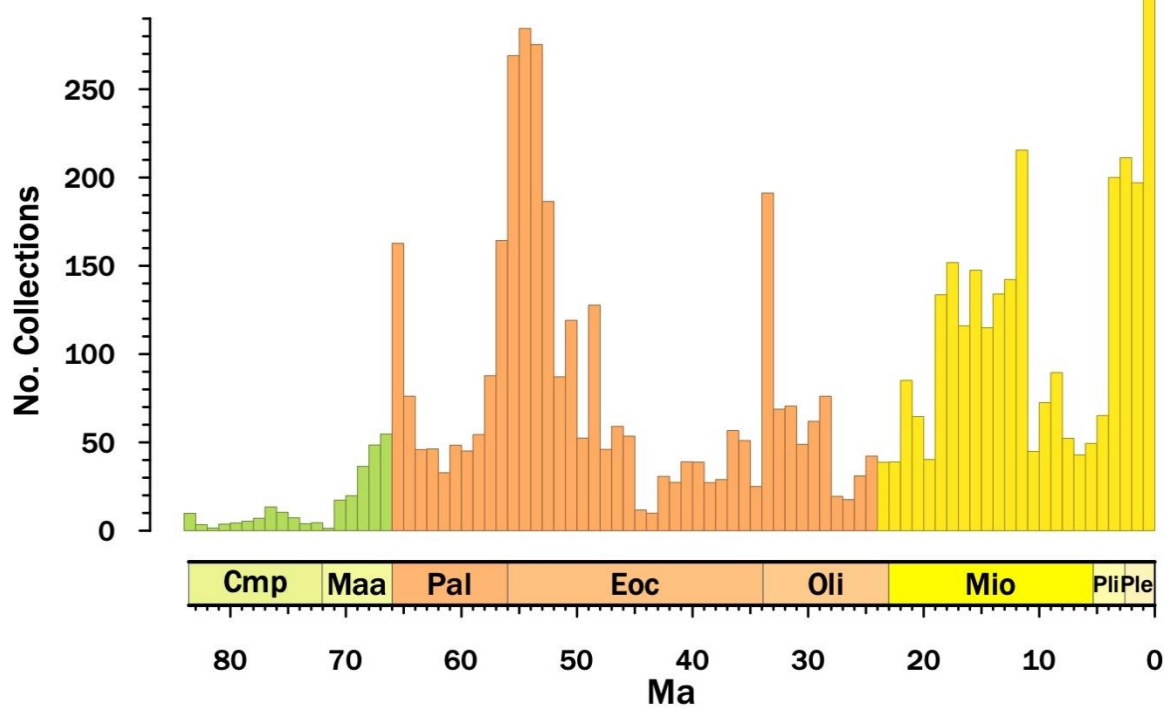
Figure S7. **The number of collections found in each 1-million year time bin across the last 85 million years.**
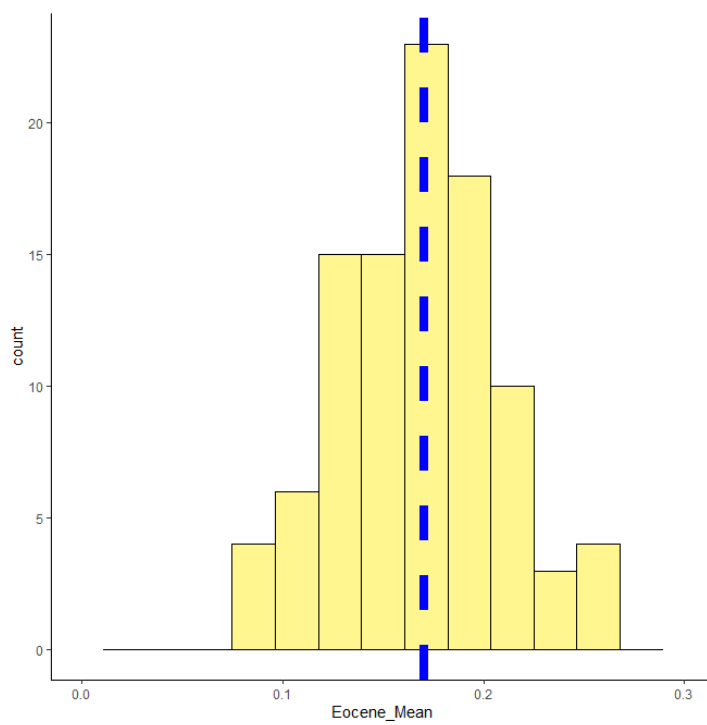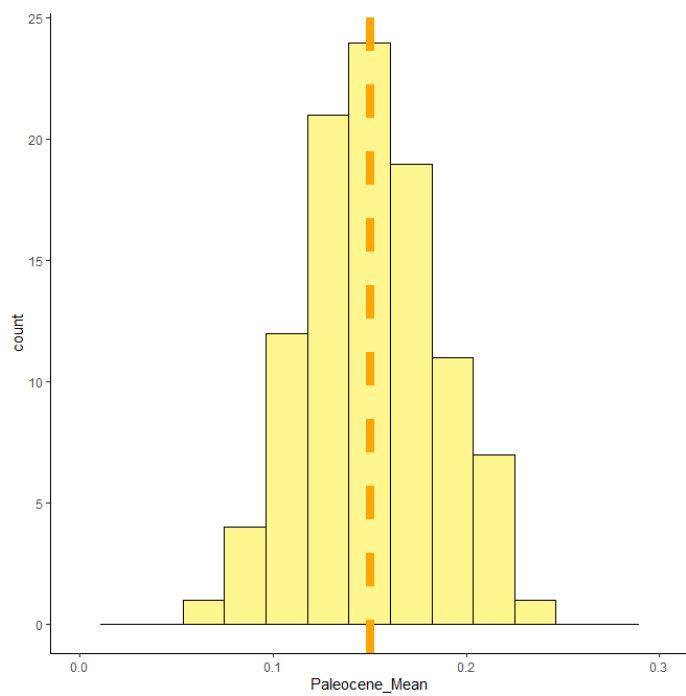
Figure S8. **Histograms showing the distributions of mean local scale functional richness values after sub-sampling with replacement down to 5 paleocommunities in the 10 million years of the Paleocene and the first 10 million years of the Eocene.** This sub-sampling routine was preformed 100 times. The Paleocene has the orange bar making the overall mean of the distribution and the Eocene has the blue bar. 5 paleocommunities were chosen because it was the lowest number of paleocommunities found in a North American Land Mammal Age in the Paleocene and Eocene. We ran this sub-sampling routine and ran a t-test to compare the distributions (t = 3.5567, df = 187.2, p-value = 0.0004757*) to determine if the Eocene had higher functional diversity values due to a larger number of paleocommunities. Our results demonstrate that the rise in functional richness is not due to the increase in the number of paleocommunities, but instead due to an overall higher average of functional richness.
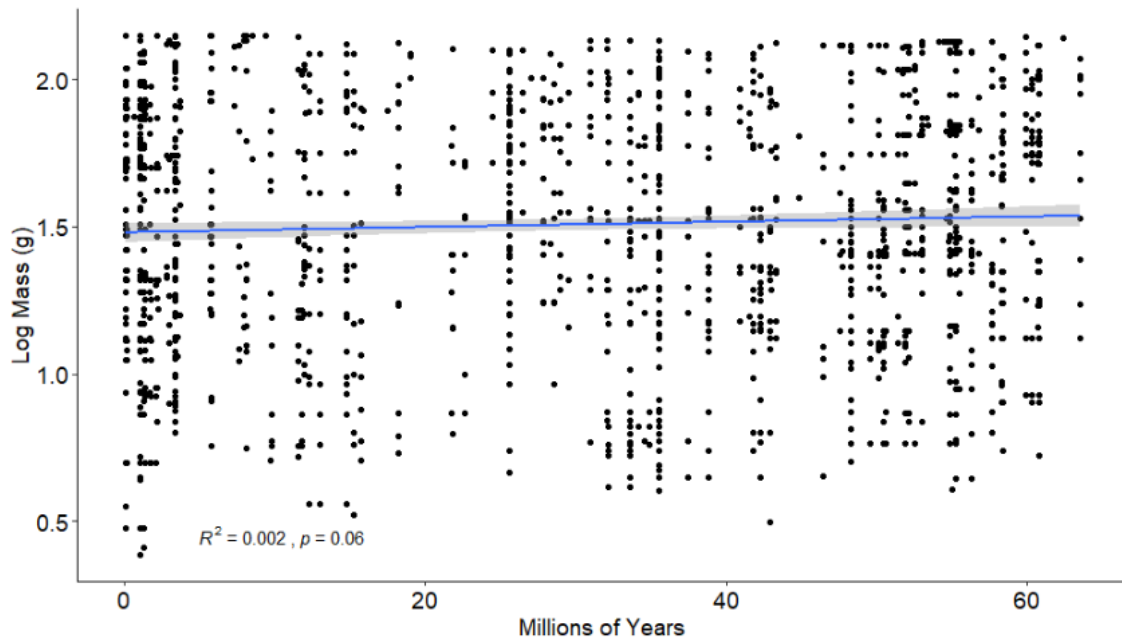
Figure S9. **The bottom quartile of all mammal body masses (log grams) in the database plotted through time.** This suggest that there was not a size bias in our data to skew our results.
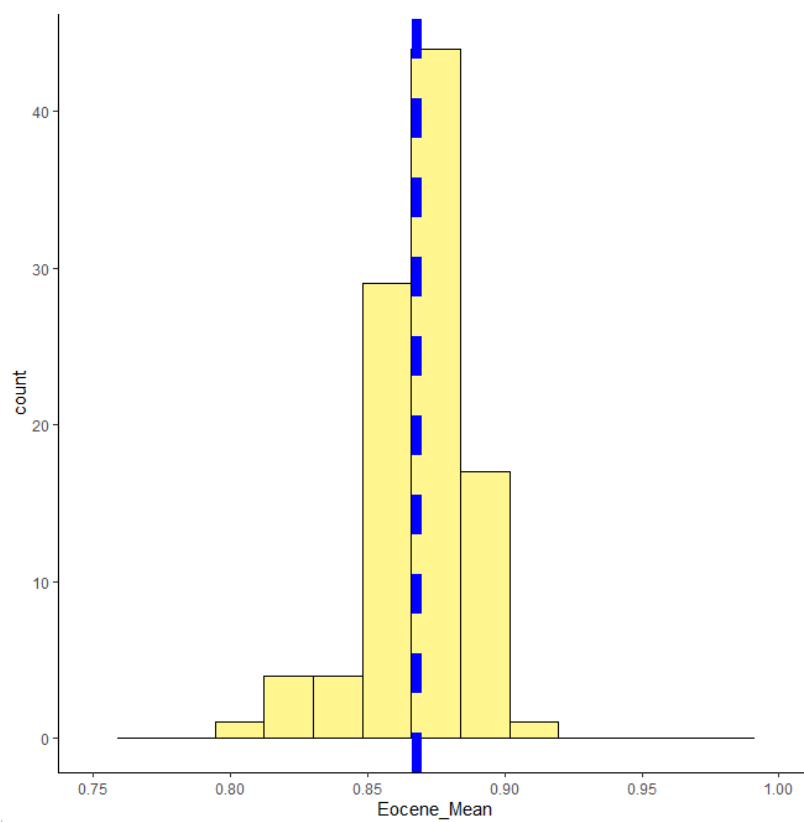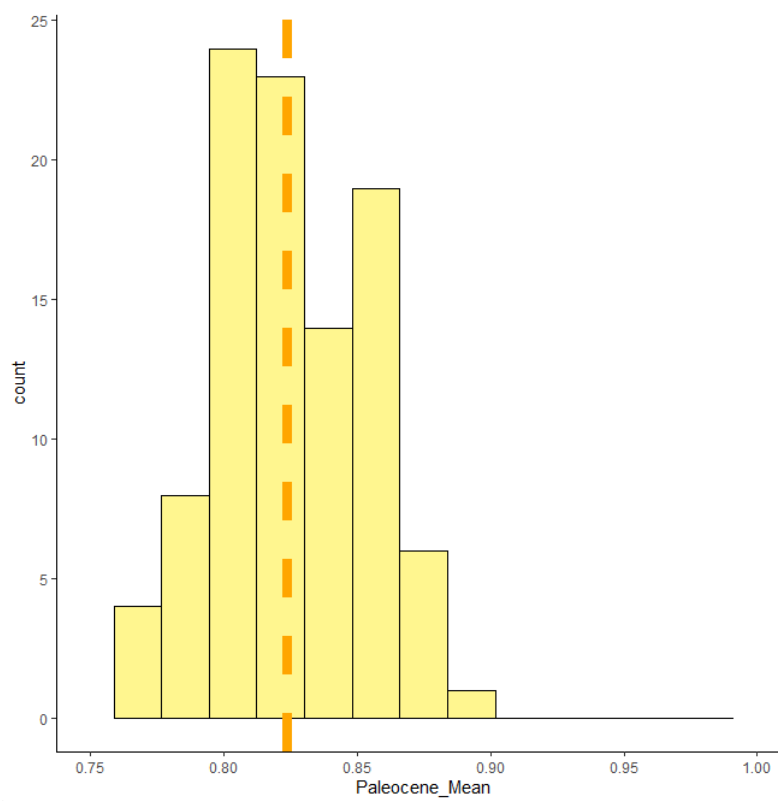
Figure S10. **Histograms showing the distributions of mean local scale functional divergence values after sub-sampling with replacement down to 5 paleocommunities in the 10 million years of the Paleocene and the first 10 million years of the Eocene.** The Paleocene has the orange bar making the overall mean of the distribution and the Eocene has the blue bar. 5 paleocommunities were chosen because it was the lowest number of paleocommunities found in a North American Land Mammal Age in the Paleocene and Eocene. We ran this sub-sampling routine and ran a t-test to compare the distributions ($t = 13.476$, $df = 166.98$, p-value $< 2.2e-16$ *) to determine if the Eocene had higher functional diversity values due to a larger number of paleocommunities. Our results demonstrate that the rise in functional divergence is not due to the increase in the number of paleocommunities, but instead due to an overall higher average of functional divergence.
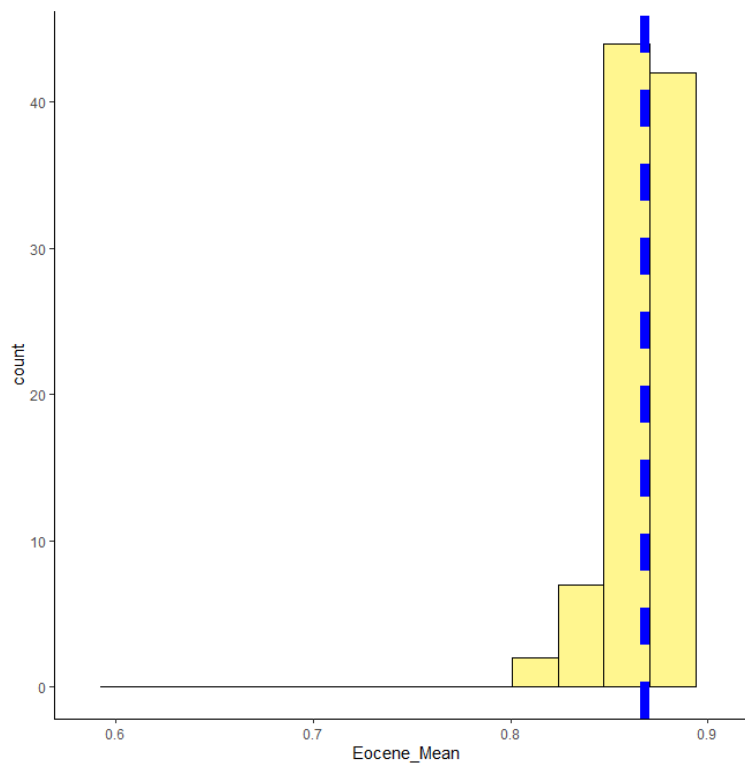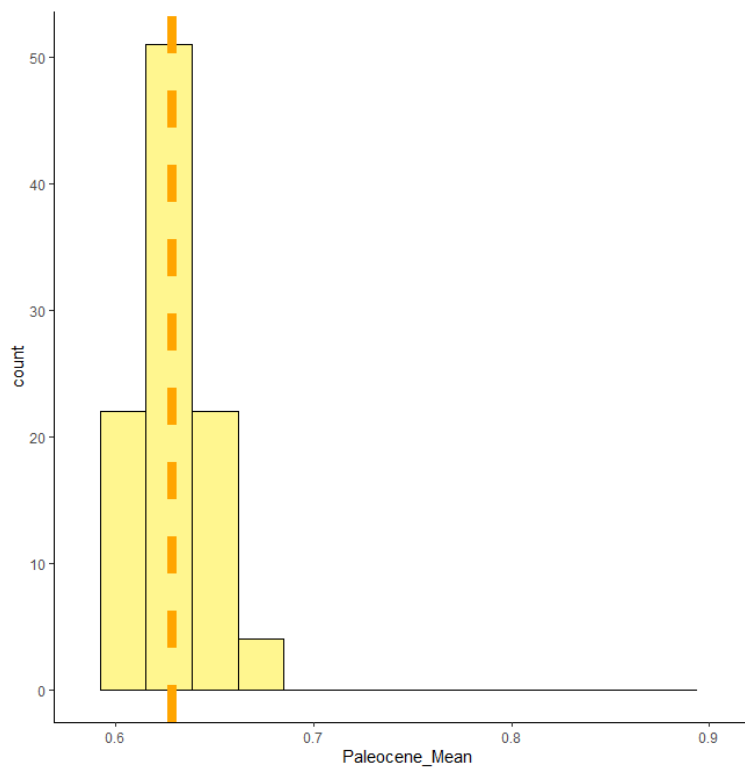
Figure S11. Histograms showing the distributions of mean local scale functional evenness values after sub-sampling with replacement down to 5 paleocommunities in the 10 million years of the Paleocene and the first 10 million years of the Eocene. The Paleocene has the orange bar making the overall mean of the distribution and the Eocene has the blue bar. 5 paleocommunities were chosen because it was the lowest number of paleocommunities found in a North American Land Mammal Age in the Paleocene and Eocene. We ran this sub-sampling routine and ran a t-test to compare the distributions (t = 97.712, df = 197.95, p-value < 2.2e-16*) to determine if the Eocene had higher functional diversity values due to a larger number of paleocommunities. Our results demonstrate that the rise in functional evenness is not due to the increase in the number of paleocommunities, but instead due to an overall higher average of functional evenness.
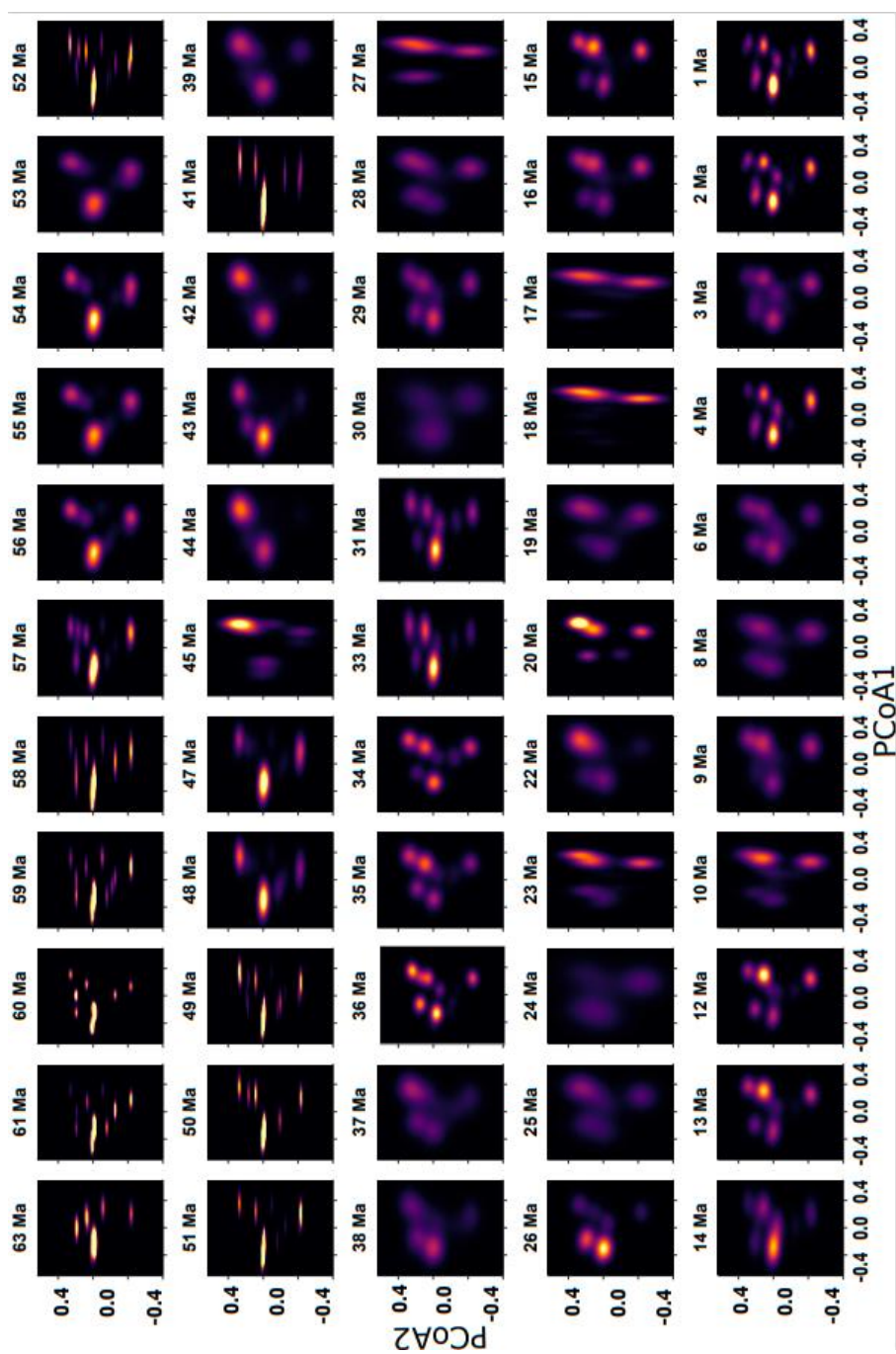
Figure S12. **Trait space density of North American mammals in 1-million-year time bins across the Cenozoic.** Plot elements as in Figure 4.
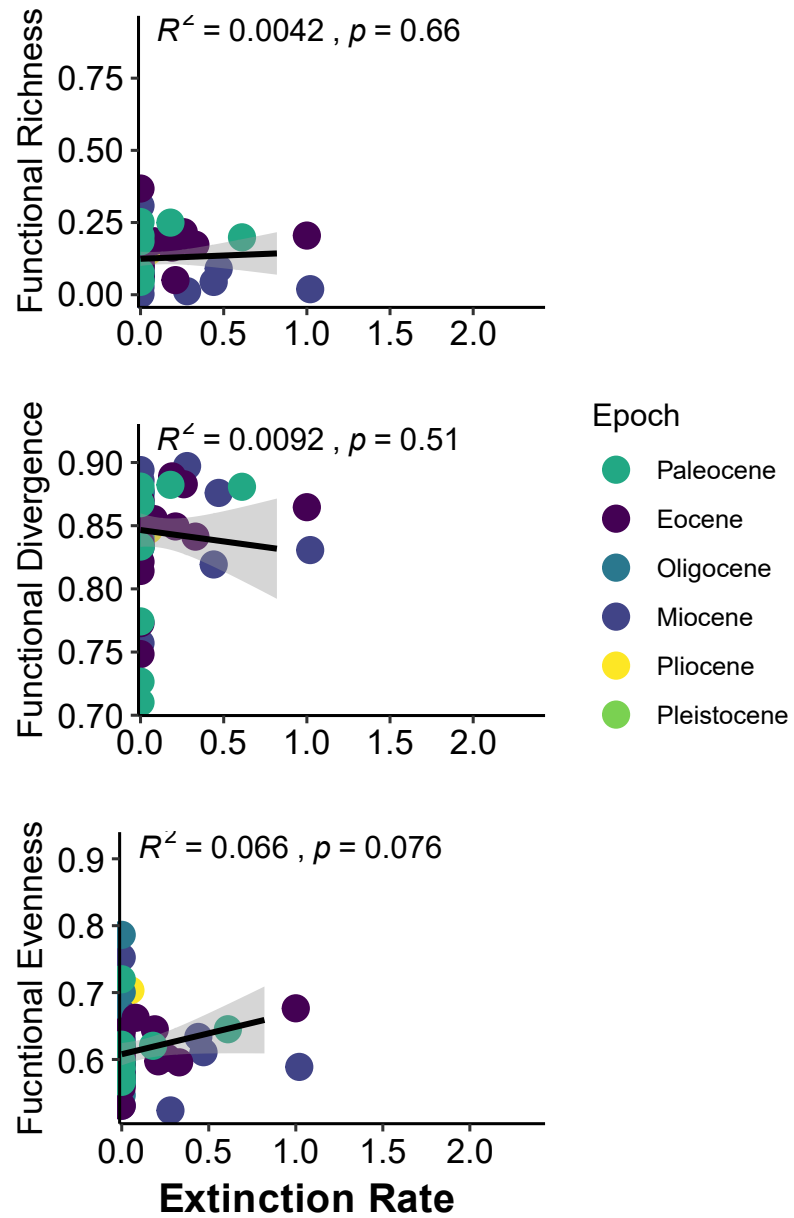
Figure S13. **Regressions of mammal species extinction rates plotted against each local functional diversity index.** The communities are color coded by epoch matching colors in Figure S1.
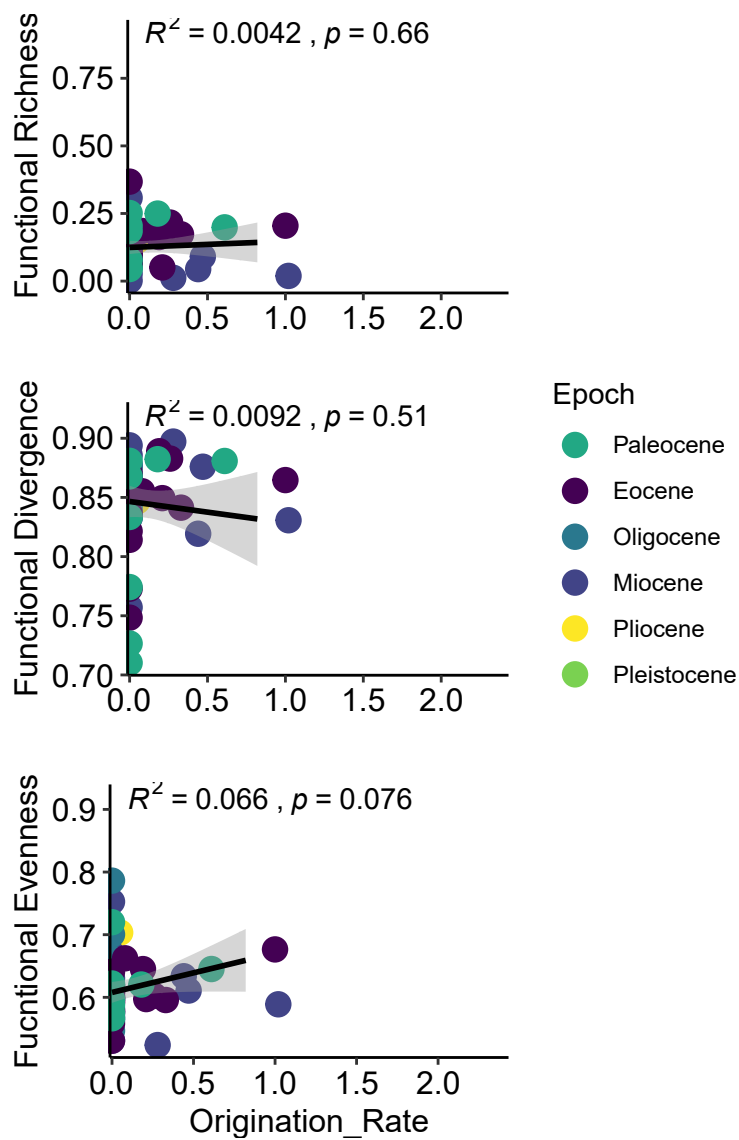
Figure S14. **Regressions of mammal origination rates plotted against each local functional diversity index.** Communities are color coded by epoch matching colors in Figure S1.
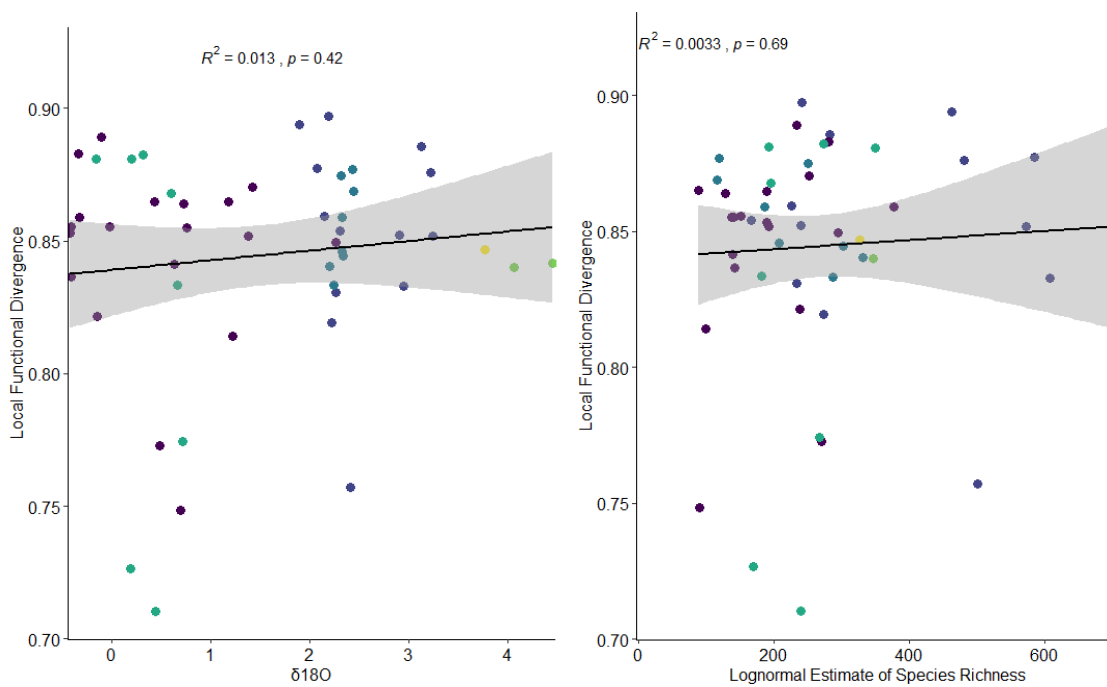
Figure S15. **Generalized linear regression between local functional divergence averaged in 1-million year time bins against the averaged $\delta^{18}O$ values and the lognormal species richness estimate for each time. (See Figure S2).**
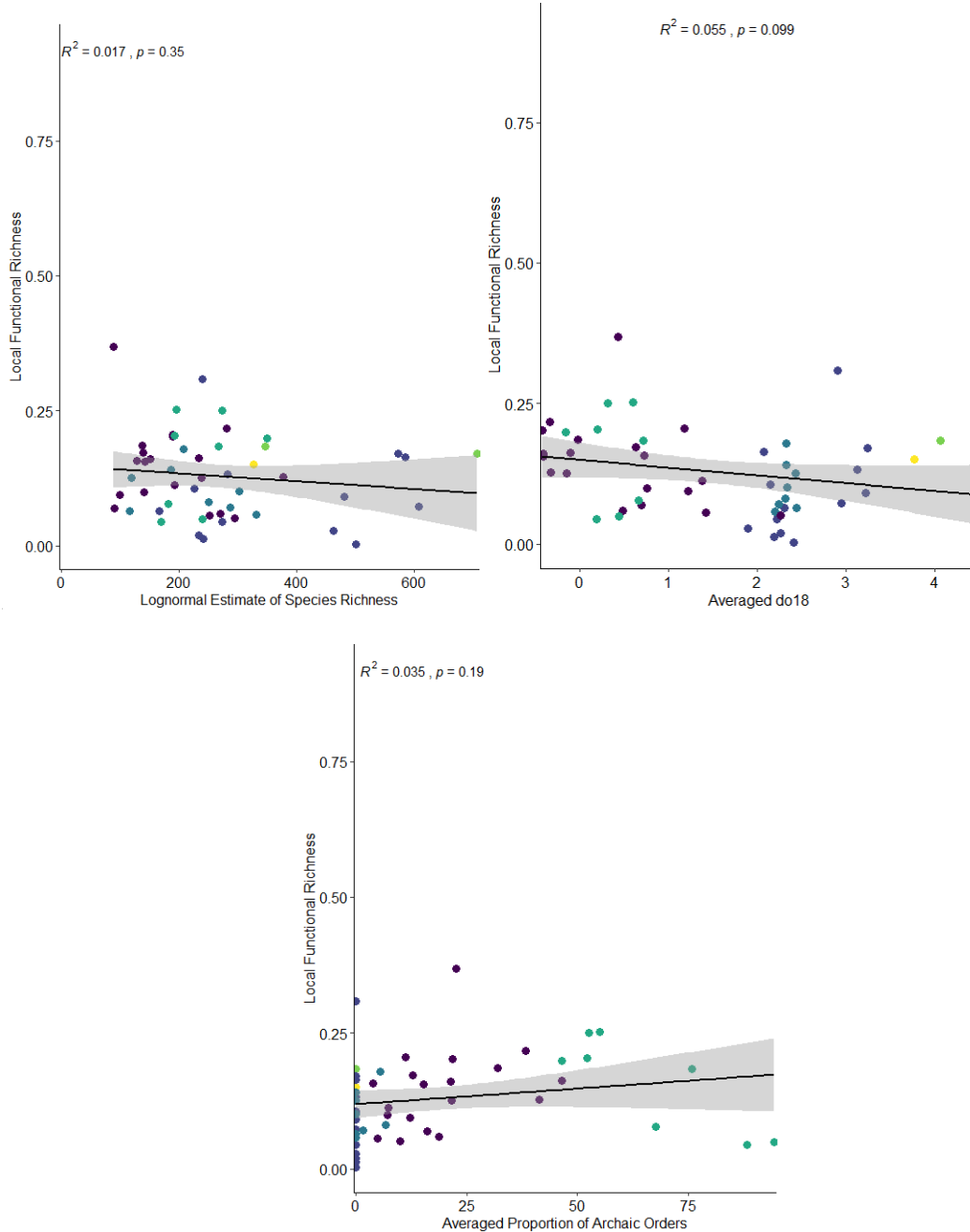
Figure S16. **Generalized linear regression between local functional richness averaged in 1-million year time bins against the averaged δ¹⁸O values, the average proportion of archaic orders in 1-million year time bins and the lognormal species richness estimate for each time. (See Figure S2).**
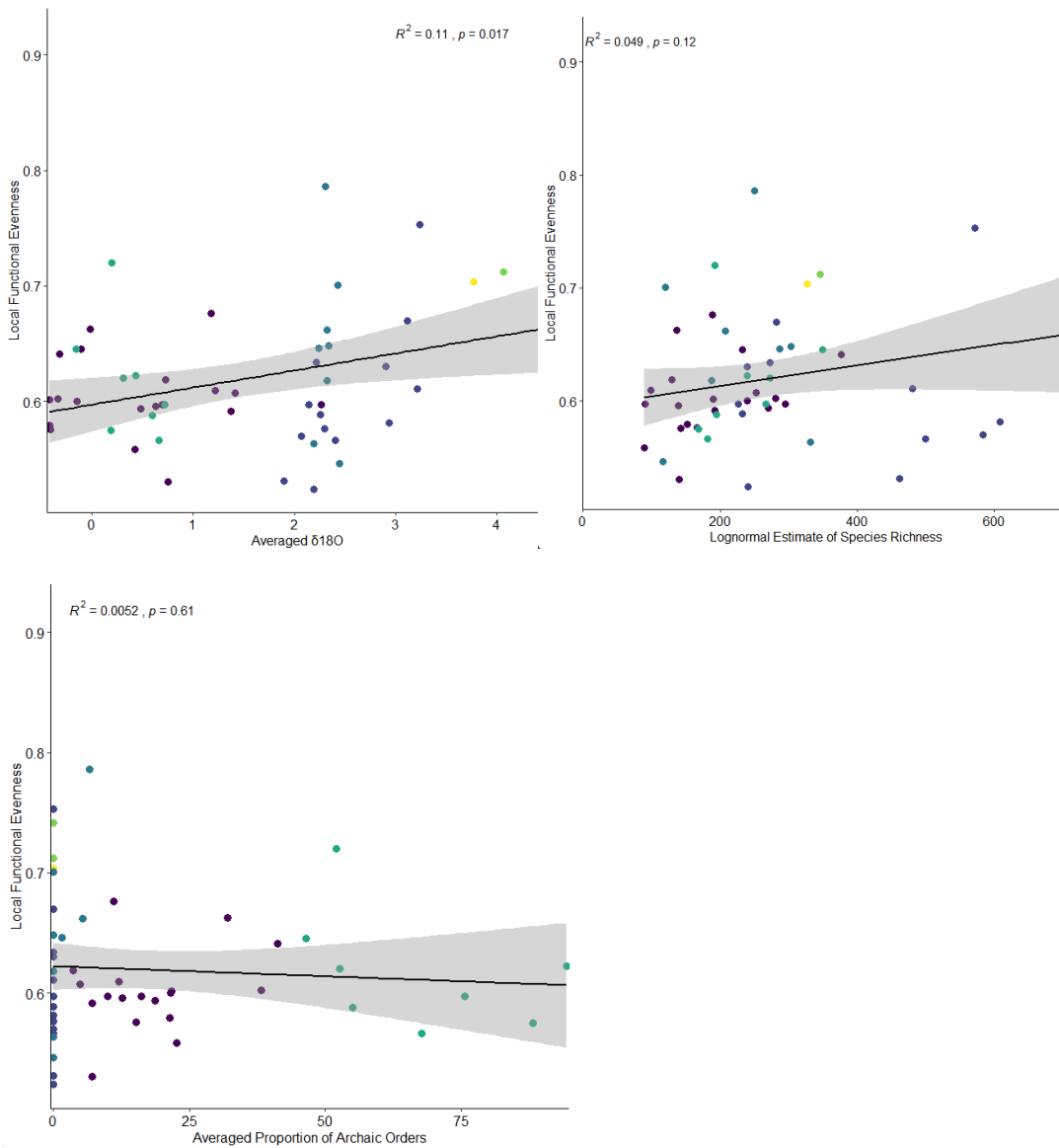
Figure S17. **Generalized linear regression between local functional evenness averaged in 1-million year time bins against the averaged δ¹⁸O values, the average proportion of archaic orders in 1-million year time bins and the lognormal species richness estimate for each time. (See Figure S2).**

Figure S18. **The proportion of extinct orders within each community through time.**

The communities are color coded by epoch matching colors in Figure S2.
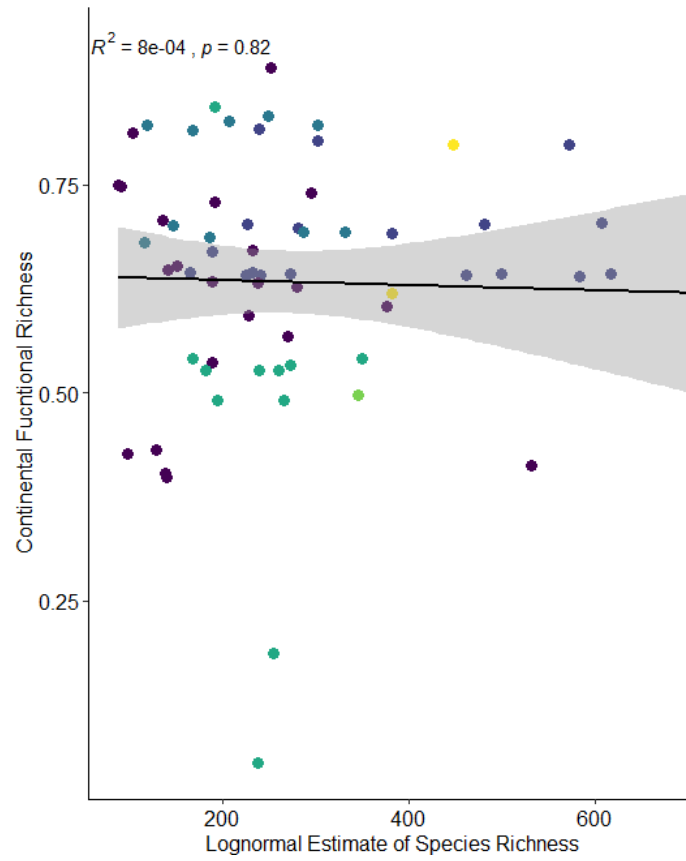
Figure S19. **Generalized linear regression between continental functional richness averaged in 1-million year time bins and the lognormal species richness estimate for each time. (See Figure S2).**
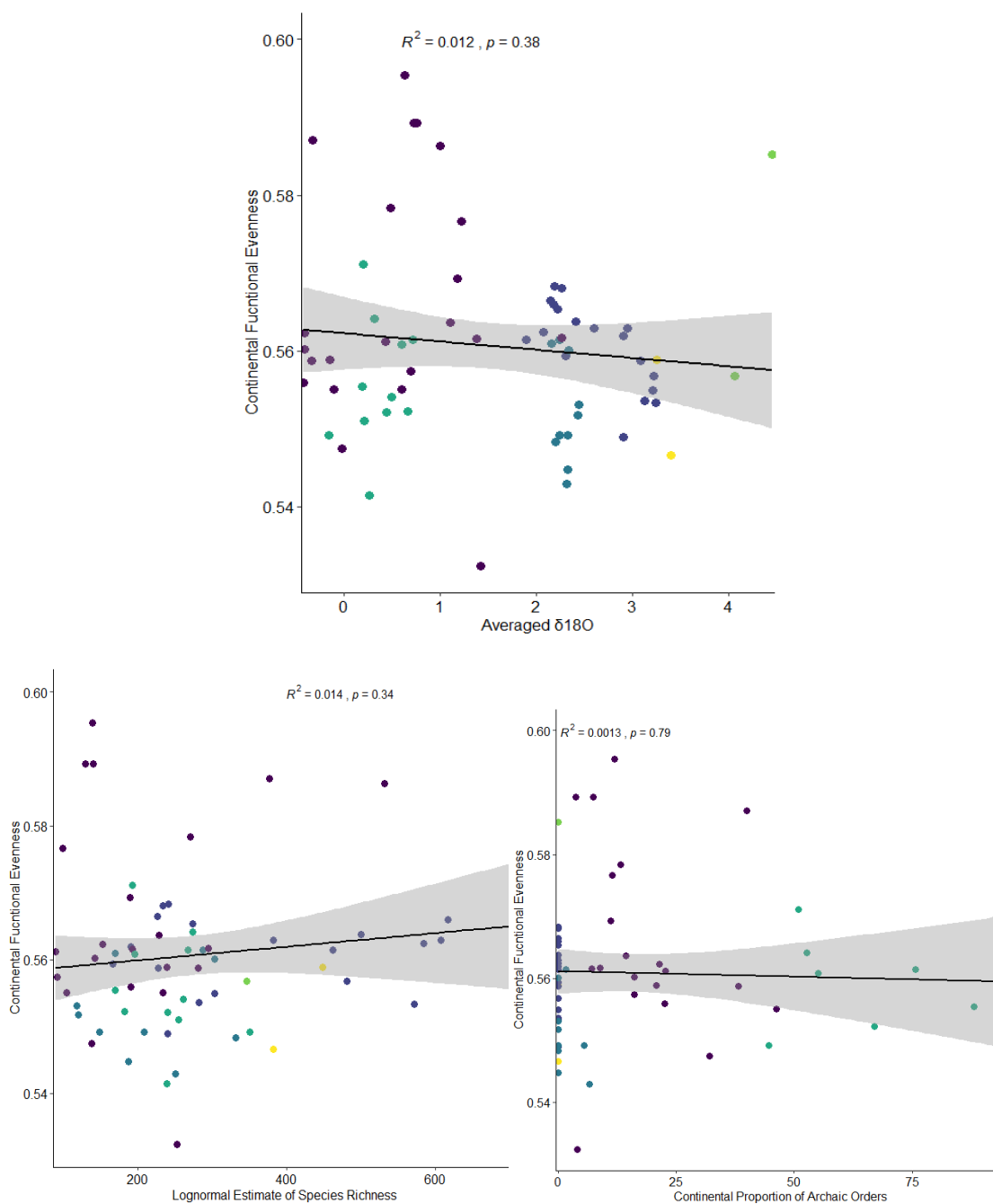
Figure S20. **Generalized linear regression between continental functional evenness averaged in 1-million year time bins against the averaged δ¹⁸O values, the average proportion of archaic orders in 1-million year time bins and the lognormal species richness estimate for each time. (See Figure S2).**

Figure S21. **Regressions of the local and continental proportion of archaic mammals excluding any time bins after archaic orders completely go extinct by 30 Ma.** Local functional divergence and proportion of archaic orders have a slightly stronger relationship when eliminating the last 30 Ma. However, continental functional richness and the continental proportion of archaic orders no longer have a significant relationship, suggesting the relationship is not real.
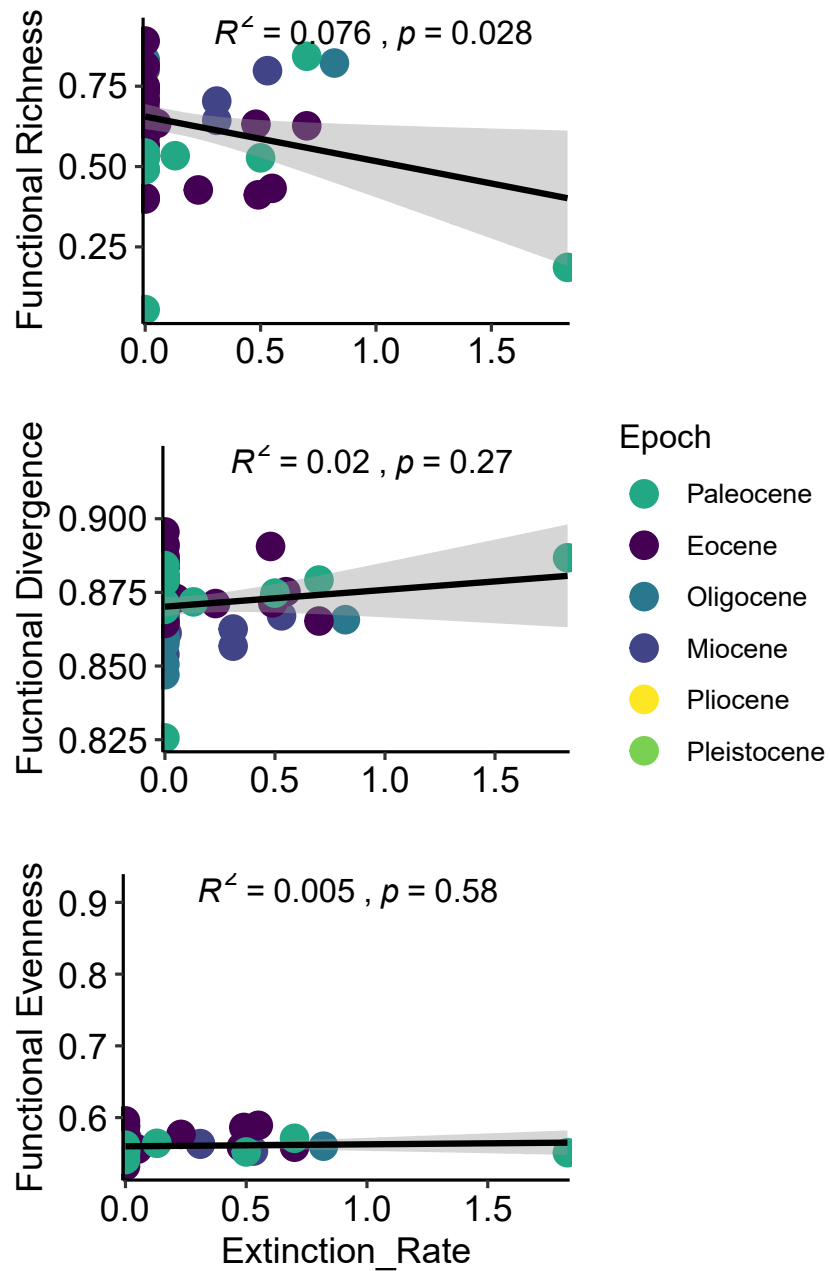
Figure S22. **Regressions of mammal species extinction rates (middle bounds) plotted against each continental functional diversity index.**
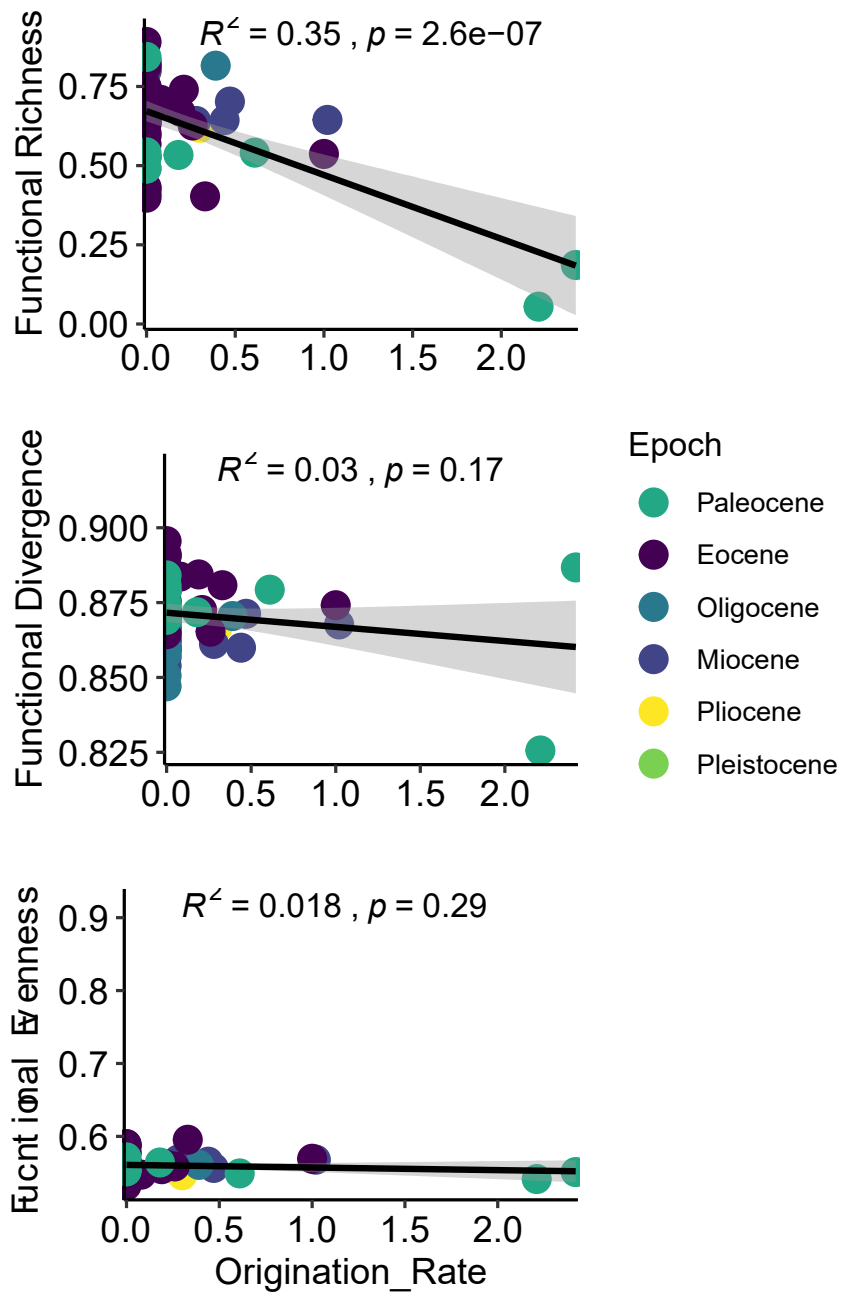
Figure S23. **Regressions of mammal species extinction rates (middle bounds) plotted against each continental functional diversity index.** Although functional richness does have significant relationship with origination rate, it is solely driven by the two earliest Paleocene time bins.

Table S1. **Traits and trait categories used in this study to define each mammal species functionality.**

Diet	Locomotion	Life Habit	Mass
Mixed Feeder	Saltatorial	Arboreal	Log (grams)
Grazer	Plantigrade	Ground-dwelling	
Browser	Graviportal	Amphibious	
Carnivore	Digitigrade	Semifossorial	
Frugivore	Unguligrade	Fossorial	
Insectivore			
Omnivore			

Table S2. **Functional diversity metrics used to analyze Cenozoic mammal communities in our study.**

Indices	Description	Reference
Functional Richness (FRic)	The volume of the minimum convex hull including all species, or the amount of functional space filled by the community in multidimensional trait space.	Villéger et al. (2008)
Functional Evenness (FEve)	The equitability of trait distribution in multidimensional space. High values of FEve indicate that trait values are evenly distributed throughout the trait space; low values indicate an uneven or clumped distribution.	Villéger et al. (2008)
Functional divergence (FDiv)	The trait distribution regarding the mean distance from the multidimensional center of gravity.	Villéger et al. (2008)

Table S3. **List of possible number of breakpoints for estimating paleocommunity FRic breakpoints in package "breakpoint" along with their AICc values. NA is placed in columns where a breakpoint was not found.**

# of Breakpoints	AICc Value	Breakpoint #1	Breakpoint #2	Breakpoint #3	Breakpoint #4
1	-519.8071	19.2 2.976			
2	**-535.1356**	**58.302 1.693**	**20.550 2.634**		
3	-531.2139	58.278 1.333	33.627 5.302	9.990 4.496	
4	-531.122	58.684 1.725	33.726 1.695	29.838 3.338	20.359 3.241

Table S4. List of possible number of breakpoints for estimating paleocommunity FDiv breakpoints in package "breakpoint" with the AICc values.

# of Breakpoints	AICc Value	Breakpoint #1	Breakpoint #2	Breakpoint #3	Breakpoint #4
1	-942.8987	58.509 1.211			
2	-956.9382	57.359 0.744	48.667 2.909		

3	**-960.9602**	**57.287 0.703**	**48.252 1.836**	**7.501 4.507**	
4	-960.7354	57.307 0.689	44.802 2.024	35.535 2.943	7.400 5.801

Table S5. List of possible number of breakpoints for estimating paleocommunity FEve breakpoints in package "breakpoint" with the AICc values.

# of Breakpoints	AICc Value	Breakpoint #1	Breakpoint #2	Breakpoint #3	Breakpoint #4
1	-719.05	12.171 1.378			
2	-712.3829	22.877 1.464	20.552 2.313		
3	-732.4748	56.300 0.864	51.807 1.499	12.042 1.544	
4	**-735.5713**	**56.300±1.191**	**49.883±1.561**	**28.133±3.092**	**16.524±1.680**

Table S6. **List of possible number of breakpoints for estimating North American continental fauna FRic breakpoints in package "breakpoint" with the AICc values.**

Max # of Breakpoints Allowed	AICc Value	Breakpoint #1	Breakpoint #2	Breakpoint #3	Breakpoint #4
1	-85.1777	63.639±0.568			
2	-93.5545	63.725±0.502	5.00±1.774		
3	-83.1767	60.923±2.395	56.722±15.602	4.873±1.834	
4	**-124.5737**	63.996±0.382	45.326±0.652	41.667±0.554	34.999±1.089

Table S7. List of possible number of breakpoints for estimating North American continental fauna FDiv breakpoints in package "breakpoint" with the AICc values.

Max # of Breakpoints Allowed	AICc Value	Breakpoint #1	Breakpoint #2	Breakpoint #3	Breakpoint #4
1	-418.6731	62.969±0.605			

2	- 427.2197	48.923±1.883	26.036±3.081		
3	**-** **430.6329**	61.962±1.175	44.735±2.726	27.951±2.795	

Table S8. List of possible number of breakpoints for estimating North American continental fauna FEve breakpoints in package "breakpoint" with the AICc values.

Max # of Breakpoints Allowed	AICc Value	Breakpoint #1	Breakpoint #2	Breakpoint #3	Breakpoint #4
1	-387.531	43.003±6.131			
2	**-405.1936**	39.652±1.648	35.011±2.083		

Table S9. **AIC values for generalized linear regressions looking at the relationship between biotic and abiotic variables and the functional diversity indices across spatial scales.**

Generalized Linear Model		df	AIC	Species Richness	d018 _p- value	PropArchaic_p- value
Local_Fric	glm(formula = Fric_mean ~ log(Species Richness) + do18 + Proportion of Archaic, family = gaussian, data = MixedModel_Data)	47	-111.23	0.879	0.414	0.726
	glm(Fric_mean~+do18+MixedModel _Data$Local_PropArchaic_Mean, data=MixedModel_Data)	48	-113.2	NA	0.3	0.739
	glm(Fric_mean~MixedModel_Data$L ocal_PropArchaic_Mean, data=MixedModel_Data)	49	-114.05	NA	NA	0.187
	glm(Fric_mean~do18, data=MixedModel_Data)	49	-115.08	NA	0.0989	NA

	glm(Fric_mean~log(Species Richness), data=MixedModel_Data)	4 9	- 113. 12	0.35 5	NA	NA
	glm(Fric_mean~log(Species Richness)+do18, data=MixedModel_Data)	4 8	- 113. 09	0.92 2	0.175	NA
	glm(Fric_mean~log(Species Richness)+MixedModel_Data$Local_ PropArchaic_Mean, data=MixedModel_Data)	4 8	- 112. 5	0.52	NA	0.258
Local_F div	glm(formula = Fric_mean ~ log(Species Richness) + do18 + Proportion of Archaic, family = gaussian, data = MixedModel_Data)	4 7	- 182. 46	0.61 87	0.152 86	0.00256 **
	glm(Fric_mean~+do18+MixedModel _Data$Local_PropArchaic_Mean, data=MixedModel_Data)	4 8	- 184. 19	NA	0.168 56	0.00264 **
	glm(Fric_mean~MixedModel_Data$L ocal_PropArchaic_Mean, data=MixedModel_Data)	4 8	- 184. 15	NA	NA	0.00484 **

	glm(Fric_mean~do18, data=MixedModel_Data)	4	9	-176.48	NA	0.423	NA
	glm(Fric_mean~log(Species Richness), data=MixedModel_Data)	4	9	-175.98	0.69	NA	NA
	glm(Fric_mean~log(Species Richness)+do18, data=MixedModel_Data)	4	8	-174.48	0.988	0.492	NA
	glm(Fric_mean~log(Species Richness)+MixedModel_Data$Local_PropArchaic_Mean, data=MixedModel_Data)	4	8	-182.22	0.80442	NA	0.00558 **
Local_Feve	glm(formula = Fric_mean ~ log(Species Richness) + do18 + Proportion of Archaic, family = gaussian, data = MixedModel_Data)	4	7	-145.17	0.8388	0.0251*	0.1835
	glm(Fric_mean~+do18+MixedModel_Data$Local_PropArchaic_Mean, data=MixedModel_Data)	4	8	-147.13	NA	0.00719**	0.1632

	glm(Fric_mean~MixedModel_Data$Local_PropArchaic_Mean, data=MixedModel_Data)	49	-141.37	NA	NA	0.614
	glm(Fric_mean~do18, data=MixedModel_Data)	49	-147.04	NA	0.0175*	NA
	glm(Fric_mean~log(Species Richness), data=MixedModel_Data)	49	-143.65	0.12	NA	NA
	glm(Fric_mean~log(Species Richness)+do18, data=MixedModel_Data)	48	-145.23	0.672	0.0676	NA
	glm(Fric_mean~log(Species Richness)+MixedModel_Data$Local_PropArchaic_Mean, data=MixedModel_Data)	48	-141.67	0.143	NA	0.875
Continental_Fric	glm(formula = Fric_mean ~ log(Species Richness) + do18 + Proportion of Archaic, family = gaussian, data = MixedModel_Data)	55	-83.008	0.501	0.435	0.136

glm(Fric_mean~+do18+MixedModel_Data$Local_PropArchaic_Mean, data=MixedModel_Data)	5 6	-84.519	NA	0.592	0.11
glm(Fric_mean~MixedModel_Data$Local_PropArchaic_Mean, data=MixedModel_Data)	6 3	-86.214	NA	NA	0.00952 **
glm(Fric_mean~do18, data=MixedModel_Data)	6 3	-62.145	NA	0.008 14 **	NA
glm(Fric_mean~log(Species Richness), data=MixedModel_Data)	6 3	-54.915	0.82 3	NA	NA
glm(Fric_mean~log(Species Richness)+do18, data=MixedModel_Data)	6 2	-63.142	0.09 217	0.001 87**	NA
glm(Fric_mean~log(Species Richness)+MixedModel_Data$Local_PropArchaic_Mean, data=MixedModel_Data)	5 6	-84.349	0.72 179	NA	0.00992 **

Continental_Fdiv	glm(formula = Fric_mean ~ log(Species Richness) + do18 + Proportion of Archaic, family = gaussian, data = MixedModel_Data)	55	-395.75	0.961	5.01E-06	0.714
	glm(Fric_mean~+do18+MixedModel_Data$Local_PropArchaic_Mean, data=MixedModel_Data)	56	-397.75	NA	3.63E-07	0.705
	glm(Fric_mean~MixedModel_Data$Local_PropArchaic_Mean, data=MixedModel_Data)	57	-372.24	NA	NA	0.00044***
	glm(Fric_mean~do18, data=MixedModel_Data)	63	-408.77	NA	7.84e-07***	NA
	glm(Fric_mean~log(Species Richness), data=MixedModel_Data)	63	-389.26	0.0177*	NA	NA
	glm(Fric_mean~log(Species Richness)+do18, data=MixedModel_Data)	62	-406.89	0.734	1.63e-05***	NA

	glm(Fric_mean~log(Species Richness)+MixedModel_Data$Local_PropArchaic_Mean, data=MixedModel_Data)	5	6	-375.2	0.03076*	NA	0.00228**
Continental_Feve	glm(formula = Fric_mean ~ log(Species Richness) + do18 + Proportion of Archaic, family = gaussian, data = MixedModel_Data)	5	5	-353.02	0.1782	0.0209*	0.0961
	glm(Fric_mean~+do18+MixedModel_Data$Local_PropArchaic_Mean, data=MixedModel_Data)	5	6	-353.06	NA	0.0553	0.1353
	glm(Fric_mean~MixedModel_Data$Local_PropArchaic_Mean, data=MixedModel_Data)	5	7	-351.16	NA	NA	0.787
	glm(Fric_mean~do18, data=MixedModel_Data)	6	3	-385.57	NA	0.381	NA
	glm(Fric_mean~log(Species Richness), data=MixedModel_Data)	6	3	-385.71	0.343	NA	NA

	glm(Fric_mean~log(Species Richness)+do18, data=MixedModel_Data)	6 2	- 386. 04	0.12 6	0.137	NA
	glm(Fric_mean~log(Species Richness)+MixedModel_Data$Local_ PropArchaic_Mean, data=MixedModel_Data)	5 6	- 349. 25	NA	0.767	0.852

Table S10. **Best sampling distribution models over time.**

	Invariant				Exponential					Lognormal		
bin	scale	S	lnL	AICc	scale	decay	S	lnL	AICc	scale	mag_var	S
70-69	0.00843	481	-5128.4	10260.72	18.06583	1.013010	911	-1589.1	3182.2	4.240609	5.908207	707
69-68	0.01459	224	-528.3	1060.52	4.05143	1.013304	893	-423.4	850.7	3.187473	3.064796	342
68-67	0.01649	200	-602.6	1209.24	4.64251	1.017579	693	-428.3	860.6	3.132712	3.395724	311
67-66	0.02044	228	-824.3	1652.69	7.05639	1.016566	731	-521.8	1047.6	4.730879	4.253278	382
66-65	0.01938	154	-153.1	310.3	2.55646	1.040000	329	-177.1	358.2	3.028799	3.921114	410
65-64	0.02959	194	-255.9	515.8	15.58000	1.025000	503	-251.0	505.9	5.942870	4.907785	624
64-63	0.04221	119	-187.5	379.06	10.45939	1.029077	439	-169.8	343.7	4.868411	4.474871	340
63-62	0.03137	160	-206.6	417.29	4.41509	1.040000	329	-234.6	473.2	4.962800	2.861239	276
62-61	0.02579	215	-425.0	854.08	6.85285	1.018182	672	-348.4	700.7	5.552593	4.221229	481
61-60	0.02924	89	-168.2	340.42	4.24661	1.036746	355	-134.9	273.8	2.386092	4.357749	227
60-59	0.02222	75	-54.2	112.57	2.33333	1.050000	269	-55.0	114.2	1.640215	3.553514	192
59-58	0.02019	227	-999.1	2002.15	10.21506	1.018621	658	-524.8	1053.7	4.774803	7.233175	608
58-57	0.02512	135	-420.1	844.26	4.65571	1.025667	491	-285.2	574.5	3.380467	4.250188	240
57-56	0.02614	199	-582.5	1169.06	6.53125	1.016626	729	-406.3	816.5	5.461223	4.675386	382
56-55	0.02705	172	-400.1	804.12	4.76080	1.020000	616	-339.0	682.1	4.616655	2.615069	226
55-54	0.01892	255	-657.0	1318.08	6.45531	1.013333	891	-472.2	948.4	4.684934	4.566888	577
54-53	0.01666	177	-284.4	572.8	5.55198	1.020000	616	-259.6	523.2	2.867497	3.493389	359
53-52	0.01978	172	-408.0	819.94	5.39474	1.025000	503	-354.4	712.9	3.346490	2.808079	240
52-51	0.02486	133	-340.0	683.93	5.28907	1.022222	560	-282.2	568.5	3.230523	2.681581	175
51-50	0.01213	185	-51.3	106.69	1.56098	1.066667	208	-90.8	185.8	2.241195	3.268798	500
50-49	0.02526	134	-189.6	383.3	3.92406	1.020645	599	-157.4	318.8	3.230933	5.966273	617
49-48	0.01865	169	-206.6	417.16	3.34884	1.028571	446	-217.9	439.8	3.126389	2.653773	273
48-47	0.01981	88	-42.8	89.78	0.84615	1.100000	145	-70.6	145.4	1.743590	1.000000	88
47-46	0.04513	50	-64.3	132.8	2.46154	1.066667	208	-66.8	137.8	2.256473	1.906244	60
46-45	0.02744	139	-124.7	253.53	6.48837	1.033333	388	-138.6	281.3	3.815086	3.445424	326
45-44	0.04812	61	-75.0	154.12	4.70714	1.048369	277	-69.2	142.5	2.819282	4.610799	192
44-43	0.02849	39	-12.2	29.07	1.83333	1.100000	145	-13.5	31.7	1.111185	1.810320	50
43-42	0.05313	16	-12.9	30.58	1.20000	1.200000	80	-13.6	32.0	0.850891	1.744527	19
42-41	0.03577	118	-303.4	610.86	8.69861	1.030549	420	-218.3	440.6	3.908893	5.021026	303
41-40	0.03679	96	-196.4	396.8	7.39638	1.036660	356	-160.8	325.7	3.430973	4.636984	241
40-39	0.03366	77	-127.6	259.2	6.11187	1.051252	263	-105.7	215.5	2.941189	5.321855	208
39-38	0.03102	89	-163.8	331.7	5.32394	1.050000	269	-152.6	309.2	2.883727	3.741217	169
38-37	0.03455	99	-219.8	443.6	7.78231	1.038198	343	-172.1	348.3	3.323256	5.959695	328
37-36	0.03121	130	-839.0	1681.9	9.02556	1.037395	350	-343.9	691.7	4.105925	7.704479	295
36-35	0.05531	81	-90.3	184.7	7.25143	1.036193	360	-83.7	171.5	4.286017	4.317142	252
35-34	0.05529	133	-300.8	605.7	13.89989	1.024881	506	-260.5	524.9	7.401848	2.921263	192
34-33	0.03098	171	-223.4	450.9	5.05263	1.028571	446	-246.7	497.4	5.275452	2.172826	228
33-32	0.05600	141	-167.2	338.5	5.37931	1.040000	329	-200.0	404.0	7.862221	2.024251	182
32-31	0.05195	77	-79.7	163.6	5.57143	1.040000	329	-89.1	182.4	4.009999	1.763759	92
31-30	0.04070	109	-164.0	332.0	5.03984	1.027772	458	-128.9	261.8	4.146444	6.150879	532
30-29	0.06061	77	-147.3	298.6	4.83789	1.037188	351	-123.4	250.8	4.491167	3.150006	129

CHAPTER 2

TAXONOMIC AND FUNCTIONAL BETA DIVERSITY OF CENOZOIC NORTH AMERICAN MAMMALS

Abstract

Taxonomic beta diversity has been widely used to examine the spatial structure of mammalian communities. More recently, functional beta diversity, a taxon-free approach that uses traits as the unit of measure, has been used to more directly evaluate changes in ecosystem function. Ecologists studying extant taxa find that the relationship between taxonomic and functional beta diversity can differ by habitat and spatial scale. Furthermore, ecological mechanisms driving spatial structure are not well understood. The North American fossil record of mammals over the last 66 million years encompasses various major environmental and ecological events making it an ideal system to evaluate beta diversity of mammals on a geologic timescale. We compiled 264 mammal paleocommunities spanning the Cenozoic. Each mammalian genus was given four functional traits to evaluate functional trait distributions: locomotion, body mass, life habit and diet. The two dimensions of beta diversity were calculated in 5-million years sliding window bins to avoid autocorrelation. We find that the dimensions of beta diversity are strongly correlated across the Cenozoic. Both dimensions peak during the initial opening of the forests and grassland expansion, likely an result of increased habitat heterogeneity. We highlight the importance of using taxonomic and functional approaches to better understand the underlying processes. Furthermore, we demonstrate

the importance of examining diversity patterns on long time scales and across various types of disturbances to examine the differing effects on mammalian dynamics.

Introduction

Temporal changes in mammalian diversity can vary with spatial scale, potentially reflecting different drivers and mechanisms (1). Diversity is often divided into three categories that reflect the spatial scale at which they are measured: alpha, beta and gamma (1-5). Alpha diversity addresses the composition of a single locality or community. It provides information on resource distribution within a community and how mammals are dividing niches (1–3). Beta diversity is the measure of compositional change across space, such as across environmental gradients, reflecting habitat utilization on the landscape (1–3). Gamma represents the "landscape diversity" and is the result of alpha and beta patterns (1, 4, 5). Therefore, by evaluating all three scales of diversity through time we can better understand ecological dynamics that lead to large-scale changes in mammalian faunas.

Traditionally, diversity at different spatial scales was explored primarily using taxonomic composition because it can be easily measured and quantified (1, 5, 6). However, taxonomic identities change, and the definition of a species, as well as higher taxonomic levels, is highly variable (7). Functional diversity (FD) is an approach that uses traits to define the ecological role of an organism (6, 8). Moreover, it offers a quantifiable approach to assess changes in ecosystem functioning by identifying changes in trait space (8–10) including the increase, decrease, or a shift in occupied trait space. Significant changes in trait space can suggest a change in ecosystem services provided by

the biological community, leading to a cascade effect. Shupinski et al. (10) used functional diversity to evaluate alpha and gamma of North American mammal paleocommunities across the last 66 Ma. They found that shifts in functional diversity were frequent and primarily disassociated between continental and local scales. Most of the continental shifts in functional diversity occurred during the middle of the Cenozoic while local functional diversity occurred throughout the Cenozoic, overlapping with major ecological and environmental events. Most profoundly, they found a synchronous rise in trait space during the early Cenozoic radiation of mammals on both spatial scales (11). Here, we continue the exploration of mammalian ecological dynamics over the last 66 Ma by quantifying changes in beta diversity using a taxonomic and functional approach.

Traditionally, beta diversity has been quantified using species richness and used to compare similarities in taxonomic composition among communities (12). However, a focus on similarities in traits as well as taxa allows for a more direct examination of habitat specialization and utilization, as well as the potential processes driving turnover across space (12, 13). For example, communities can have different taxonomic compositions but share similar ecological roles (12). Analyses of beta diversity from a taxonomic and functional perspective have provided a deeper understanding of the underlying mechanisms driving changes in species distributions by examining variation in the relationship between beta diversity dimensions (12, 14). Indeed, the relationship between taxonomic and functional beta diversity varies by spatial scale, organismal group and geographic region (12, 13, 15, 16). For example, a global analysis of phylogenetic,

taxonomic and functional mammal beta diversity found variation between beta diversity dimensions depending on the region (15). Tropical forests had high taxonomic beta diversity but low trait diversity, likely a result of greater niche packing and trait redundancy (15). In contrast, temperate biomes had low taxonomic and trait beta diversity attributed to greater range size of these mammals (15). Other variables such as biogeographical history and past climatic events can also affect beta diversity patterns (15, 17). For example, climatic cycling during the Pleistocene led to greater overlap in North American mammal ranges (17). However, these broad-scale studies addressing the relationship between taxonomic and functional beta diversity are primarily based on modern data using already anthropogenically altered communities (12, 13, 15, 16). As such, it is difficult to determine how much of the variation across space is a product of human impacts.

Modern diversity patterns have been drastically altered by humans, diminishing our ability to infer environmental and ecological drivers of mammal dynamics (18). Moreover, anthropogenic activities have variable effects and differ in intensity by region, further hampering out ability to infer community assembly processes (15). We therefore advocate an approach that uses data from the fossil record that predates human impacts. Although previous studies have evaluated mammal beta diversity in the fossil record, they concentrated on specific periods (e.g. Eocene, Miocene, Pleistocene) (17, 19–21). Furthermore, the variation in the temporal and spatial scales of these different studies makes broader inferences through comparison difficult. Moreover, because of the variation in scale, any approach used to control for distance-decay relationships in beta

diversity cannot be standardized among studies. Here, the geographic and temporal extent of the data allows us to use consistent time bins and geographic constraints to examine North American mammalian beta diversity across Cenozoic climatic, environmental, and ecological events.

Throughout the Cenozoic, North America experienced a cooling trend that led to a transition from widespread sub-tropical forests to savannahs (22). There was a gradual reduction in forests that began during the Eocene with the eventual development of grassland habitats by the Oligocene epoch (23). Grasslands were widespread by the early Miocene. By the late Miocene, grasslands were the dominant habitat in North America (23). This climatic transition across the Cenozoic also involved several biotic interchanges, diversification events and extinctions (22, 24–27). These changes resulted in the modification of the mammalian fauna present in North America, providing a unique opportunity to explore the impacts on taxonomic and functional beta diversity, as well as the relationship between the spatial distributions of taxa and traits (10, 20–22, 28).

Here, we examine broad, evolutionary changes in beta diversity of North American mammals across the Cenozoic. We examine spatial distributions of taxa and traits, allowing us to assess the relationship between taxonomic and functional beta diversity through time. By observing changes across the Cenozoic, we address how associated ecological, environmental, and climatic events affect beta diversity. This provides a baseline for how mammals filter into communities from the regional pool prior to human influence.

Methods

Data

We compiled 264 North American paleocommunities from published databases (Alroy 1998, Smith et al. 2018, Paleobiology Database; paleobiodb.org/) that included 2,462 mammal species (Datafile1: Mammal_Traits_Localities, fig. S1). The most updated taxonomic name for each species was collected from the Paleobiology Database. The estimated date ranges for each paleocommunity based on geologic location were refined when possible, using primary literature (Datafile1: Locality Dating, fig. S1). The refining of locality dates resulted in an average age range of 1.539 million years. Each genus in our database has an average body mass, locomotion, life habit and diet (Table S1). To buffer preservation biases in the fossil record and allow for the best representation of the paleocommunities, we required a minimum of 15 species and the presence of multiple trophic levels. Only terrestrial communities were included in our study but the order Chiroptera was excluded.

Analyses

We calculated taxonomic and functional beta diversity at the genus-level due to the temporal extent of our time bins. To run the FD analysis, each genus required a single set of traits. Genus-level traits were averaged from the species in the database. Body mass was averaged across species within each genus. Categorical traits were based on the most common category found among the species of that genus. For example, if the majority of Equus species were listed as grazers while some species were mixed feeders, the genus was identified as a grazer. However, with the exception of genera whose species varied

between differing types of herbivory (e.g. mixed feeder, browser, grazer), the large majority of traits were highly conserved and consistent within each genus. With these traits we used the R package "FD" to calculate functional diversity and get PCoA coordinates for each genus (7). A species-trait matrix with rows as the genus and the columns as traits was converted into a distance matrix using Gower's dissimilarity method. The 'dbFD' function ran the distance matrix through a Principal Coordinates Analysis (PCoA) to ordinate each genus in multidimensional trait space using PCoA axes (9). The coordinates of the genera were then used to calculate functional beta diversity.

Taxonomic and functional beta diversity were calculated using the r package "betapart" (27). The betapart package uses the genus coordinates provided by the "FD" package during the calculation of functional diversity to form the convex hull for each paleocommunity. Pairs of paleocommunities were then plotted together in multidimensional space and the volume of overlap was calculated to determine the dissimilarity in trait composition. Taxonomic beta diversity quantifies the number of matching genera between pairs of paleocommunities to determine the level of dissimilarity. All values were standardized between 0 and 1. 1 represents the highest level of dissimilarity and a value of 0 represents the most similar.

The functional and taxonomic dissimilarity scores across all paleocommunity pairs were averaged in 5-million-year window bins. The bins shift by one million years (65-60 Ma, 64-59 Ma, 63-58 Ma, etc.) resulting in a total of 61 window bins to avoid an autocorrelation bias. We avoided issues with the well-documented distance-decay relationship in beta diversity (as the distance between two sites increases, the

dissimilarity correspondingly increases) (28), by finding the smallest-maximum geographic distance of the window bins. We then restricted all pairs of paleocommunities to those with a geographic distance equal to or less than that distance (1,117,679 m).

Results

Functional Beta Diversity

Total functional beta diversity of North American mammal paleocommunities fluctuates across the Cenozoic with three major peaks (Fig. 1). The first peak occurs in the Paleocene, the earliest part of the Cenozoic. However, it quickly declines and remains low until the early to middle Eocene around 50 Ma followed by higher and fluctuating values until ~35 Ma. Values then decline until ~24 Ma before reaching the largest peak. The peak around the 20-million-year time bin leads to a sharp decline into the latest Cenozoic. We addressed possible biases in our data by examining the relationship of functional beta diversity between the number of paleocommunities within a time bin, the average geographic distance between paleocommunity pairs and the average age difference between paleocommunity pairs. There is a significant relationship between average functional beta diversity and the number of paleocommunities within a time bin (fig. S1; $R^2 = 0.27$, p = <0.01) and the average geographic distance of paleocommunity pairs within a time bin (fig. S4; $R^2 = 0.18$, p = <0.01). However, we were able to determine that these relationships are not driving our results (fig. S2, S3, S7, S8). There was no significant relationship between the average age difference between paleocommunity pairs (fig. S9; $R^2 = 0.025$, p = 0.23).

Nestedness and Turnover of Functional Beta Diversity

Functional nestedness is the highest contributor to total functional beta diversity for most of the Cenozoic (Fig. 1). There are only three points where turnover is a greater contributor to total functional beta diversity than nestedness. Turnover is higher than nestedness during the Paleocene at ~43 Ma and during the early Miocene at ~22 Ma (Fig.1). Nestedness peaks at four different times during the Cenozoic. Nestedness is highest around 50 Ma and between 40-35 Ma. The final peak is smaller but prominent between 27 Ma and 24 Ma time bins (Fig. 1).

Taxonomic Beta Diversity

Total taxonomic beta diversity has consistently higher values than functional beta diversity across the Cenozoic but less temporal variation (Fig. 1). Taxonomic beta diversity is higher during two periods from approximately 50-40-million-year time bins, and the second period occurs between 28-20-million-year time bins. Taxonomic beta diversity is initially low Paleocene but increases and fluctuates, reaching the first peak around the 50-million-year time bin. It remains higher until about 40 Ma before declining. However, by 34 Ma it begins to increase again, reaching the second peak that lasts from the 29 – 24-million-year time bins. From there, it gradually rises into the second peak and keeps consistently higher values until ~20 Ma. Afterward taxonomic beta diversity drops and remains lower for the rest of the Cenozoic.

We addressed possible biases in our data by examining the relationship of taxonomic beta diversity between the number of paleocommunities within a time bin, the average geographic distance between paleocommunity pairs and the average age difference between paleocommunity pairs. We found that there was a significant

relationship between taxonomic beta diversity and the number of paleocommunity pairs within a time bin (fig. S1; $R^2 = 0.26$, p = <0.01), the average geographic distance between paleocommunity pairs within a time bin (fig. S4; $R^2 = 0.23$, p = <0.01) and the average age difference between paleocommunity pairs within a time bin (fig. S9; $R^2 = 0.13$, p = <0.01). However, we were able to determine that these relationships are not driving our results (fig. S2, S3, S5, S6, S10, S11).

Turnover and Nestedness of Taxonomic Beta Diversity

Turnover heavily drives total taxonomic beta diversity across the Cenozoic (Fig. 1). Taxonomic turnover reflects the same fluctuations demonstrated by total taxonomic beta diversity. Nestedness remains close to zero for the entirety of the Cenozoic. Interestingly, we find that nestedness is lowest during the periods of highest taxonomic beta diversity increases in the middle Eocene and late Oligocene to early Miocene (Fig. 1).

Taxonomic and Functional Beta Diversity Relationship

Average functional and taxonomic beta diversity are significantly correlated across the Cenozoic (Fig. 4; r = 0.6, p =<0.01), and have heightened levels during similar intervals. Taxonomic and functional beta diversity have sustained peaks in the middle Eocene to early Oligocene. They both reach the highest levels in the early Miocene (Fig. 1).

We also analyzed the relationship between taxonomic and functional beta diversity within each time bin (Fig. 4). We find that taxonomic and functional beta diversity are strongly correlated across the Cenozoic except during initial rises in

functional beta diversity. In particular, taxonomic and functional beta diversity become decoupled during periods of increasing functional nestedness (Fig. 4).

Discussion

Functional and taxonomic beta diversity of North American mammal paleocommunities fluctuates throughout the Cenozoic, driven be different components of beta diversity (Fig. 1). Taxonomic beta diversity is almost solely influenced by turnover in genera through time with little influence from low nestedness. However, nestedness is the greatest contributor to functional beta diversity overall, but there are periods during the Cenozoic when turnover is greater than nestedness. Functional beta diversity has more temporal variation than taxonomic beta diversity but taxonomic and functional dissimilarity across space reach the highest levels during the same time periods (Fig. 1).

Disassociation in the Earliest Cenozoic

Earliest Cenozoic paleocommunities exhibit high dissimilarities in functional trait composition. The greatest dissimilarity is primarily driven by higher nestedness and lower turnover. This suggests that paleocommunities shared a core set of ecological roles. These roles were likely fulfilled by a consistent set of mammalian genera as well, reflected by the greater similarity in taxa across space due to low turnover. Although nestedness has limited influence on taxonomic beta diversity, it does reach its highest point at the 65- and 64-million-year time bins (65-59 Ma). This further supports the hypothesis that paleocommunities had a similar set of ecological roles being filled by the analogous taxa. Two likely explanations for our findings; 1) The landscape was relatively homogenous due to the flat temperature gradient at this time allowing for widespread

sub-tropical habitats (29), and 2) these time bins reflect paleocommunities of the early to middle Paleocene epoch, which took place soon after the extinction of the non-avian dinosaurs (~66 Ma) (30, 31). Although mammals radiated rapidly during this epoch, mammal diversity remained relatively low until around 60 Ma (30).

Middle Eocene Rise in Beta Diversity

North American paleocommunities become less similar and sustain higher taxonomic and functional dissimilarity throughout much of the middle to late Eocene (Fig. 1). This interval corresponds with a rapid increase in mammal species richness (23, 33). Furthermore, the climate becomes more arid and cooler with greater seasonality (23). Taxonomic beta diversity maintains higher levels between the 49-41 Ma time bins (~49–36 Ma). The rise in taxonomic dissimilarity coincides with an increase in mammal species richness that occurred during the cooling and drying of the climate (23, 33, 35). there is a rise in the dissimilarity of functional traits as well (~43-28 Ma). Higher functional beta diversity is likely attributed to the opening of forests in the late Eocene marking the first evidence of grasses (24, 36) and development of the first grasslands in the early Oligocene (25, 37, 38). At this time there is an increase in in cursoriality (24), likely due to the opening of forests. The gradual transition to a more open landscape in North America led to greater habitat heterogeneity, and in turn, greater spatial variation in mammal ecological roles.

Greatest Beta Diversity of the Cenozoic – The Early to Middle Miocene

Functional and taxonomic beta diversity both reach their peaks between the 21 and 18-million-year time bins, covering 21 Ma to 14 Ma (Fig. 1). During this interval, the

expansion of grasslands facilitated various changes to the North American mammal fauna (21, 34). There is a diversification of open-landscape mammals with the spread of the new habitat, particularly in grazing ungulates, such as horses (21). They rapidly diversified until approximately 16-14 Ma before species richness began to decline again (21). There is also a rise in the taxonomic diversity of carnivores (24). Additionally, true felids and proboscideans arrive in North America at this time (36). The sharp decline in beta diversity following this period may be a result of the middle Miocene Climate Transition (~14 Ma), which was another shift to a cooler climate (32). Thereafter, savanna's dominated North America, homogenizing the landscape (21).

Conclusion

Taxonomic and functional beta diversity are strongly associated across evolutionary timescales. The intervals with the greatest spatial dissimilarity of mammal traits and taxa occur during the middle to late Eocene and early Miocene. During these intervals habitat heterogeneity is increasing due to changes in climate. In future research it will be important to further investigate the changes we find in taxonomic and functional beta diversity to determine if specific geographic regions, clades, or functional groups are influencing these temporal fluctuations. However, the aim of this study is to evaluate overlying patterns of beta diversity across evolutionary timescales and the relationship between taxa and traits. This macroecological approach can improve our understanding of mammal spatial distributions by comparing intervals of heightened beta diversity, allowing us to better infer associated ecological, environmental, or climatic events.

References

1. J. J. Sepkoski, Alpha, beta, or gamma: where does all the diversity go? Paleobiology **14**, 221–234 (1988).

2. R. H. Whittaker, Evolution and Measurement of Species Diversity. TAXON **21**, 213–251 (1972).

3. R. H. Whittaker, Vegetation of the Siskiyou Mountains, Oregon and California. Ecological Monographs **30**, 279–338 (1960).

4. W. Rh, Evolution of species diversity in land communities. Evolutionary biology **10**, 1–67 (1977).

5. L. Arellano, G. Halffter, Gamma diversity: derived from and a determinant of Alpha diversity and Beta diversity. An analysis of three tropical landscapes. Acta zoológica mexicana, 27–76 (2003).

6. J. Zak, M. Willig, D. Moorhead, H. Wildman, Zak JC, Willig MR, Moorhead DL, Wildman HG.. Functional diversity of microbial communities: a quantitative approach. Soil Biol Biochem 26: 1101-1108. Soil Biology and Biochemistry **26**, 1101–1108 (1994).

7. E. Laliberté, P. Legendre, A distance-based framework for measuring functional diversity from multiple traits. Ecology **91**, 299–305 (2010).

8. E. Laliberté, P. Legendre, B. Shipley, FD: Measuring functional diversity from multiple traits, and other tools for functional ecology. R package version **1**, 0–12 (2014).

9. S. Villéger, N. W. H. Mason, D. Mouillot, New Multidimensional Functional Diversity Indices for a Multifaceted Framework in Functional Ecology. Ecology **89**, 2290–2301 (2008).

10. S. Villéger, J. R. Miranda, D. F. Hernandez, D. Mouillot, Low Functional β-Diversity Despite High Taxonomic β-Diversity among Tropical Estuarine Fish Communities. PLoS ONE **7**, e40679 (2012).

11. A. Siefert, C. Ravenscroft, M. D. Weiser, N. G. Swenson, Functional beta-diversity patterns reveal deterministic community assembly processes in eastern North American trees. Global Ecology and Biogeography **22**, 682–691 (2013).

12. I. S. Martins, J. C. G. Ortega, V. Guerra, M. M. S. Costa, F. Martello, F. A. Schmidt, Ant taxonomic and functional beta-diversity respond differently to changes in forest cover and spatial distance. Basic and Applied Ecology **60**, 89–102 (2022).

13. C. Penone, B. G. Weinstein, C. H. Graham, T. M. Brooks, C. Rondinini, S. B. Hedges, A. D. Davidson, G. C. Costa, Global mammal beta diversity shows parallel assemblage structure in similar but isolated environments. Proceedings of the Royal Society B: Biological Sciences **283**, 20161028 (2016).

14. A. S. Melo, T. F. L. V. B. Rangel, J. A. F. Diniz-Filho, Environmental drivers of beta-diversity patterns in New-World birds and mammals. Ecography **32**, 226–236 (2009).

15. E. B. Davis, Mammalian beta diversity in the Great Basin, western USA: palaeontological data suggest deep origin of modern macroecological structure: Deep origin of beta diversity in the Great Basin. Global Ecology and Biogeography **14**, 479–490 (2005).

16. S. Faurby, J.-C. Svenning, Historic and prehistoric human-driven extinctions have reshaped global mammal diversity patterns. Diversity and Distributions **21**, 1155–1166 (2015).

17. S. K. Lyons, A Quantitative Model for Assessing Community Dynamics of Pleistocene Mammals. The American Naturalist **165**, E168–E185 (2005).

18. D. Fraser, S. K. Lyons, Mammal Community Structure through the Paleocene-Eocene Thermal Maximum. The American Naturalist **196**, 271–290 (2020).

19. W. C. Clyde, P. D. Gingerich, Mammalian community response to the latest Paleocene thermal maximum: An isotaphonomic study in the northern Bighorn Basin, Wyoming. Geol **26**, 1011 (1998).

20. B. Figueirido, C. Janis, J. Pérez-Claros, M. De Renzi, P. Palmqvist, Cenozoic climate change influences mammalian evolutionary dynamics. Proceedings of the National Academy of Sciences of the United States of America **109**, 722–7 (2011).

21. C. M. Janis, J. Damuth, J. M. Theodor, The origins and evolution of the North American grassland biome: the story from the hoofed mammals. Palaeogeography, Palaeoclimatology, Palaeoecology **177**, 183 (2002).

22. M. O. Woodburne, G. F. Gunnell, R. K. Stucky, Climate directly influences Eocene mammal faunal dynamics in North America. PNAS **106**, 13399–13403 (2009).

23. C. D. Bacon, P. Molnar, A. Antonelli, A. J. Crawford, C. Montes, M. C. Vallejo-Pareja, Quaternary glaciation and the Great American Biotic Interchange. Geology **44**, 375–378 (2016).

24. G. D. Wesley-Hunt, The morphological diversification of carnivores in North America. Paleobiology **31**, 35–55 (2005).

25. C. A. E. Strömberg, Decoupled taxonomic radiation and ecological expansion of open-habitat grasses in the Cenozoic of North America. Proceedings of the National Academy of Sciences **102**, 11980–11984 (2005).

26. S. A. F. Darroch, A. E. Webb, N. Longrich, J. Belmaker, Palaeocene–Eocene evolution of beta diversity among ungulate mammals in North America. Global Ecology and Biogeography **23**, 757–768 (2014).

27. betapart: an R package for the study of beta diversity - Baselga - 2012 - Methods in Ecology and Evolution - Wiley Online Library. https://besjournals-onlinelibrary-wiley-com.libproxy.unl.edu/doi/full/10.1111/j.2041-210X.2012.00224.x.

28. C. Graco-Roza, S. Aarnio, N. Abrego, A. T. R. Acosta, J. Alahuhta, J. Altman, C. Angiolini, J. Aroviita, F. Attorre, L. Baastrup-Spohr, J. J. Barrera-Alba, J. Belmaker, I. Biurrun, G. Bonari, H. Bruelheide, S. Burrascano, M. Carboni, P. Cardoso, J. C. Carvalho, G. Castaldelli, M. Christensen, G. Correa, I. Dembicz, J. Dengler, J. Dolezal, P. Domingos, T. Erös, C. E. L. Ferreira, G. Filibeck, S. R. Floeter, A. M. Friedlander, J. Gammal, A. Gavioli, M. M. Gossner, I. Granot, R. Guarino, C. Gustafsson, B. Hayden, S. He, J. Heilmann-Clausen, J. Heino, J. T. Hunter, V. L. M. Huszar, M. Janišová, J. Jyrkänkallio-Mikkola, K. K. Kahilainen, J. Kemppinen, Ł. Kozub, C. Kruk, M. Kulbiki, A. Kuzemko, P. Christiaan le Roux, A. Lehikoinen, D. Teixeira de Lima, A. Lopez-Urrutia, B. A. Lukács, M. Luoto, S. Mammola, M. M. Marinho, L. S. Menezes, M. Milardi, M. Miranda, G. A. O. Moser, J. Mueller, P. Niittynen, A. Norkko, A. Nowak, J. P. Ometto, O. Ovaskainen, G. E. Overbeck, F. S. Pacheco, V. Pajunen, S. Palpurina, F. Picazo, J. A. Campos, I. F. Rodil, F. M. Sabatini, S. Salingré, M. De Sanctis, A. M. Segura, L. H. S. da Silva, Z. D. Stevanovic, G. Swacha, A. Teittinen, K. T. Tolonen, I. Tsiripidis, L. Virta, B. Wang, J. Wang, W. Weisser, Y. Xu, J. Soininen, Distance decay 2.0 – A global synthesis of taxonomic and functional turnover in ecological communities. Global Ecology and Biogeography **31**, 1399–1421 (2022).

29. P. J. Rose, D. L. Fox, J. Marcot, C. Badgley, Flat latitudinal gradient in Paleocene mammal richness suggests decoupling of climate and biodiversity. Geology **39**, 163–166 (2011).

30. J. Alroy, The Fossil Record of North American Mammals: Evidence for a Paleocene Evolutionary Radiation. Systematic Biology **48**, 107–118 (1999).

31. Time Scales of Critical Events Around the Cretaceous-Paleogene Boundary | Science. https://www-science-org.libproxy.unl.edu/doi/full/10.1126/science.1230492.

32. T. Westerhold, N. Marwan, A. J. Drury, D. Liebrand, C. Agnini, E. Anagnostou, J. S. K. Barnet, S. M. Bohaty, D. De Vleeschouwer, F. Florindo, T. Frederichs, D. A. Hodell, A. E. Holbourn, D. Kroon, V. Lauretano, K. Littler, L. J. Lourens, M. Lyle, H. Pälike, U. Röhl, J. Tian, R. H. Wilkens, P. A. Wilson, J. C. Zachos, An astronomically dated record of Earth's climate and its predictability over the last 66 million years. Science **369**, 1383–1387 (2020).

33. S. Manchester, Update on the megafossil flora of Florissant, Colorado. ser **4**, 137–161 (2001).

34. C. A. E. Strömberg, Evolution of Grasses and Grassland Ecosystems. Annual Review of Earth and Planetary Sciences **39**, 517–544 (2011).

35. C. A. E. Strömberg, The origin and spread of grass-dominated ecosystems in the late Tertiary of North America: preliminary results concerning the evolution of hypsodonty. Palaeogeography, Palaeoclimatology, Palaeoecology **177**, 59–75 (2002).

36. T. Rothwell, A Partial Skeleton of Pseudaelurus (Carnivora: Felidae) from the Nambé Member of the Tesuque Formation, Española Basin, New Mexico. novi **2001**, 1–31 (2001).

Tables and Figures
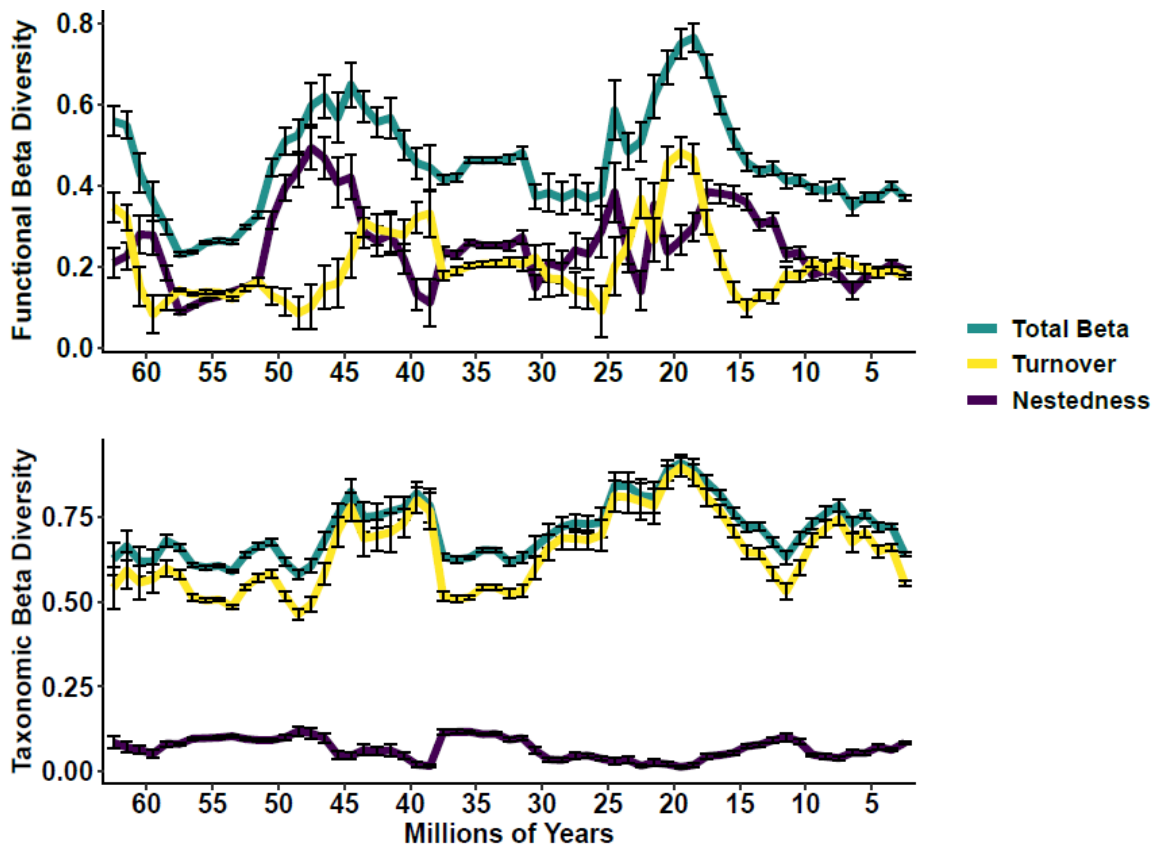
Figure 1. **Line plot of Cenozoic taxonomic and functional beta diversity of mammalian genera calculated in 5-million-year window bins.** The time bins are plotted at the midpoint of the 5-million years. For example, the 65-60 Ma bin is plotted at 63.5 Ma. The plots also include turnover and nestedness components to demonstrate the variation and contribution of the additive components to total beta diversity over time.
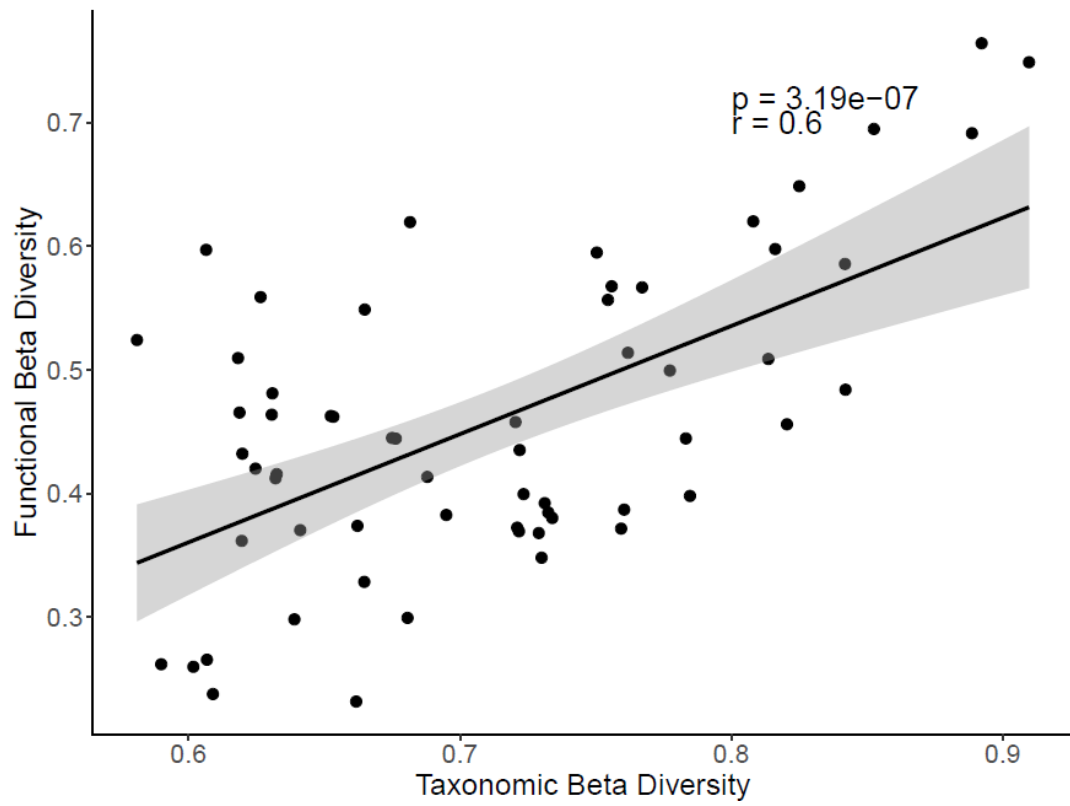
Figure 2. **Correlation plot showing the relationship between taxonomic and functional beta diversity (r = 0.6, p =<0.01).**
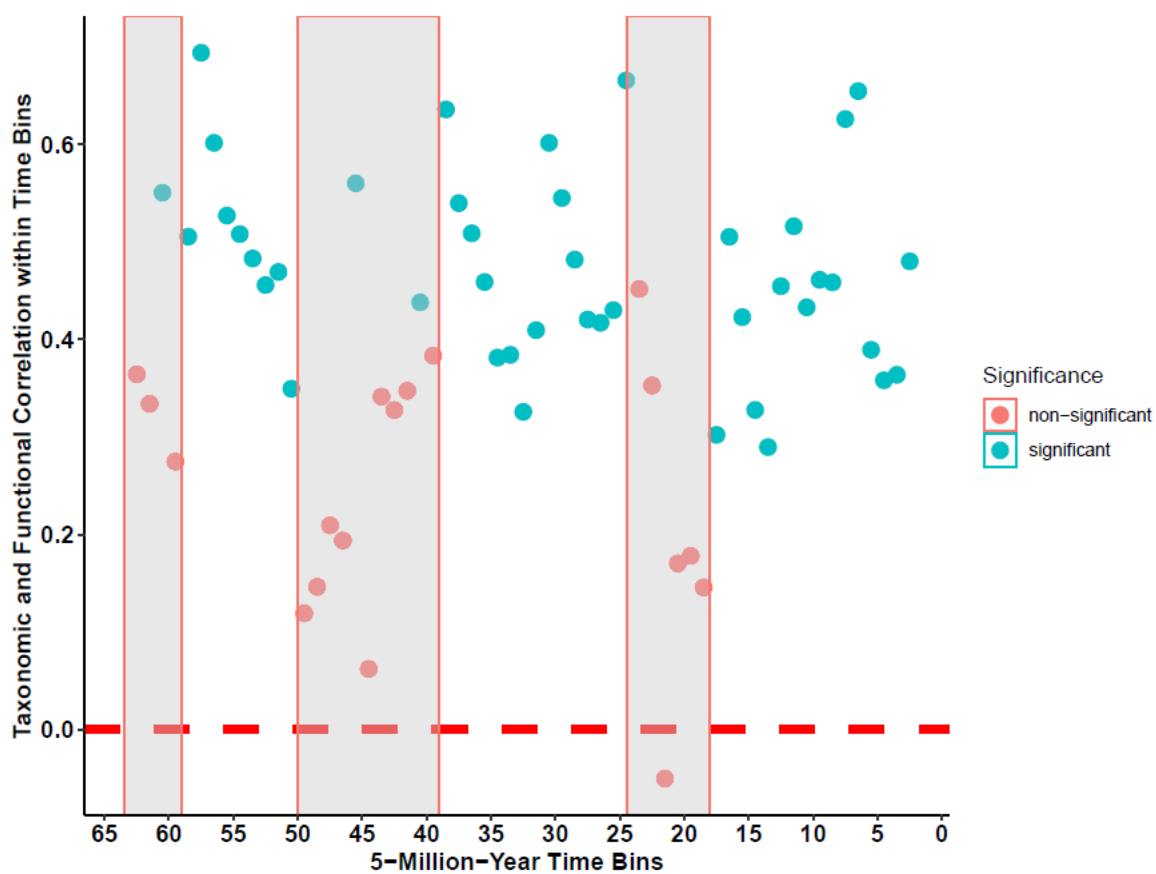
Figure 3. **Correlation coefficient of taxonomic and functional beta diversity relationship within each 5-million-year time bin.** The points are color coded by significance. Pink dots are not significant correlations, while blue dots are significant correlations ($p <= 0.05$).
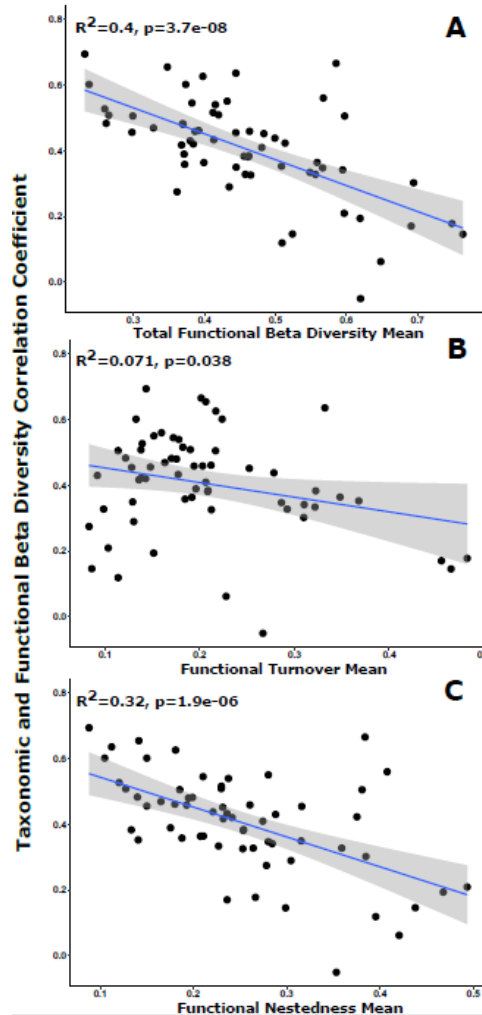
Figure 4. **Regressions showing the relationship between the taxonomic and functional beta diversity correlation coefficient through time (see fig. S5) and the components of functional beta diversity (total (top), turnover (middle), nestedness (bottom)).** Functional turnover has a very weak, yet significant relationship ($R^2 = 0.071$, p = 0.038). Total beta diversity has a significant relationship ($R^2 = 0.4$, p= <0.01). However, functional nestedness shares a significant, negative relationship with the correlation coefficient through time ($R^2 = 0.32$, p = <0.01)

Table S1. **Species traits and categories used to calculate functional beta diversity.**

Body Mass	Life Habit	Locomotion	Diet
Average Log Mass	Arboreal	Saltatorial	Omnivore
	Ground-dwelling	Plantigrade	Carnivore
	Fossorial	Digitigrade	Mixed Feeder
	Semi-fossorial	Graviportal	Frugivore
	Amphibious		Grazer
			Browser
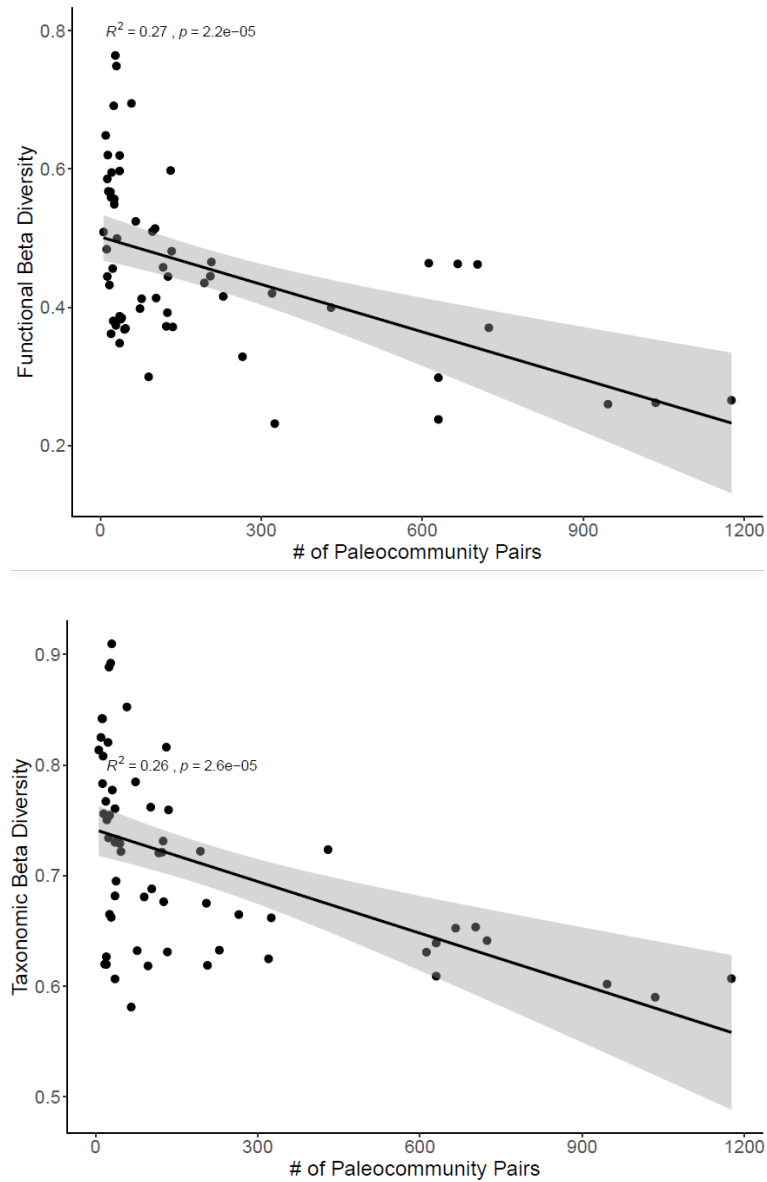
Figure S1. **Relationship between total taxonomic beta diversity (functional and taxonomic) and the number paleocommunity pairs in each window bin to determine if the number of paleocommunity pairs drives our patterns.** There is a significant, negative relationship between the number of pairs and total functional beta diversity (Top: $R^2 = 0.27$, p = <0.01), as well as taxonomic beta diversity ($R^2 = 0.26$, p=<0.01).
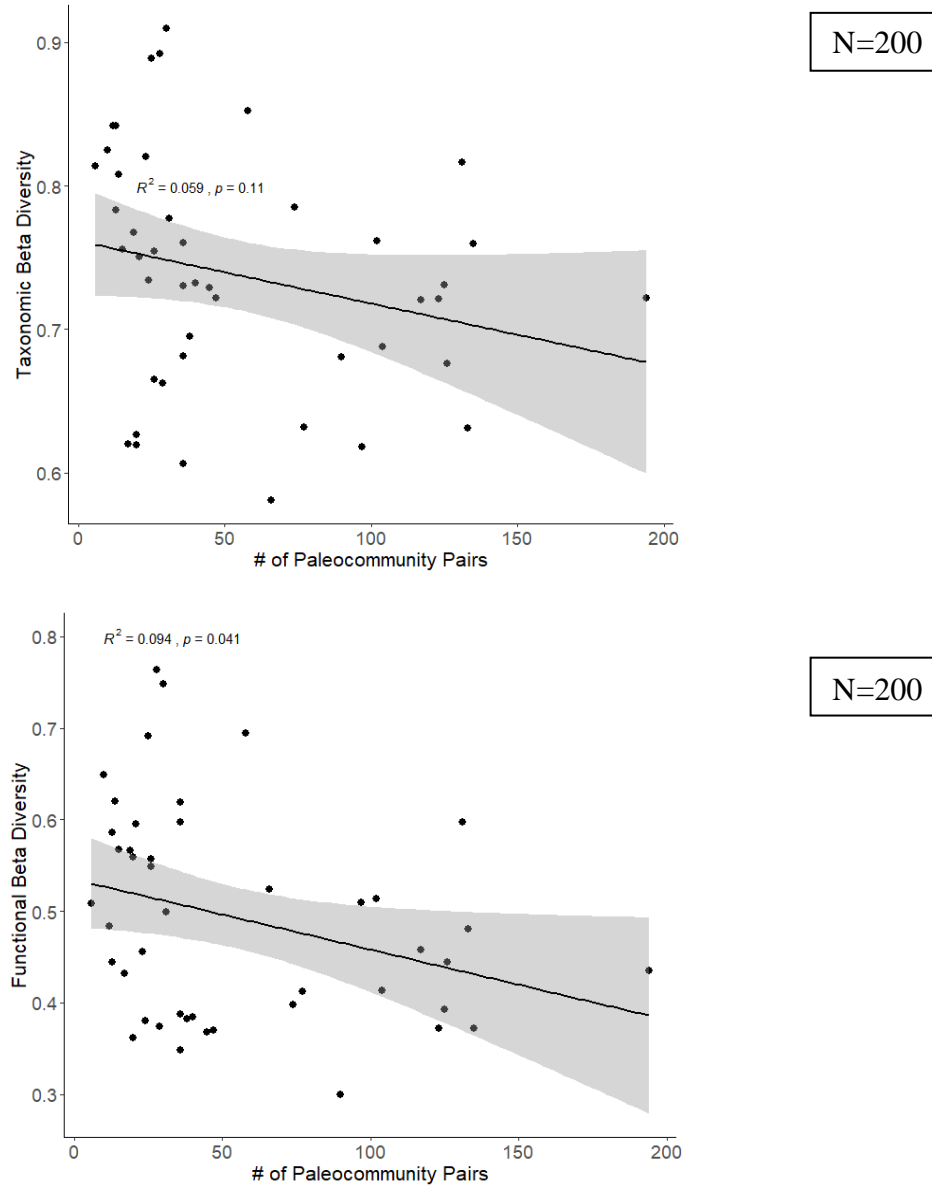
Figure S2. **Regression demonstrating the relationship between all time bins with less than 200 paleocommunity pairs**. All time bins with an average greater than 200 were removed. This is the threshold at which the relationship between beta diversity and the number of paleocommunity pairs in each time bin is lost.
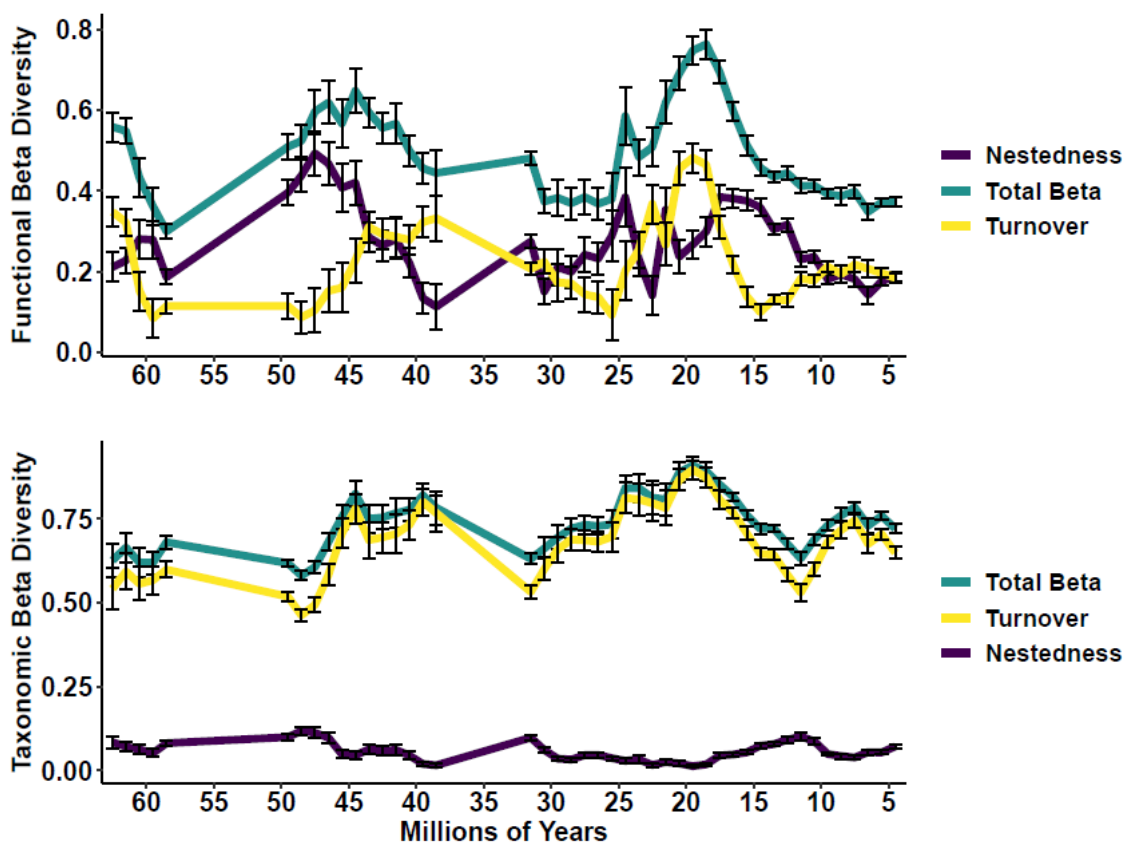
Figure S3. **A line plot of taxonomic beta diversity across the Cenozoic with all time bins with more than 200 paleocommunity pairs removed to assess the effect of high number of paleocommunities in time bins on our results.** 200 paleocommunity pairs is the threshold at which the relationship between both beta diversity dimensions and the number of paleocommunity pairs is no longer present. The pattern in beta diversity over the Cenozoic remains intact, suggesting the relationship is not driving our results.
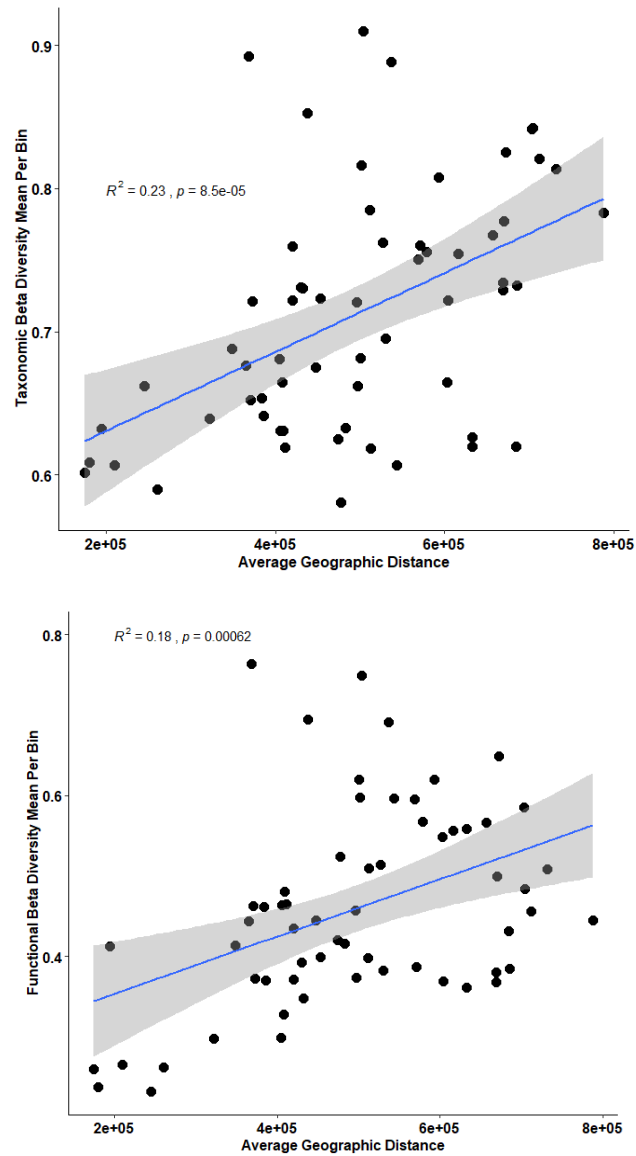
Figure S4. **Regressions of taxonomic and functional beta diversity against the average distance between paleocommunity pairs averaged for each time bin.** There is a significant, positive relationship between both dimensions of beta diversity and average distance (Taxonomic: $R^2 = 0.23$, p = <0.01, Functional: ($R^2 = 0.18$, p = <0.01).
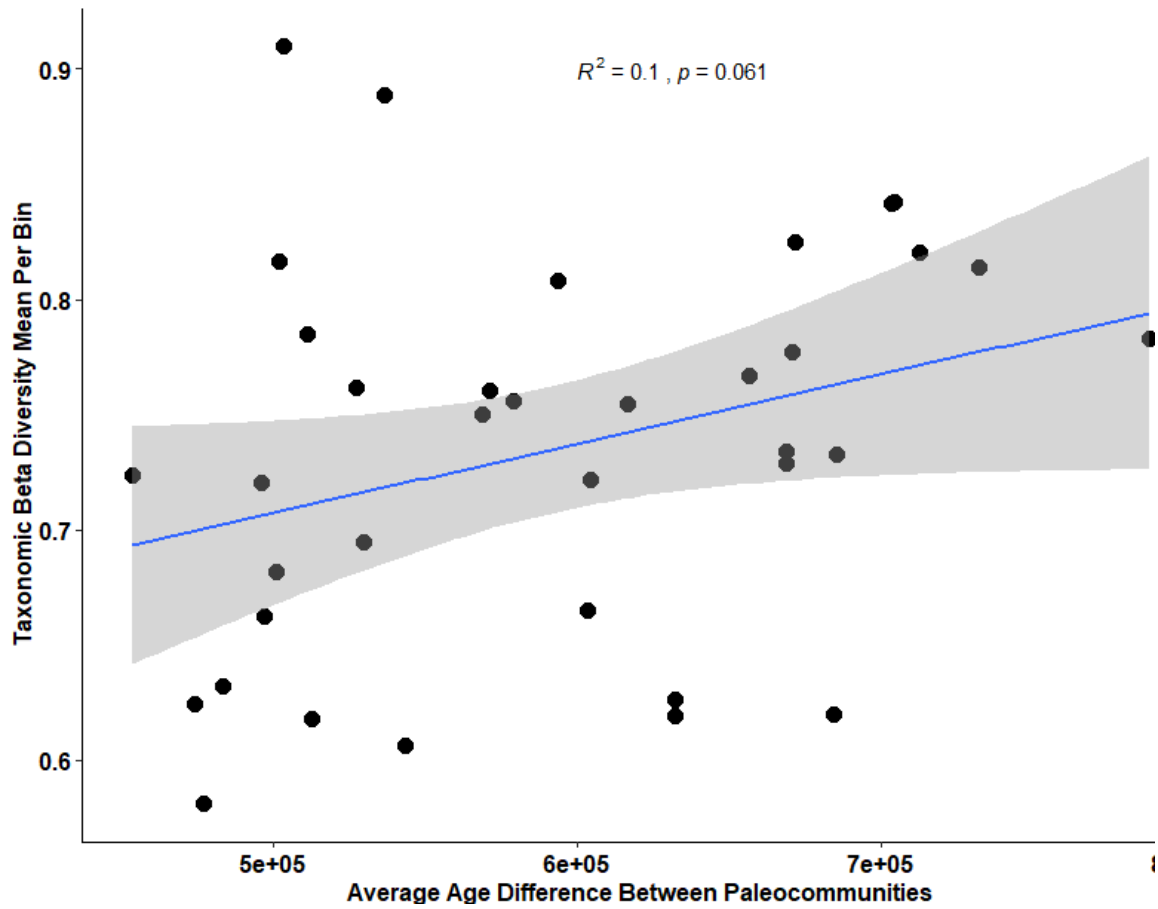
Figure S5. **Regression showing the relationship between average geographic difference between paleocommunities and taxonomic beta diversity per time bin.** In this regression all bins were removed that had an average geographic difference less than 450,000 meters. 450,000 meters is the threshold at which the relationship between age difference and taxonomic beta diversity is no longer significant (R^2=0.1, p=0.061). This suggests that the relationship between average geographic distance and taxonomic beta diversity in time bins is primarily driven by the time bins with very low geographic spread.
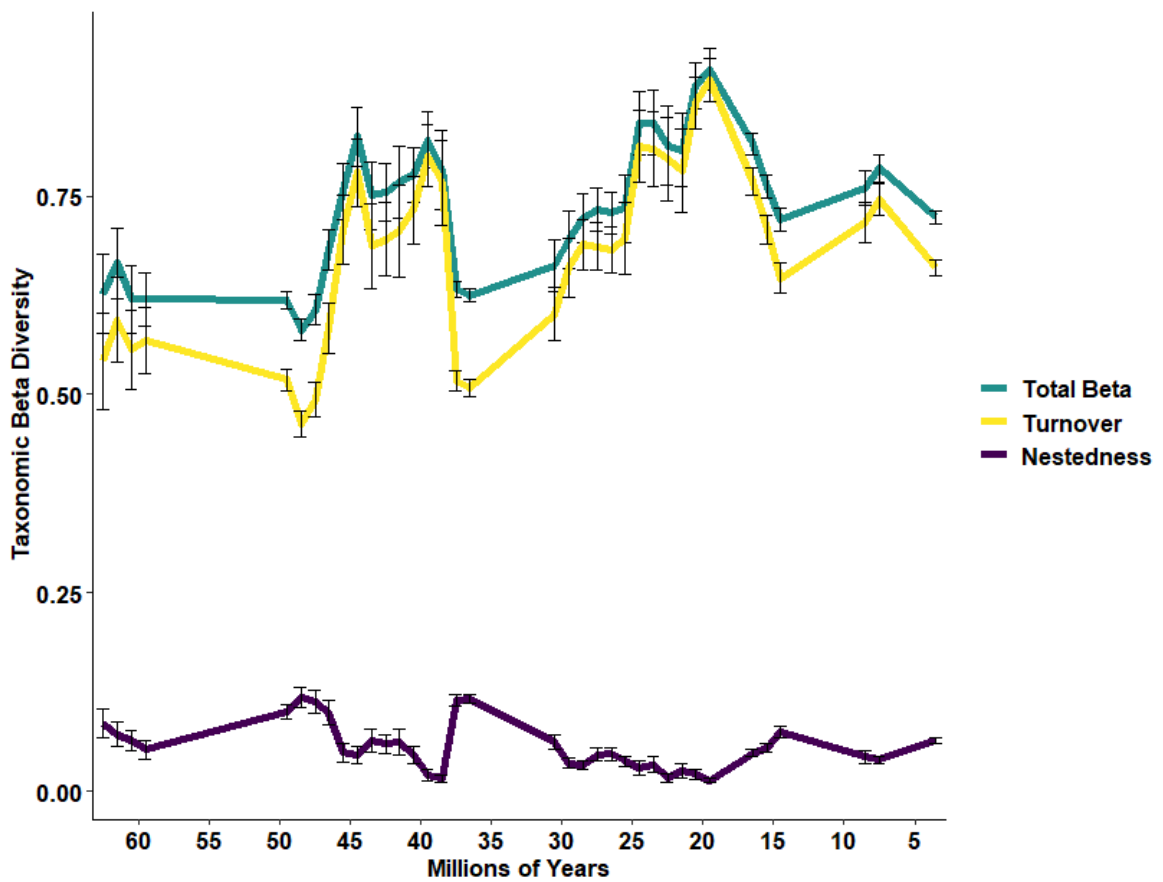
Figure S6. **Taxonomic beta diversity replotted after removing all time bins with an average geographic distance between paleocommunity pairs less 450,500 meters.** These results are consistent with the original findings.
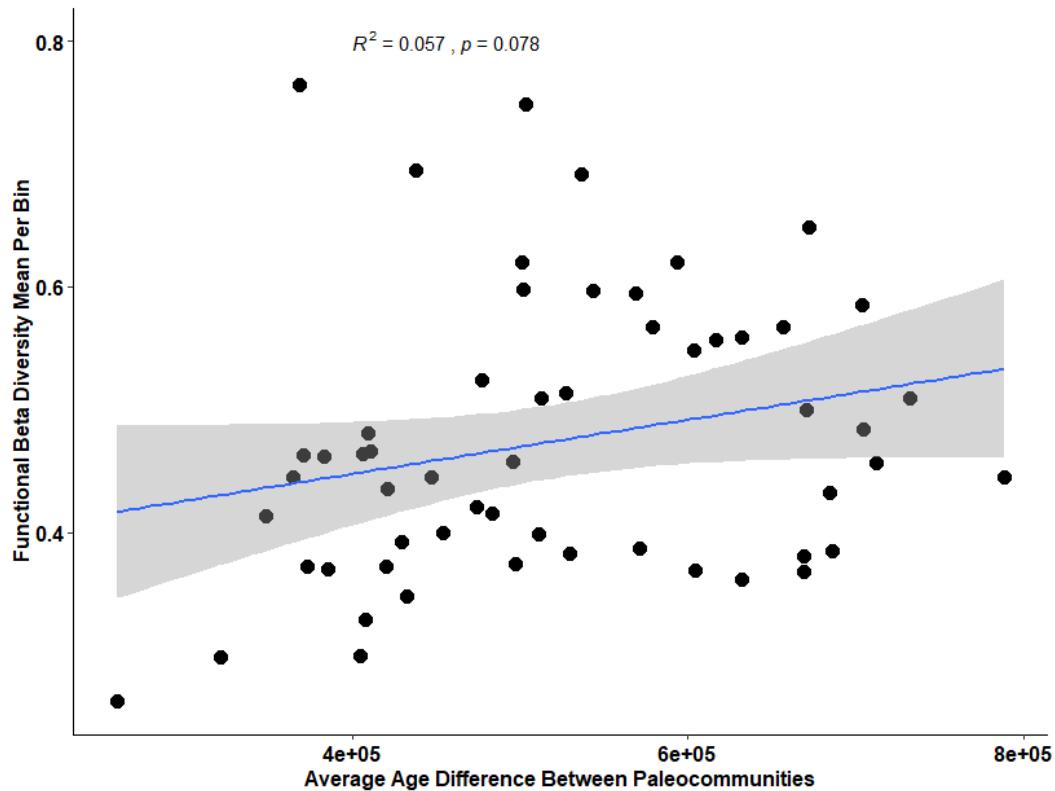
Figure S7. **Regression showing the relationship between average geographic difference between paleocommunities and functional beta diversity per time bin.** In this regression all bins were removed that had an average geographic difference less than 200,000 meters. 200,000 meters is the threshold at which the relationship between age difference and functional beta diversity is no longer significant (R^2=0.057, p=0.078). This suggests that the relationship between average geographic distance and functional beta diversity in time bins is primarily driven by the time bins with very low geographic spread.
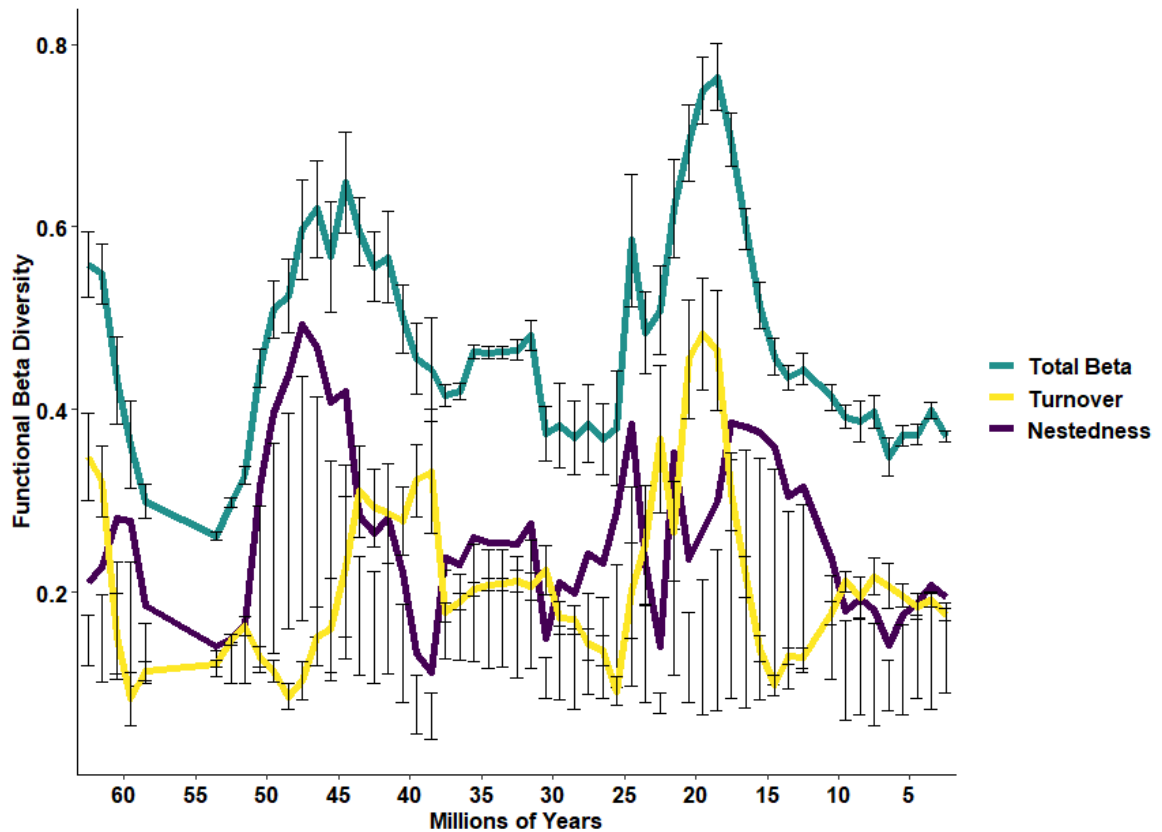
Figure S8. **Functional beta diversity replotted after removing all time bins with an average geographic distance between paleocommunity pairs less 200,000 meters.** These results are consistent with the original findings.
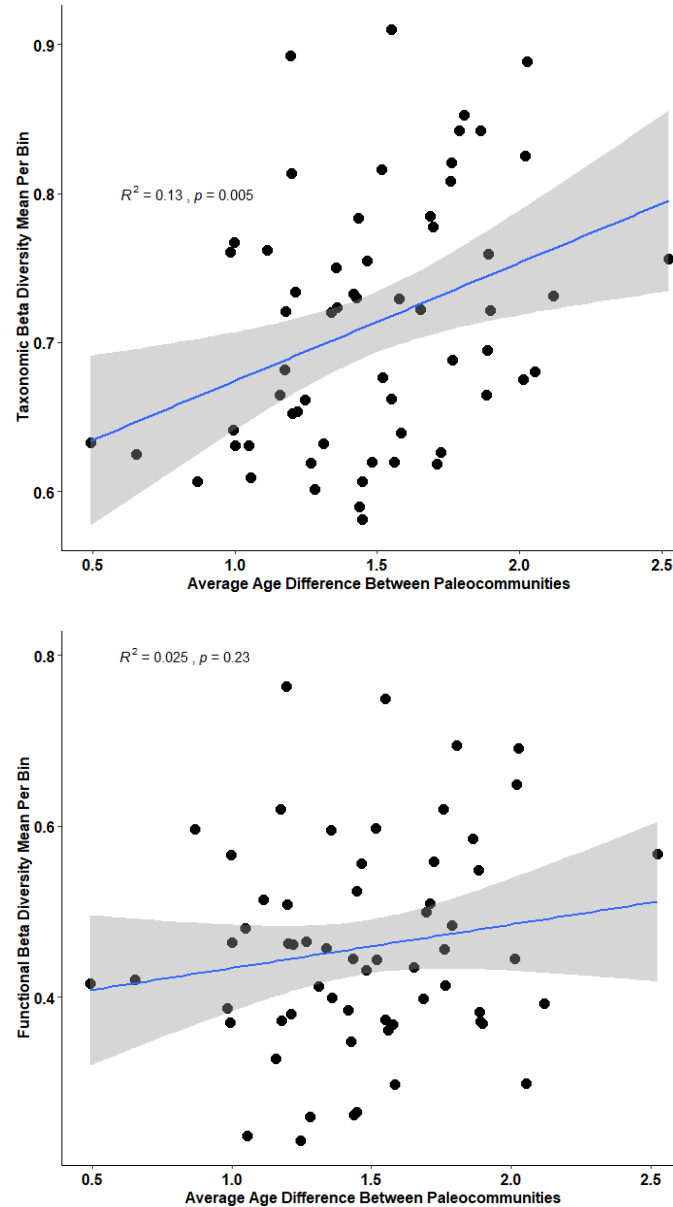
Figure S9. **Regression plots showing the relationship between average taxonomic (top) and functional (bottom) beta diversity and average age difference between paleocommunity pairs.** There is a weak, positive relationship with taxonomic beta diversity (R^2 = 0.13, p = <0.01). There is no significant relationship with functional beta diversity (R^2 = 0.025, p = 0.23)
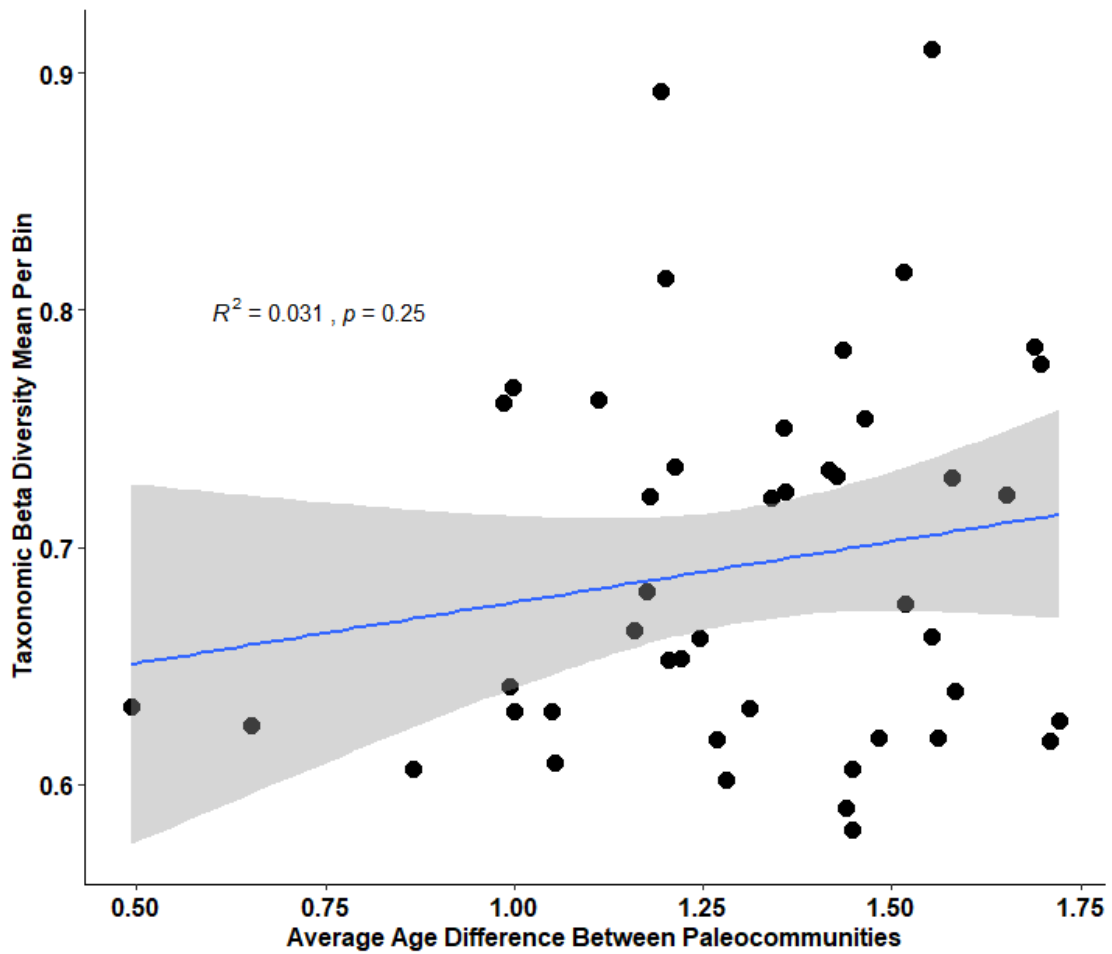
Figure S10. **Regression demonstrating the relationship between all time bins with less than an average age difference between paleocommunities of 1.75 Ma.** All time bins with an average greater than 1.75 were removed. This is the threshold at which the relationship between taxonomic beta diversity mean per bin is lost.
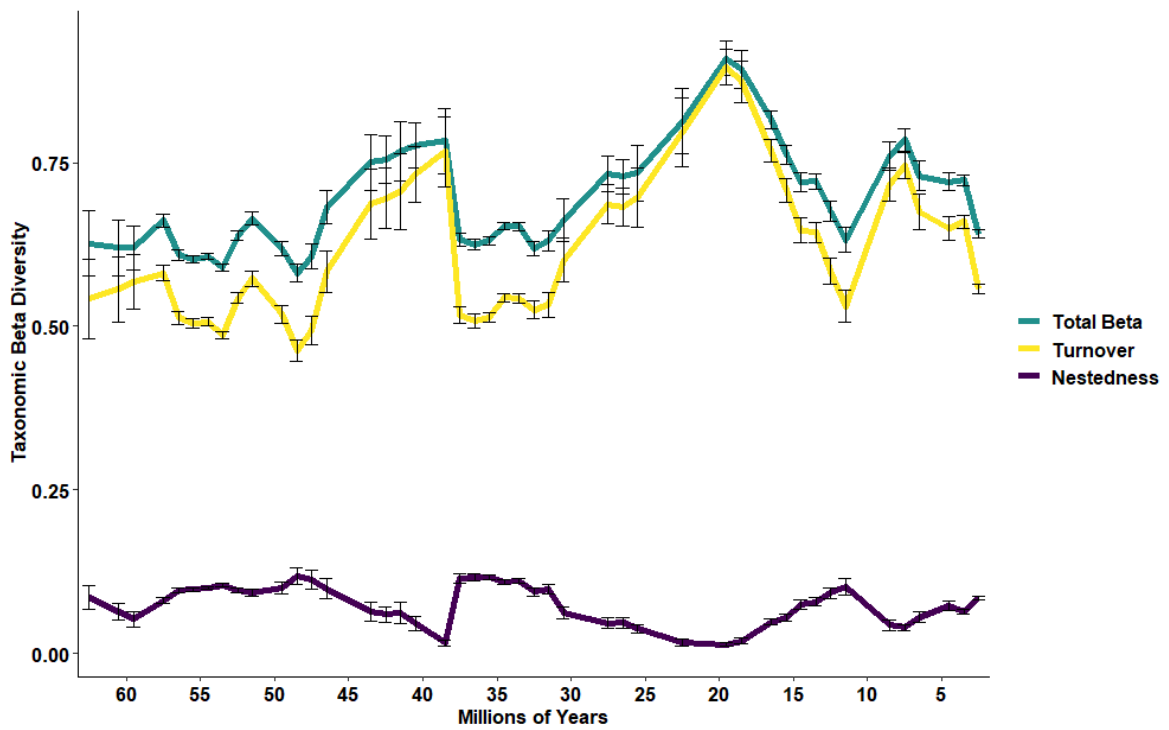
Figure S11. **Taxonomic beta diversity replotted following the removal of all time bins that have an average age difference of 1.75 Ma or greater.** This plot demonstrates that the overall pattern is consistent with original findings and the age difference between paleocommunities is not driving the results.

CHAPTER 3

DIFFERENT MAMMALS, SAME STRUCTURE: CO-OCCURRENCE

STRUCTURE ACROSS THE PLIO-PLEISTOCENE TRANSITION

Abstract

A central goal in ecology is investigating the impact of major perturbations on the structure of biological communities, such as invasion. One promising line of inquiry is using co-occurrence analyses to examine how species traits mediate co-existence and how major ecological, climatic, and environmental disturbances can affect this relationship and underlying mechanisms. However, present communities are heavily influenced by anthropogenic activities and may exhibit greater or lesser resistance to invasion than communities existing before human arrival. Here, we use the North American fossil record to evaluate the co-occurrence structure of mammals across the Great American Biotic Interchange. We compiled 126 paleocommunities from the late Pliocene (4–2.5 Ma) and early Pleistocene (2.5–1 Ma). Genus-level co-occurrence was calculated to identify significantly aggregated (co-occur more than expected) and segregated (co-occur less than expected) genus pairs. A functional diversity analysis was used to calculate functional distance between genus pairs to evaluate the relationship between pair association strength and functional role. We found that the strength distribution of aggregating and segregating genus pairs does not significantly change from the late Pliocene to the early Pleistocene even with different mammals forming the pairs, including immigrant mammals from South America. However, the distribution of functional distances between genus pairs became significantly shorter in the early

Pleistocene. Due to different mammals and ecological roles forming significant associations and the stability of co-occurrence structure across this interval, our study suggests that mammals have fundamental ways of assembling that may have been altered by humans.

Introduction

Understanding the impacts of major ecological, environmental, and climatic transitions on biological communities is a primary focus for conservation paleobiology and modern ecology (1–8). Community structure plays a key role in maintaining ecosystem functioning and resiliency against disturbances. However, the exploration and investigation of changes in community structure is exceptionally complex because structure is driven by numerous components of biological systems and interactions (8). Traditionally, species diversity, richness and abundance are some of the most examined components (8, 9). However, modern ecologists are increasingly using quantitative methods to examine the importance of biological relationships and functional roles on community structure (10–12) Furthermore, paleoecologists have begun applying these methods to encompass critical intervals in the fossil record. This allows us to understand how events such as climate shifts and biological invasions result in the reorganization of community structure. For example, periods of major climate transitions, can lead to dramatic shifts in vegetation distributions resulting in non-analog habitats (13–15). Altering resource availability for other species can lead to range shifts, as well as extinctions due to shifts in geographic ranges (16). This leads to the loss or gain of species interactions (17). Similarly, large-scale immigration likely impacts species

associations, such as competition, mutualisms, and facilitations, altering the relative importance of underlying mechanisms that drive how organisms assemble (16, 17). Thus, evaluating changes in community structure across space and time during past disturbances is particularly informative in understanding mammalian community assembly.

The closing of the Isthmus of Panama was a major environmental perturbation for South and North American ecosystems. The exact timing of the closing is still contested but may have occurred between 3-2.5 Ma. It both triggered the intermingling of North and South American biota and may have facilitated the transition into a colder climate that drastically modified North and South American mammal communities (18–22). While this land bridge was likely in place nearly 10 million years ago. Some studies suggest that it continuously flooded until the late Pliocene (18, 23–25). By 3 Ma uplift caused by the meeting of the North and South American plates permanently divided the Gulf of Mexico and the Pacific Ocean and the ocean circulation between the Americas ceased (25, 26). The reorganization of ocean currents may have helped drive the onset of glaciation in the Northern Hemisphere (27, 28). The shift towards a cooling climate and the rapid expansion of glaciers in North America(18, 29) pushed mammals to lower latitudes (30); steppe-tundra habitats were displaced southward (30).

These events led to extensive interchange of mammals between the Americas; an immigration process called the Great American Biotic Interchange (GABI). Many important studies have evaluated the taxonomic identification, functional roles and the timing of movements (19, 21, 31). For example, although portions of the Isthmus of

Panama may have been uplifted much earlier, the migration of mammals between continents remained minor until ~3-2.5 Ma (18–20), and only a few mammal taxa crossed prior to this time (18). One of the earliest migrants into North America were giant ground sloths, which are large and more ecological generalists. By the middle to late Pliocene, armadillos, porcupines and capybara-like rodents followed (19, 24). Occurrences of South American taxa in North America were fairly rare before the Plio-Pleistocene transition, increasing by 50% afterward (18, 20). The South American mammals that ultimately immigrated represent a diversity of functional roles and 36 families (24). Although some of these groups were successful and remain part of the North American fauna, others did not move northward beyond the subtropics or are no longer found in North America (31). In contrast, North American migrants into South America experienced far greater success, likely due to the higher extinction rates of native South American taxa during this period (31). Previous studies have also evaluated migration, extinction, and origination rates across this interval (18–20, 31). Mammals in North America underwent increased origination and extinction rates and temporal turnover in community composition was high during the invasion of South America migrants (21, 32, 33). The combined impact of changing functional diversity, loss of native genera and the range shifts to lower latitudes due to glacier expansion on community structure remains largely unexplored. However, with recently developed methods and increased computing power, we can better understand the impact of this event on mammal community structure.

One method that has been used to quantify changes in mammalian community structure is a pairwise co-occurrence analysis (1, 4, 34). Co-occurrence analysis uses species pairs to examine the extent to which they occupy the same communities (1, 34). Species can be segregated (appearing together less often than expected) aggregated (appearing together more often than expected), or random (not significantly aggregating or segregating). Patterns of species associations over time and space give important insight into the mechanisms that determine how mammals filter into communities including, dispersal limitations, environment filtering, and competition (35). Moreover, species functional traits provide a link to ecosystem functioning by interacting with these mechanisms in shaping communities and species associations (12, 36–38). Functional traits (e.g. body mass, diet, life habit, locomotion) define a mammal's ecological role in an ecosystem (12, 39) and species associations are heavily influenced by the functional roles of the constituent species (40, 41). Combining information on functional diversity with co-occurrence strengths allows us to characterize changes in community structure more fully and infer the underlying mechanisms driving mammal community structure (41).

The closing of the Isthmus of Panama played an important role in shaping the modern North American mammalian fauna through major climatic, ecological, and environmental changes. Various studies have recorded taxonomic turnover associated with the interchange of species between the two continents, changes in generic richness and the timing of the arrival of different genera into each continent (24, 31). However, the effects on community structure are largely unknown. Here we identify changes in

western North American mammal community structure using species associations and functional diversity across the Plio-Pleistocene transition. Specifically, we ask if there is a change in the relative proportions of significant aggregations versus segregations. We investigate whether the extinction of North American genera or the invasion of South American genera contributed to changes in co-occurrence structure. Finally, we ask whether the functional roles or body size of species that form significant pairs change across this interval.

Methods & Data

Occurrence Data

Our study includes 126 North American localities spanning the Plio-Pleistocene transition. Data on occurrence come from the Paleobiology Database (https://paleobiodb.org/#/) and includes a total of 118 genera (Datafile1). Paleocommunities are divided into two equal time bins, pre-glaciation (4-2.5 Ma) and early Pleistocene (2.5-1 Ma). Each paleocommunity was a fossil locality or a combination of fossil localities. Paleocommunities were constrained using the following criteria: 1. because data were limited for the eastern region, we only used localities between -125 to -90 degrees longitude and less than 55 degrees in latitude. 2. Due to preservation biases, only mammals above 1 kg were included. 3. Only terrestrial and non-volant mammal genera were included. Genera were defined as South American or North American based on the earliest occurrence of the family before 10 Ma. The continental species pool was also compiled using all terrestrial mammalian genera over 1kg

occurring in North America (minus Mexico) between 4-1 Ma. This database also only included non-volant, terrestrial mammals.

Co-occurrence Analysis

We examined co-occurrence at the genus level. A minimum of 5 genera were required for a paleocommunity to be included in the co-occurrence analysis (1). Any paleocommunities with the same estimated date range and located within 5 km of each other were combined into a single site. Co-occurrence analysis was run separately for the late Pliocene time bin (4-2.5 Ma) and the early Pleistocene time bin (2.5-1 Ma) using the 'cooccur' R package (42). The Veech 2013 pairwise method was used to determine if significant genus pairs either aggregated or segregated by comparing the observed number of times two genera occur together against the expected frequency (10, 11, 43). To account for differences in sample size between time bins, we ran a random sub-sampling routine for 100 iterations. Each iteration provided a list of significantly aggregating and segregating genus pairs. The Fisher's exact Test mid-P variant provided a weight to score the strength of each significant pair (1, 10). The raw scores were then z-transformed using the qnorm function in R to standardize them between positive and negative infinity (1). This resulted in segregated pairs having negative scores and aggregated pairs having positive scores. The mid-P variant was then averaged over the 100 subsampling routines for each pair to provide an average strength. The list of pairs can be found in Datafile2 of the supplementary material. A Kolmogorov–Smirnov test was conducted to determine if there was a significant difference in the distribution of pair strengths between time bins. By identifying significant changes in pair strengths

distributions, it can demonstrate shifts in community structure that may otherwise not be found when evaluating other components of community structure (e.g., species richness, diversity, etc.).

Functional Diversity and Functional Distance

Functional diversity was calculated using four functional traits for each genus (body mass category, diet, locomotion and life habit). The functional traits for each genus were adjusted from species trait data from Datafile3 where all trait references can be found. References for the primary literature of the fossil localities can be found in Datafile4. Body masses were averaged, and categorical traits were chosen based on the most prevalent category found in that genus. Numeric body mass categories were based on Pinedo-Munoz and Alroy 2016, who found that these body mass categories were highly associated with the ecological role of a species (Table 1). Diet was a single category based on the most common dietary preference of the species within the genera. Locomotion was the morphological limb structure that determines a mammal's stance and was highly conserved across species within each genus. Life habitat reflected the commonly preferred habitat of the genera and the most abundant category across species in a genus was chosen (Table 1). Functional diversity was calculated for all mammalian genera occurring in North America above a latitude of 31° N, during the two-time bins (4-1 Ma), not just genera included in the co-occurrence analysis. We used the coordinates from this analysis to plot genera in trait space. Using coordinates calculated from all genera ensured that we did not under or overestimate the variation in ecological roles. A genus by trait matrix was used to make a distance matrix with the Gower's dissimilarity

method. In the distance matrix, categorical traits are not ranked or ordered. Between two genera they are identified as a 1 (match) or 0 (no match). The distance matrix was analyzed with the 'dbFD' function from the 'FD' R package (44). A square root correction was applied to the non-Euclidean dataset. Principle Coordinate Analysis (PCoA) coordinates were created for each genus to ordinate them in multidimensional space. To calculate Euclidean distances between each pair of genera, we used the first four PCoA axes and applied them to the excel equation - =SQRT(SUMXMY2(array_x,array_y)). Array x was the first four axes of one genus and array y would the first four axes of the second genus. Kolmogorov–Smirnov tests were employed to assess differences in the distribution of functional distance between genera for significant associations pre and early Pleistocene.

Extinction versus Survivorship of Genera

Survivorship of mammalian genera across the Plio-Pleistocene transition was evaluated by whether it had fossil occurrences past 1 Ma in North America. Information on first and last appearances can be found in Datafile5. We used the Paleobiology Database to collect information on the maximum and minimum date of the last appearance. We used the youngest estimated date (most recent) of their survival for all graphs in the main text but included graphs using the oldest estimated date of extinction in the supplementary material (See Supplementary Information).

Results

1.1 Co-occurrence Structure

The co-occurrence structure of western North American mammal paleocommunities remains stable across the Plio-Pleistocene transition. The distribution of co-occurrence strengths for segregating and aggregating genus pairs does not significantly change even though significant pairs decline from pre to post glaciation (Kolmogorov-Smirnov: $p = 0.5731$; Number of Significant Pairs: Pre = 291, Post = 255; Fig. 1). In addition, our results show that both time slices have a greater proportion of aggregations than segregations. Moreover, the association strengths of segregations tend to be weaker than those of aggregations on average. While the overall pattern of aggregations and segregations does not change, the identity of genera forming significant pairs does change (DataFile1).

1.2 South American Migrants vs. North American Native Mammal Co-occurrence Structure

South American mammals increase in the number of significant pairs they form following the Plio-Pleistocene transition. There are 37 significant pairs including a South American genus and a North American genus (NA-SA) in the late Pliocene time bin compared to 63 NA-SA pairs in the early Pleistocene (Fig. 2). Meanwhile, pairs with only North American genera (NA-NA) decrease (pre = 252, post = 191). Interestingly, South American genera form few pairs with each other (SA-SA) in either time period (Pre = 2, Post = 1). In addition, the NA-SA pairs that occur in the early Pleistocene are not filling in ecological space vacated by the NA-NA pairs and these areas are less densely occupied (Fig. 2). Instead, they are spread throughout the ecological space defined by co-occurrence strength and functional distance. In addition, the proportions of

segregations to aggregations do not vary between genus pairs of different continental origins or the same continental origin (Fig. 3).

2.1 Functional Roles

We find that the average functional distance between significant associations decreases across the Plio-Pleistocene transition (Kolmogorov–Smirnov Test: p = 0.004; Fig. 4). This pattern persists even when aggregated and segregated pairs are analyzed separately (Kolmogorov–Smirnov Test: Aggregating p =1.581e-07, Segregating p = 0.001429). The decrease in functional distance of significant pairs is not caused by differences in the geographic distributions of the fossil localities between time bins (Kolmogorov-Smirnov Test: p = 0.1063; fig. S1, S2). These results also are not determined by differences in community species richness distributions between each time bin (Kolmogorov–Smirnov Test: p = 0.2866).

We also identified changes in trait category distributions of mammalian genera in the late Pliocene and early Pleistocene. We found that locomotion, diet, and body mass category distributions change significantly, while mammal distributions across life habit categories remains the same (p-values: locomotion = 1.184e-12, diet = 3.458e-05, body mass = 6.661e-11, life habit = 0.6931).

2.2 South American vs. North American Functional Roles

The diversity of South American functional types is much lower than North American functional types (Fig. 5), with South American mammals occupying the center of functional space whereas, North American genera have a greater abundance along the

outside (Fig. 5). This pattern is more obvious when South American genera are only plotted with North American survivors (Fig. 6). However, the extinct North American genera occupy similar functional extent as the surviving genera (Fig. 7). There are no extinct South American genera that form significant associations. Most South American genera aggregate with carnivores, mixed feeders, or other browsers. The number of aggregations formed by browsers increases in the early Pleistocene (fig. S3). The role of body size in mediating pair formation changes over time (figs. S4-S10). NA-SA pairs show an increase in associations between large and medium sized genera, as well as associations between large-bodied genera across the transition. In contrast, NA-NA pairs between medium and large-sized mammals and between large-bodied genera decline in abundance following the Plio-Pleistocene transition.

Discussion

Amidst the onset of a major climate transition (18, 28, 45) and the escalation of the Great Biotic Interchange (18, 19, 24), western North American mammal paleocommunities underwent high compositional turnover, and yet, community structure, as measured by species co-occurrence patterns, remains stable. No difference occurred across the Plio-Pleistocene transition in either the proportion of aggregated and segregated genus pairs or in the strengths of the associations (Fig. 1, 3). Our results are consistent with several recent studies that demonstrated the resiliency of some community structure components across major ecological and environmental change. Specifically, previous studies have shown that co-occurrence structure over evolutionary timescales is consistent across periods of climate change and mass extinctions unless

humans are part of the ecosystem (1, 4). Indeed, plant and mammal communities primarily form aggregations rather than segregations for approximately 300 ma until the Holocene (4). In our study, western North American mammals shift their distributions in response to climate change and the invasion of new species and form new associations. Furthermore, they were able to maintain co-occurrence structure with the formation of non-analog habitats (Fig 1.). The individualistic responses to glaciation by vegetative species led to non-analog habitats with the expansion and retraction of their fundamental niche space (46, 47). Thus, even with new members, different climatic gradients and formation of non-analog habitats due to glaciation (46, 47) they still formed the same types of associations in similar proportions (Fig. 1, 3). Our study, among others, may suggest that South and North American mammals share a fundamental way of assembling that is maintained across intervals of climatic, ecological and environmental shifts in the absence of human perturbations (1, 4, 48).

Mammals of South American origin displayed the same co-occurrence structure found in North American mammals, further supporting the idea that mammals have a fundamental way of assembling (Fig. 3). Despite originating on a continent that was isolated for millions of years, the mammals still form the same proportion of aggregations and segregations as their North American counterparts (Fig. 2). Abundance changes following the Plio-Pleistocene transition do not change the proportion of aggregate to segregated genera. The increase in South American associations early Pleistocene is likely due to heightened rate of migration between continents at ~3-2.5 Ma triggered by the closing of the Isthmus of Panama (Fig. 2; 22, 26, 27). Before this time, few South

American genera had reached western North America and they were a smaller percentage of the North American communities (24). However, it is unclear if South American genus o-occurrence structure shows a similar pattern because they are primarily paired with North American genera.

The success of some South American mammals infiltrating the North American fauna may be because they concentrate in an area of trait space, underutilized by North American genera. North American genera more densely occupy the outside of trait space (Fig. 2). Moreover, it may be that the niche space filled by those unique roles was formerly vacant. This distribution of South American genera in this unoccupied niche space is at least partially responsible for the shorter functional distances among associating genera following the glaciation event, as many of the South American genera are unlike any mammals previously found in North America. For instance, the large, browsing, plantigrade clade of ground sloths. Ground sloths form more significant pairs with North American genera than any other South American clade. Multiple genera of ground sloths migrated into North America millions of years before the closing of the Isthmus, providing time for them to form ecological relationships and even evolve species endemic to North America (19, 24). Furthermore, Glyptotherium (glyptodonts) and Erethizon (porcupines) also form a large number of significant pairs with North American genera following glaciation. Both genera commonly form segregations with grazing mammals such as horses, camels and mammoths and form aggregations with mixed feeders and other browsing mammals. Ground sloths, glyptodonts and porcupines have a strong presence in early Pleistocene paleocommunities, likely reflecting their

ecological success (Datafile 1). Glyptodonts and ground sloths survived until the late Pleistocene megafaunal extinction when many large-bodied mammals went extinct (49, 50). Porcupines survive this mass extinction and remain a common mammal in the North American fauna today (51). Due to the uniqueness of their functionality, there does not appear to be a similarity between the types of North American genera that stop forming pairs and the South American genera that begin building strong associations.

Extinct North American genera display a variety of functional roles. In fact, their distribution in functional space is similar to surviving genera (Fig. 5, 6, 7). Furthermore, the extinct genera, like surviving genera, do not overlap with South American functional roles, suggesting that competition may not have a been a strong driver in these extinctions (Fig. 5, 6, 7). However, in some areas the landscape is thought to have opened-up with a spread of drier savannah at the onset of glaciation (30). For example, Borophagus and Buisnictis were two North American genera that had a strong presence pre-glaciation, but quickly diminished following the Plio-Pleistocene transition (2.5 Ma). Borophagus was a genus of canid with robust limbs thought to specialize at ambush hunting in closed habitats (52). With a body size greater than the modern gray wolf, they likely fed on larger herbivores like tapirs (52). Buisnictis is a medium-sized transitional genus of skunk that gave rise to modern skunks (53). Based on inferences about the habitat preferences of many of the extinct genera, it is possible that many closed-habitat mammals were lost due to the opening of the landscape. Nevertheless, more quantitative assessment is needed on this topic and acquiring evidence of habitat preferences for individual genera is outside the scope of this paper.

Ecological theory predicts that factors such as invasion, climate change, and extinction have large effects on community structure (1, 54–58). In modern times, the composition of Swedish bird communities has changed rapidly in response to varying summer temperatures since the 1960's (59). Similarly, the invasion of European House Sparrows into west Mexico, led to a significant decrease in richness but increased bird abundances, resulting in a dramatic difference between invaded and non-invaded bird communities (60). Interestingly, many studies examining changes in community structure using the fossil record prior to human impacts do not find significant changes in response to these factors (2, 4, 61). For instance, the immigration of three new orders of mammals from Asia around ~56 Mya and a rapid warming event, did not result in community structure changes (2). These major environmental and ecological events in the fossil record have been explored at various temporal grades. Although our study, like many paleoecological projects, works at a large temporal grade, those using shorter timescales (e.g. 1000 years or less) (4, 62, 63) also find structural consistency across major events (4). When looking at co-occurrence structure specifically, there is no relationship between the temporal grade of the data and the proportion of aggregated to segregated pairs (4). Furthermore, taphonomic biases that vary over space and time favor the fossilization of different habitats, body types and sizes. Regardless, paleoecological studies working in different time periods and geographic regions still find consistency in mammalian community structure across major transitional events except for the climate shifts and extinctions that occur at the terminal Pleistocene to early Holocene (1, 4, 48). The novel climate at the terminal Pleistocene led to non-analog habitats due to range

shifts in plants, drastically altering the landscape (13, 15, 47, 47) . This suggests that the shift in climate occurring with glaciation at the Plio-Pleistocene transition would have likely led to similar environmental changes and ultimately, similar impacts on mammal communities. Nevertheless, community structure is not significantly altered at the Plio-Pleistocene transition. This difference is likely not driven by taphonomic biases or different temporal grades, but rather caused by the presence of humans. Anthropogenic activities are disrupting natural mechanisms that allowed for structural stability of mammal communities across past perturbations. Thus, resulting in greater susceptibility to disturbances in modern communities.

Conclusion

The closing of the Isthmus of Panama contributed to a number of ecological, environmental and climatic events that affected the composition of western North American mammal communities. South American mammals increased their rate of migration across the land bridge with some genera successfully joining the North American fauna and filling an area of niche space with low occupancy and redundancy. Moreover, and for unknown reasons, various North American mammals gradually went extinct following the Plio-Pleistocene transition. Fascinatingly, these events do not lead to a reorganization in community structure. In fact, the dispersal of mammals into North America during the Plio-Pleistocene transition may be responsible for maintaining community structure despite the extinction of some North American mammals; while the types of ecological roles forming strong associations are different, the types of associations remain the same (Fig. 1, 3). This suggests that mammal communities can

remain stable across periods of major environmental, ecological, and climatic changes without human disturbance. The deep, evolutionary timeline exhibiting these consistent mammal community patterns across major transitions is evidence for the importance of preserving natural mechanisms.

References

1. A. B. Tóth, S. K. Lyons, W. A. Barr, A. K. Behrensmeyer, J. L. Blois, R. Bobe, M. Davis, A. Du, J. T. Eronen, J. T. Faith, D. Fraser, N. J. Gotelli, G. R. Graves, A. M. Jukar, J. H. Miller, S. Pineda-Munoz, L. C. Soul, A. Villaseñor, J. Alroy, Reorganization of surviving mammal communities after the end-Pleistocene megafaunal extinction. Science **365**, 1305–1308 (2019).

2. D. Fraser, S. K. Lyons, Mammal Community Structure through the Paleocene-Eocene Thermal Maximum. Am. Nat. **196**, 271–290 (2020).

3. D. L. Pearson, A Pantropical Comparison of Bird Community Structure on Six Lowland Forest Sites. The Condor **79**, 232–244 (1977).

4. S. Kathleen Lyons, K. L. Amatangelo, A. K. Behrensmeyer, A. Bercovici, J. L. Blois, M. Davis, W. A. DiMichele, A. Du, J. T. Eronen, J. Tyler Faith, G. R. Graves, N. Jud, C. Labandeira, C. V. Looy, B. McGill, J. H. Miller, D. Patterson, S. Pineda-Munoz, R. Potts, B. Riddle, R. Terry, A. Tóth, W. Ulrich, A. Villaseñor, S. Wing, H. Anderson, J. Anderson, D. Waller, N. J. Gotelli, Holocene shifts in the assembly of plant and animal communities implicate human impacts. Nature **529**, 80–83 (2016).

5. S. Villéger, J. R. Miranda, D. F. Hernández, D. Mouillot, Contrasting changes in taxonomic vs. functional diversity of tropical fish communities after habitat degradation. Ecol. Appl. **20**, 1512–1522 (2010).

6. K. H. Bannar-Martin, Primate and Nonprimate Mammal Community Assembly: The Influence of Biogeographic Barriers and Spatial Scale. Int. J. Primatol. **35**, 1122–1142 (2014).

7. N. G. Hairston, F. E. Smith, L. B. Slobodkin, Community Structure, Population Control, and Competition. Am. Nat. **94**, 421–425 (1960).

8. H. Caswell, Community Structure: A Neutral Model Analysis. Ecol. Monogr. **46**, 327–354 (1976).

9. R. A. Kempton, The Structure of Species Abundance and Measurement of Diversity. Biometrics **35**, 307–321 (1979).

10. J. A. Veech, A probabilistic model for analysing species co-occurrence. Glob. Ecol. Biogeogr. **22**, 252–260 (2013).

11. J. A. Veech, The pairwise approach to analysing species co-occurrence. J. Biogeogr. **41**, 1029–1035 (2014).

12. S. Villéger, N. W. H. Mason, D. Mouillot, New Multidimensional Functional Diversity Indices for a Multifaceted Framework in Functional Ecology. Ecology **89**, 2290–2301 (2008).

13. H. Yang, M. Wu, W. Liu, Z. Zhang, N. Zhang, S. Wan, Community structure and composition in response to climate change in a temperate steppe. Glob. Change Biol. **17**, 452–465 (2011).

14. H. Behling, Late Quaternary vegetational and climatic changes in Brazil. Rev. Palaeobot. Palynol. **99**, 143–156 (1998).

15. M. Blinnikov, A. Busacca, C. Whitlock, Reconstruction of the late Pleistocene grassland of the Columbia basin, Washington, USA, based on phytolith records in loess. Palaeogeogr. Palaeoclimatol. Palaeoecol. **177**, 77–101 (2002).

16. M. I. Pardi, R. W. Graham, Changes in small mammal communities throughout the late Quaternary across eastern environmental gradients of the United States. Quat. Int. **530–531**, 80–87 (2019).

17. C. E. Mitchell, A. A. Agrawal, J. D. Bever, G. S. Gilbert, R. A. Hufbauer, J. N. Klironomos, J. L. Maron, W. F. Morris, I. M. Parker, A. G. Power, E. W. Seabloom, M. E. Torchin, D. P. Vázquez, Biotic interactions and plant invasions. Ecol. Lett. **9**, 726–740 (2006).

18. C. D. Bacon, P. Molnar, A. Antonelli, A. J. Crawford, C. Montes, M. C. Vallejo-Pareja, Quaternary glaciation and the Great American Biotic Interchange. Geology **44**, 375–378 (2016).

19. S. D. Webb, Mammalian Faunal Dynamics of the Great American Interchange. Paleobiology **2**, 220–234 (1976).

20. S. D. Webb, Ecogeography and the Great American Interchange. Paleobiology **17**, 266–280 (1991).

21. L. G. Marshall, S. D. Webb, J. J. Sepkoski, D. M. Raup, Mammalian Evolution and the Great American Interchange. Science **215**, 1351–1357 (1982).

22. A. O'Dea, H. A. Lessios, A. G. Coates, R. I. Eytan, S. A. Restrepo-Moreno, A. L. Cione, L. S. Collins, A. de Queiroz, D. W. Farris, R. D. Norris, R. F. Stallard, M. O. Woodburne, O. Aguilera, M.-P. Aubry, W. A. Berggren, A. F. Budd, M. A. Cozzuol, S. E. Coppard, H. Duque-Caro, S. Finnegan, G. M. Gasparini, E. L. Grossman, K. G. Johnson, L. D. Keigwin, N. Knowlton, E. G. Leigh, J. S. Leonard-Pingel, P. B. Marko, N. D. Pyenson, P. G. Rachello-Dolmen, E. Soibelzon, L. Soibelzon, J. A. Todd, G. J. Vermeij, J. B. C. Jackson, Formation of the Isthmus of Panama. Sci. Adv. **2**, e1600883 (2016).

23. Miocene Mammals and Central American Seaways | Science. https://www.science.org/doi/abs/10.1126/science.148.3667.180.

24. M. O. Woodburne, The Great American Biotic Interchange: Dispersals, Tectonics, Climate, Sea Level and Holding Pens. J. Mamm. Evol. **17**, 245–264 (2010).

25. A. G. Coates, L. S. Collins, M.-P. Aubry, W. A. Berggren, The Geology of the Darien, Panama, and the late Miocene-Pliocene collision of the Panama arc with northwestern South America. GSA Bull. **116**, 1327–1344 (2004).

26. D. Schmidt, "The closure history of the Panama Isthmus: Evidence from isotopes and fossils to models and molecules" (2007), pp. 429–444.

27. C. Huguet, A. Jaeschke, J. Rethemeyer, Paleoclimatic and palaeoceanographic changes coupled to the Panama Isthmus closing (13–4 Ma) using organic proxies. Palaeogeogr. Palaeoclimatol. Palaeoecol. **601**, 111139 (2022).

28. L. Yi, M. Medina-Elizalde, L. Tan, D. B. Kemp, Y. Li, G. Kletetschka, Q. Xie, H. Yao, H. He, C. Deng, J. G. Ogg, Plio-Pleistocene deep-sea ventilation in the eastern Pacific and potential linkages with Northern Hemisphere glaciation. Sci. Adv. **9**, eadd1467 (2023).

29. G. Balco, C. W. Rovey II, Absolute chronology for major Pleistocene advances of the Laurentide Ice Sheet. Geology **38**, 795–798 (2010).

30. G. S. Morgan, S. D. Emslie, Tropical and western influences in vertebrate faunas from the Pliocene and Pleistocene of Florida. Quat. Int. **217**, 143–158 (2010).

31. J. D. Carrillo, S. Faurby, D. Silvestro, A. Zizka, C. Jaramillo, C. D. Bacon, A. Antonelli, Disproportionate extinction of South American mammals drove the asymmetry of the Great American Biotic Interchange. Proc. Natl. Acad. Sci. **117**, 26281–26287 (2020).

32. A. K. Behrensmeyer, N. E. Todd, R. Potts, G. E. McBrinn, Late Pliocene Faunal Turnover in the Turkana Basin, Kenya and Ethiopia. Science **278**, 1589–1594 (1997).

33. J. Alroy, Constant extinction, constrained diversification, and uncoordinated stasis in North American mammals. Palaeogeogr. Palaeoclimatol. Palaeoecol. **127**, 285–311 (1996).

34. N. J. Gotelli, Null Model Analysis of Species Co-Occurrence Patterns. Ecology **81**, 2606–2621 (2000).

35. R. D. Cordero, D. A. Jackson, Species-pair associations, null models, and tests of mechanisms structuring ecological communities. Ecosphere **10**, e02797 (2019).

36. M. W. Cadotte, Functional traits explain ecosystem function through opposing mechanisms. Ecol. Lett. **20**, 989–996 (2017).

37. M. W. Cadotte, K. Carscadden, N. Mirotchnick, Beyond species: functional diversity and the maintenance of ecological processes and services. J. Appl. Ecol. **48**, 1079–1087 (2011).

38. K. Stewart, C. P. Carmona, C. Clements, C. Venditti, J. A. Tobias, M. González-Suárez, Functional diversity metrics can perform well with highly incomplete data sets. Methods Ecol. Evol. **n/a**.

39. J. F. González-Maya, L. R. Víquez-R, A. Arias-Alzate, J. L. Belant, G. Ceballos, Spatial patterns of species richness and functional diversity in Costa Rican terrestrial mammals: implications for conservation. Divers. Distrib. **22**, 43–56 (2016).

40. S. Soliveres, F. T. Maestre, M. A. Bowker, R. Torices, J. L. Quero, M. García-Gómez, O. Cabrera, A. P. Cea, D. Coaguila, D. J. Eldridge, C. I. Espinosa, F. Hemmings, J. J. Monerris, M. Tighe, M. Delgado-Baquerizo, C. Escolar, P. García-Palacios, B. Gozalo, V. Ochoa, J. Blones, M. Derak, W. Ghiloufi, J. R. Gutiérrez, R. M. Hernández, Z. Noumi, Functional traits determine plant co-occurrence more than environment or evolutionary relatedness in global drylands. Perspect. Plant Ecol. Evol. Syst. **16**, 164–173 (2014).

41. B. S. Schamp, R. Gridzak, D. A. Greco, T. M. Lavender, A. Kunasingam, J. A. Murtha, A. M. Jensen, A. Pollari, L. Santos, Examining the relative influence of dispersal and competition on co-occurrence and functional trait patterns in response to disturbance. PLOS ONE **17**, e0275443 (2022).

42. D. M. Griffith, J. A. Veech, C. J. Marsh, **cooccur** : Probabilistic Species Co-Occurrence Analysis in R. J. Stat. Softw. **69** (2016).

43. J. A. Veech, A probability-based analysis of temporal and spatial co-occurrence in grassland birds. J. Biogeogr. **33**, 2145–2153 (2006).

44. E. Laliberté, P. Legendre, B. Shipley, FD: Measuring functional diversity from multiple traits, and other tools for functional ecology. R Package Version **1**, 0–12 (2014).

45. G. Bartoli, M. Sarnthein, M. Weinelt, H. Erlenkeuser, D. Garbe-Schönberg, D. W. Lea, Final closure of Panama and the onset of northern hemisphere glaciation. Earth Planet. Sci. Lett. **237**, 33–44 (2005).

46. S. T. Jackson, J. T. Overpeck, Responses of Plant Populations and Communities to Environmental Changes of the Late Quaternary. Paleobiology **26**, 194–220 (2000).

47. J. W. Williams, S. T. Jackson, Novel climates, no-analog communities, and ecological surprises. Front. Ecol. Environ. **5**, 475–482 (2007).

48. R. Cooke, W. Gearty, A. S. A. Chapman, J. Dunic, G. J. Edgar, J. S. Lefcheck, G. Rilov, C. R. McClain, R. D. Stuart-Smith, S. Kathleen Lyons, A. E. Bates, Anthropogenic disruptions to longstanding patterns of trophic-size structure in vertebrates. Nat. Ecol. Evol. **6**, 684–692 (2022).

49. Yukon to the Yucatan: Habitat partitioning in North American Late Pleistocene ground sloths (Xenarthra, Pilosa) | Journal of Palaeosciences. (2023).

50. A. A. Carlini, J. D. Carrillo-Briceño, A. Jaimes, O. Aguilera, A. E. Zurita, J. Iriarte, M. R. Sánchez-Villagra, Damaged glyptodontid skulls from Late Pleistocene sites of northwestern Venezuela: evidence of hunting by humans? Swiss J. Palaeontol. **141**, 11 (2022).

51. H. D. AHLBERG, "Geographical Variation in the North American Porcupine Erethizon (linnaeus) Cuvier (mammalia, Rodentia)," thesis, Boston University Graduate School, United States -- Massachusetts (1969).

52. E. Bōgner, J. X. Samuels, The first canid from the Gray Fossil Site in Tennessee: new perspective on the distribution and ecology of Borophagus. J. Paleontol. **96**, 1379–1389 (2022).

53. X. Wang, Ó. Carranza-Castañeda, J. J. Aranda-Gómez, A transitional skunk, Buisnictis metabatos sp. nov. (Mephitidae, Carnivora), from Baja California Sur and the role of southern refugia in skunk evolution. J. Syst. Palaeontol. **12**, 291–302 (2014).

54. J. F. Robinson, J. E. Dickerson, Does Invasion Sequence Affect Community Structure? Ecology **68**, 587–595 (1987).

55. E. Schwindt, A. Bortolus, O. O. Iribarne, Invasion of a Reef-builder Polychaete: Direct and Indirect Impacts on the Native Benthic Community Structure. Biol. Invasions **3**, 137–149 (2001).

56. D. E. Spooner, C. C. Vaughn, A trait-based approach to species' roles in stream ecosystems: climate change, community structure, and material cycling. Oecologia **158**, 307–317 (2008).

57. M. V. Lomolino, Mammalian community structure on islands: the importance of immigration, extinction and interactive effects. Biol. J. Linn. Soc. **28**, 1–21 (1986).

58. F. A. Smith, C. P. Tomé, E. A. Elliott Smith, S. K. Lyons, S. D. Newsome, T. W. Stafford, Unraveling the consequences of the terminal Pleistocene megafauna extinction on mammal community assembly. Ecography **39**, 223–239 (2016).

59. Å. Lindström, M. Green, G. Paulson, H. G. Smith, V. Devictor, Rapid changes in bird community composition at multiple temporal and spatial scales in response to recent climate change. Ecography **36**, 313–322 (2013).

60. I. MacGregor-Fors, L. Morales-Pérez, J. Quesada, J. E. Schondube, Relationship between the presence of House Sparrows (Passer domesticus) and Neotropical bird community structure and diversity. Biol. Invasions **12**, 87–96 (2010).

61. J. Rodríguez, Stability in Pleistocene Mediterranean mammalian communities. Palaeogeogr. Palaeoclimatol. Palaeoecol. **207**, 1–22 (2004).

62. A. Bercovici, V. Vajda, D. Pearson, U. Villanueva-Amadoz, D. Kline, Palynostratigraphy of John's Nose, a new Cretaceous–Paleogene boundary section in southwestern North Dakota, USA. Palynology **36**, 36–47 (2012).

63. S. L. Wing, C. A. E. Strömberg, L. J. Hickey, F. Tiver, B. Willis, R. J. Burnham, A. K. Behrensmeyer, Floral and environmental gradients on a Late Cretaceous landscape. Ecol. Monogr. **82**, 23–47 (2012).
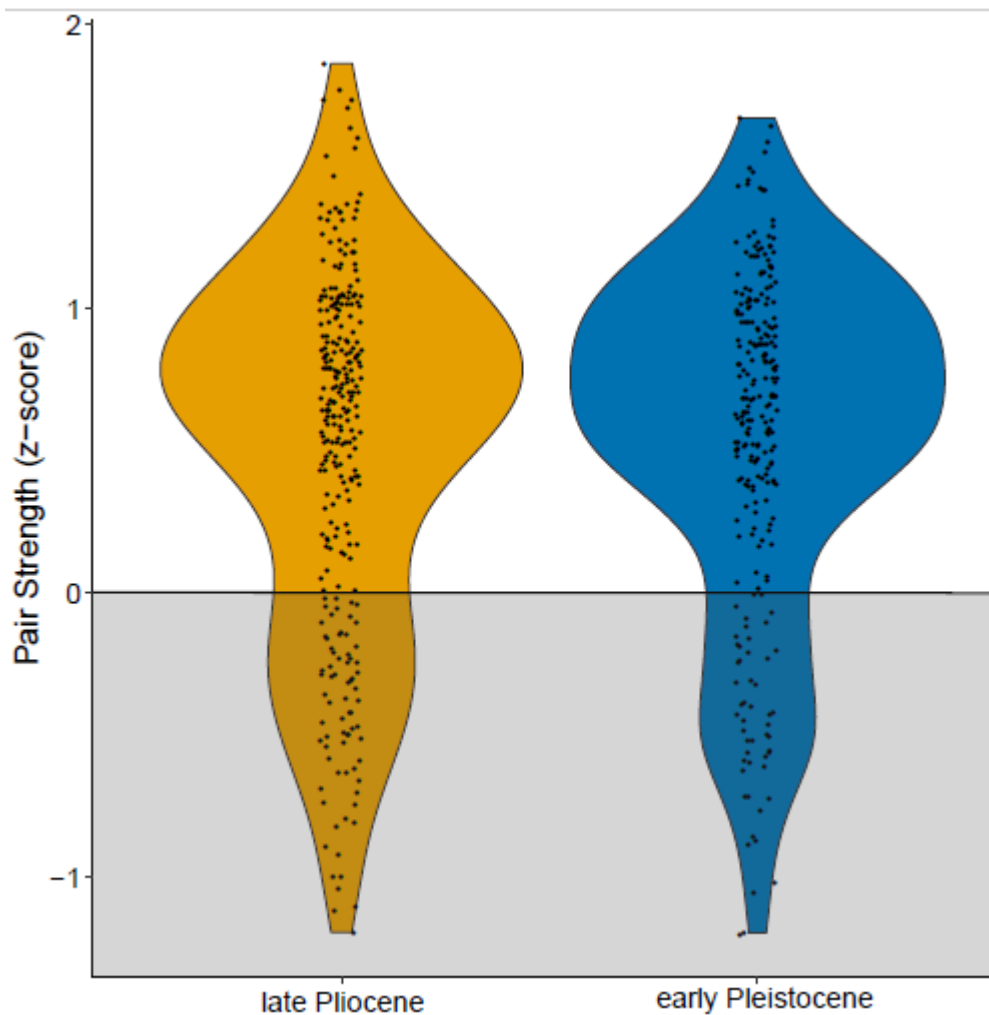
Tables and Figures

Figure 1. The distribution of z-scores for all significant pairs in pre and post-transition time bins. Scores less than zero indicate segregations, and scores greater than zero indicate aggregations. The plot widens along the y-axis based on the number of genus pairs. Areas with a greater number of pairs and becomes thinner where there are fewer pairs.
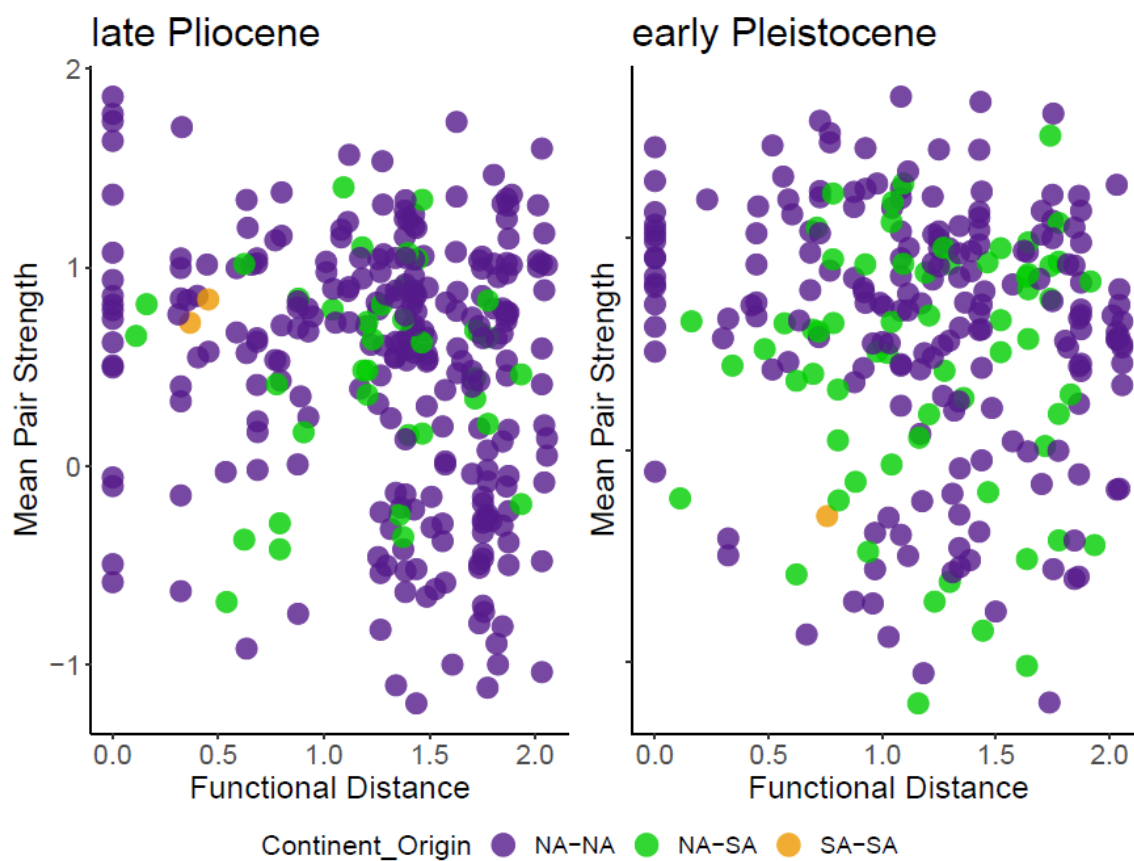
Figure 2. Graph showing the relationship between the mean strength of significant genera and the functional distance between them. The color of the points represents the origin of the genera. Functional distance is the Euclidean distance calculated between mammal genera using the four PCoA axes from the functional diversity analysis.
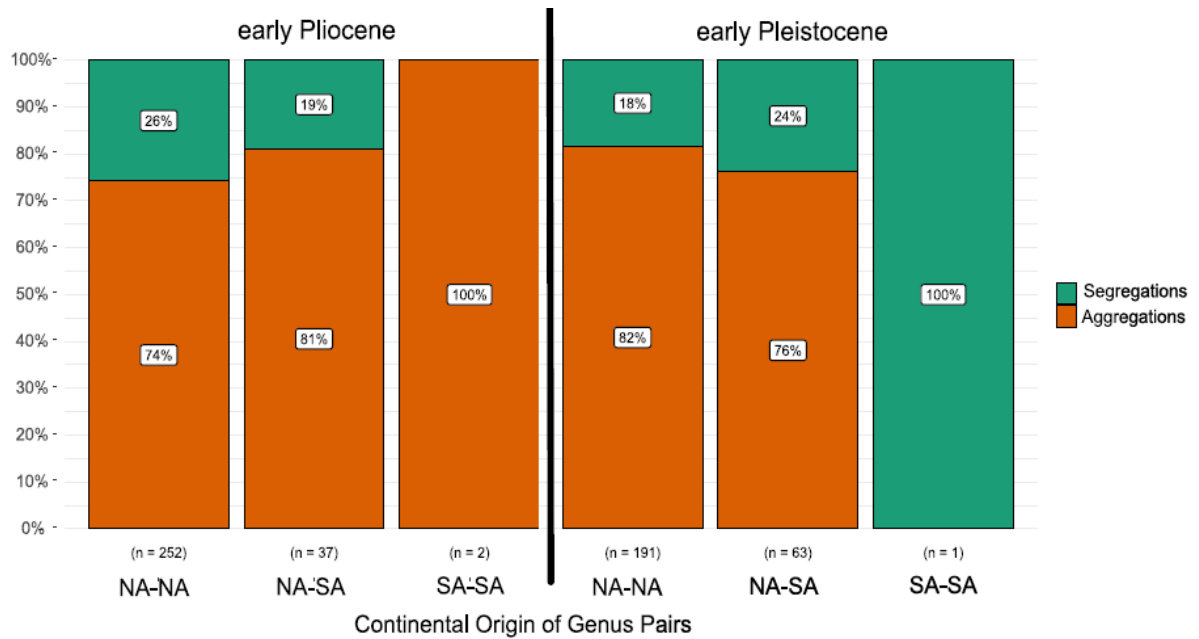
Figure 3. Within North America, proportions of genus pairs forming significant associations of the same and different continental origins. There is no significant difference in the proportion of aggregations and segregations based on the continental origins forming the pairs.
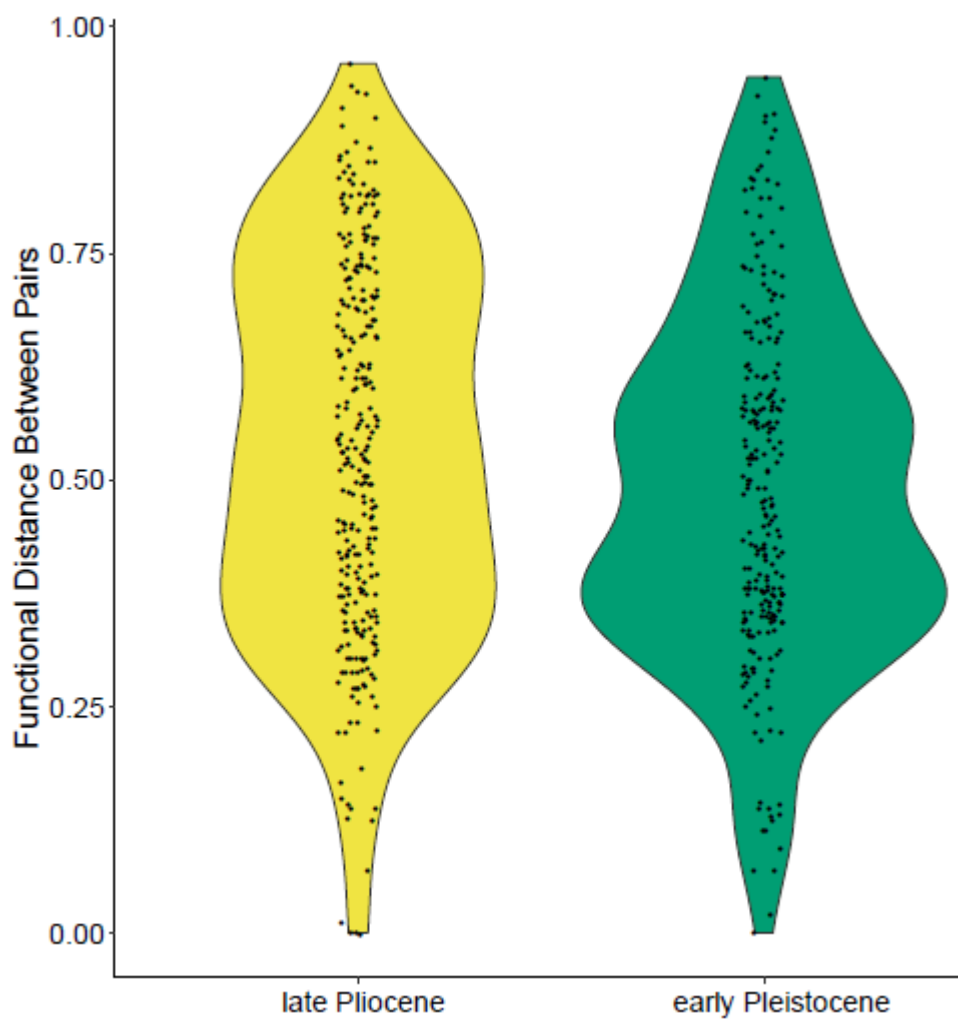
Figure 4. Distributions of functional distance between all significant pairs in the pre and early Pleistocene times bins. Functional distance of the y-axis is found by calculating the Euclidean distance between significant genus pairs in multidimensional trait space. The violin plot widens with a greater number of genus pairs and thins with fewer pairs.
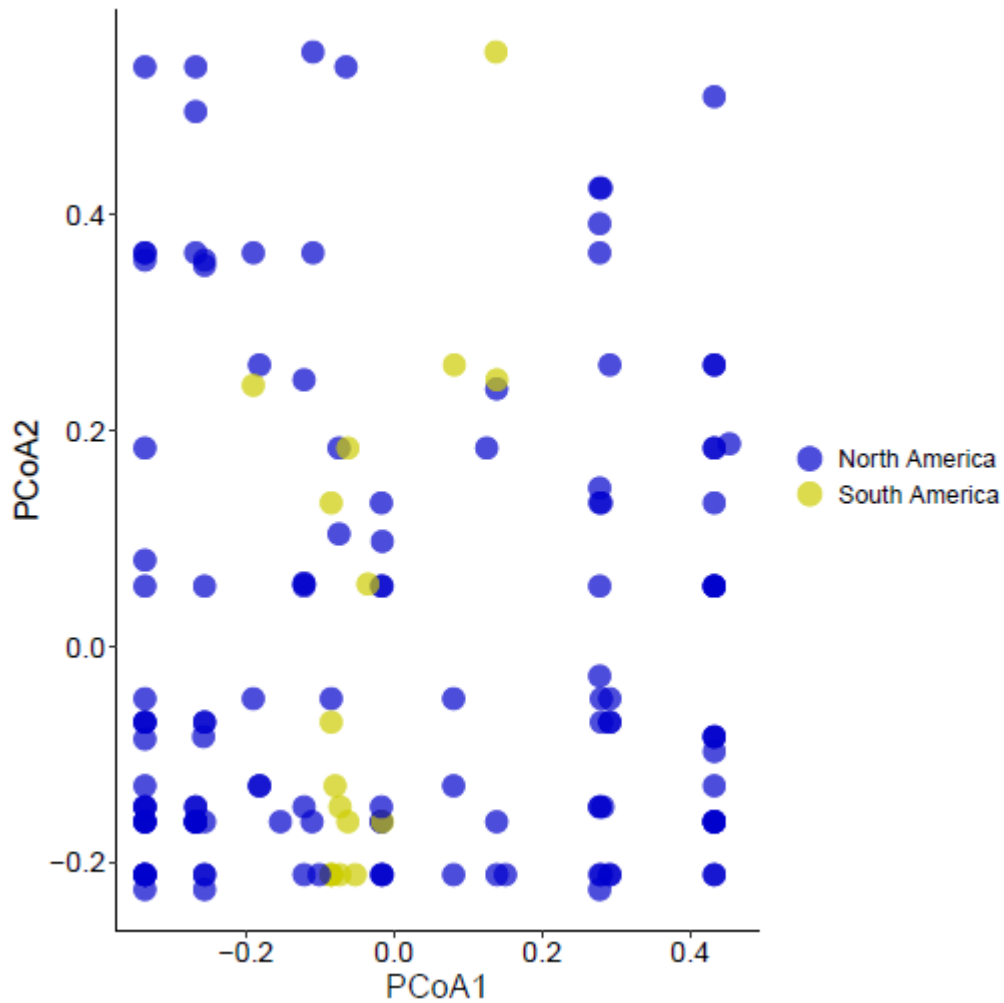
Figure 5. **Distribution of North and South American genera in multidimensional space based on functional diversity PCoA axes**. South American migrants are primarily concentrated in the lower-mid region of trait space with few overlapping North American genera.
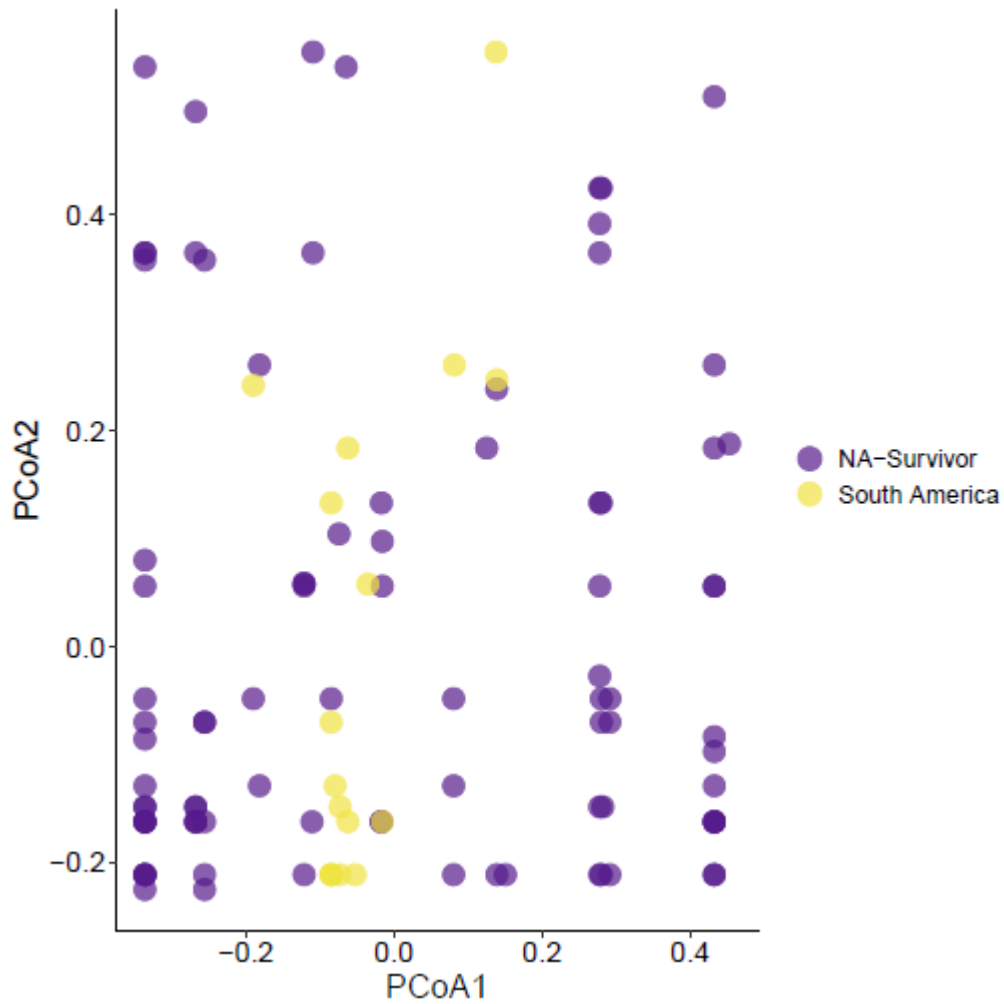
Figure 6. **Ordination of surviving North American genera and South American immigrants in functional space using the first two PCoA axes**. South American migrants are primarily concentrated in the lower-mid region of trait space with few overlapping North American genera.
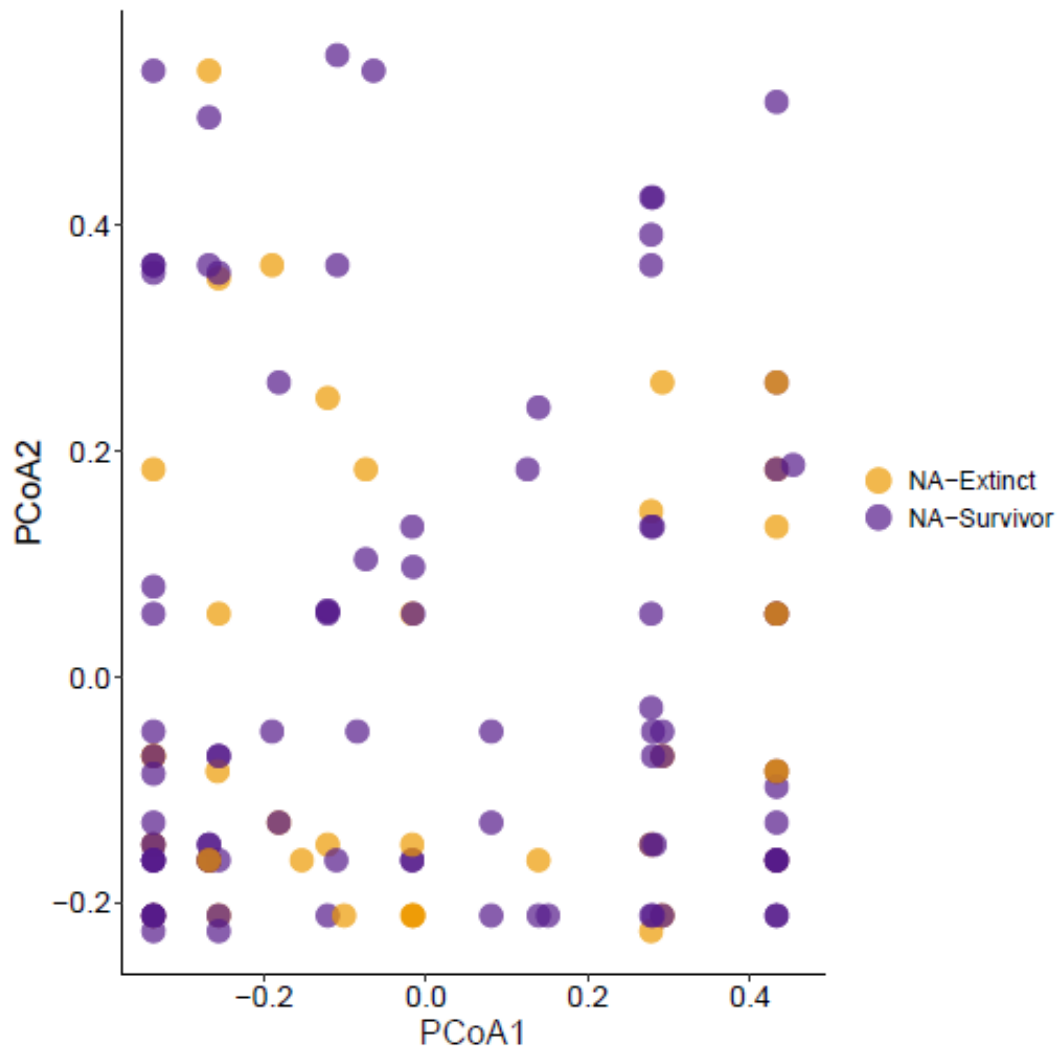
Figure 7. **Ordination of extinct and surviving North American genera in functional space using the first two PCoA axes**.
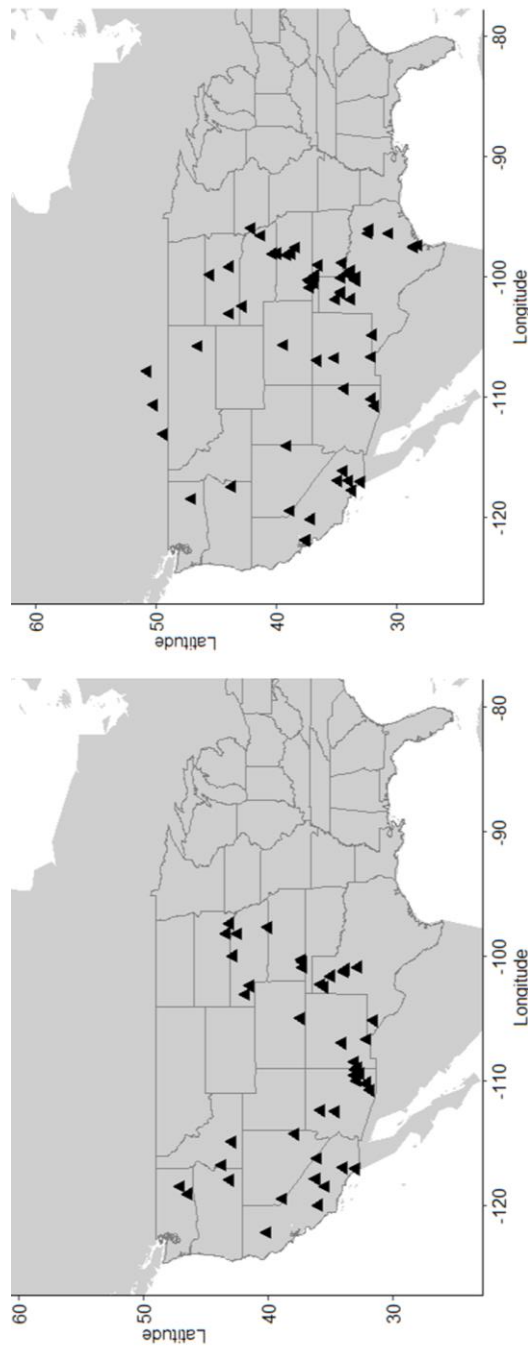
Figure S1. **Geographic locations of the fossil localities**. Late Pliocene on the left and early Pleistocene on the right.
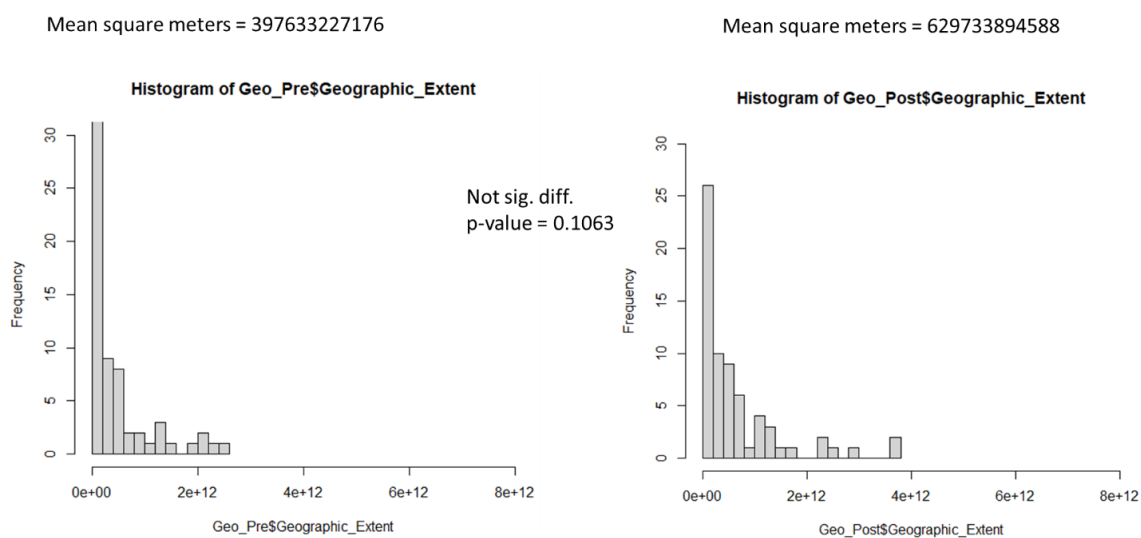
Figure S2. **Geographic distances between localities.** They are not significantly different between time bins. P-value provided by a Kolmogorov-Smirnov test. Pre represents the pre-glaciation period of the late Pliocene. Post represents the post-glaciation period of the early Pleistocene.

Figure S3. **Barplot of trait distributions using proportions from pre to post glaciation of all significant pairs**. Pre represents the pre-glaciation period of the late Pliocene. Post represents the post-glaciation period of the early Pleistocene.
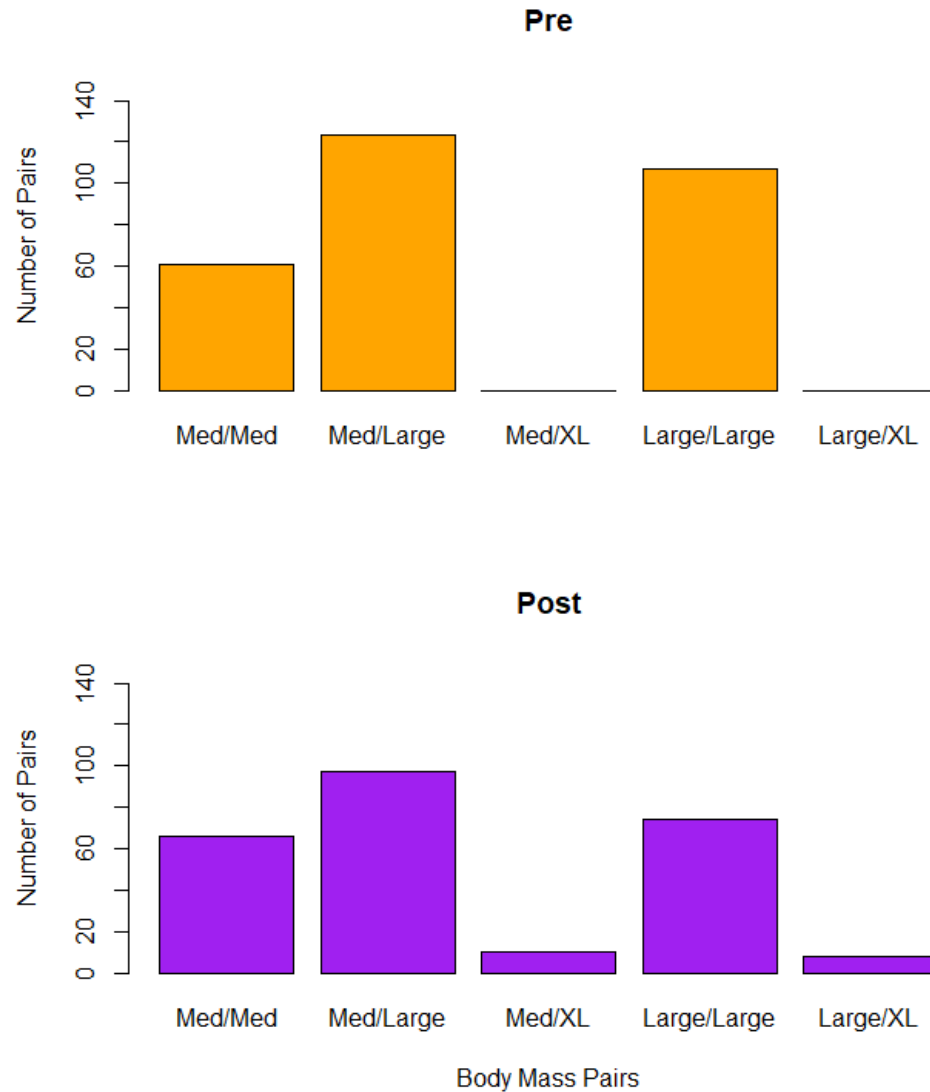
Figure S4. **Barplot of body mass category pairs between all significantly aggregating and segregating genera**. Pre represents the pre-glaciation period of the late Pliocene. Post represents the post-glaciation period of the early Pleistocene
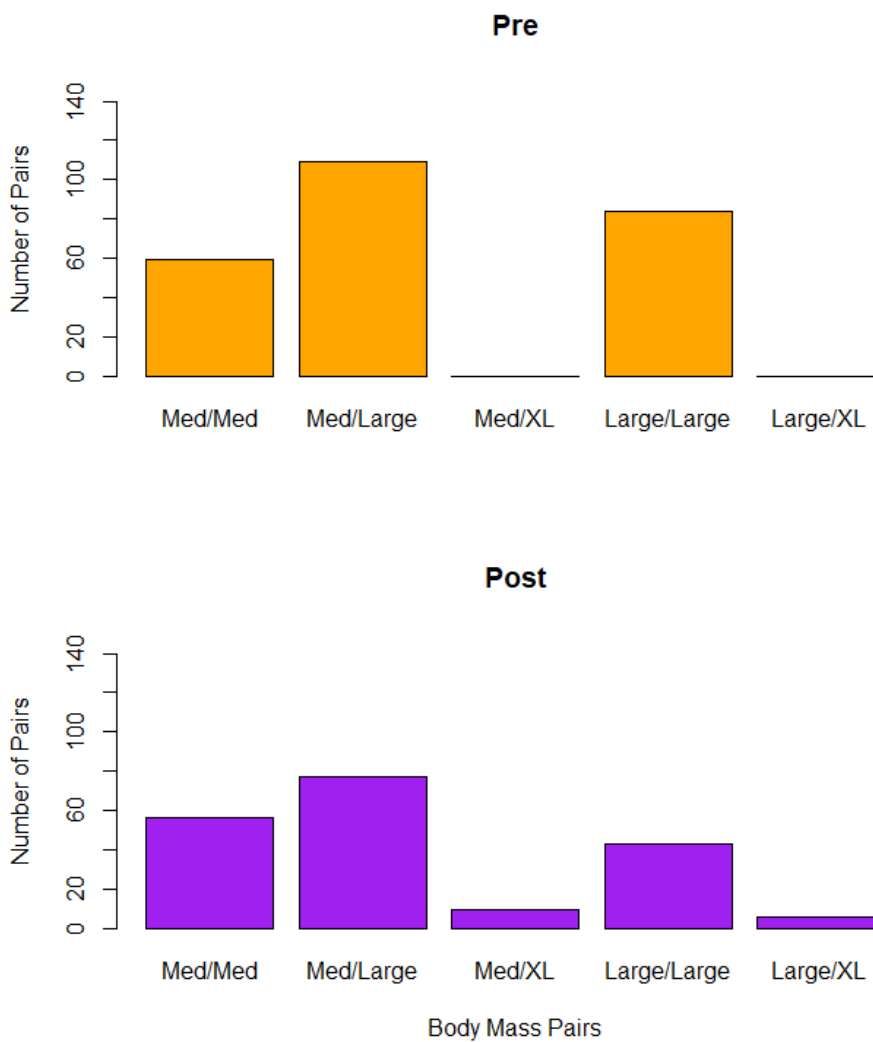
Figure S5. **Barplot of body mass category pairs between all significantly aggregating and segregating NA-NA pairs**. Pre represents the pre-glaciation period of the late Pliocene. Post represents the post-glaciation period of the early Pleistocene.
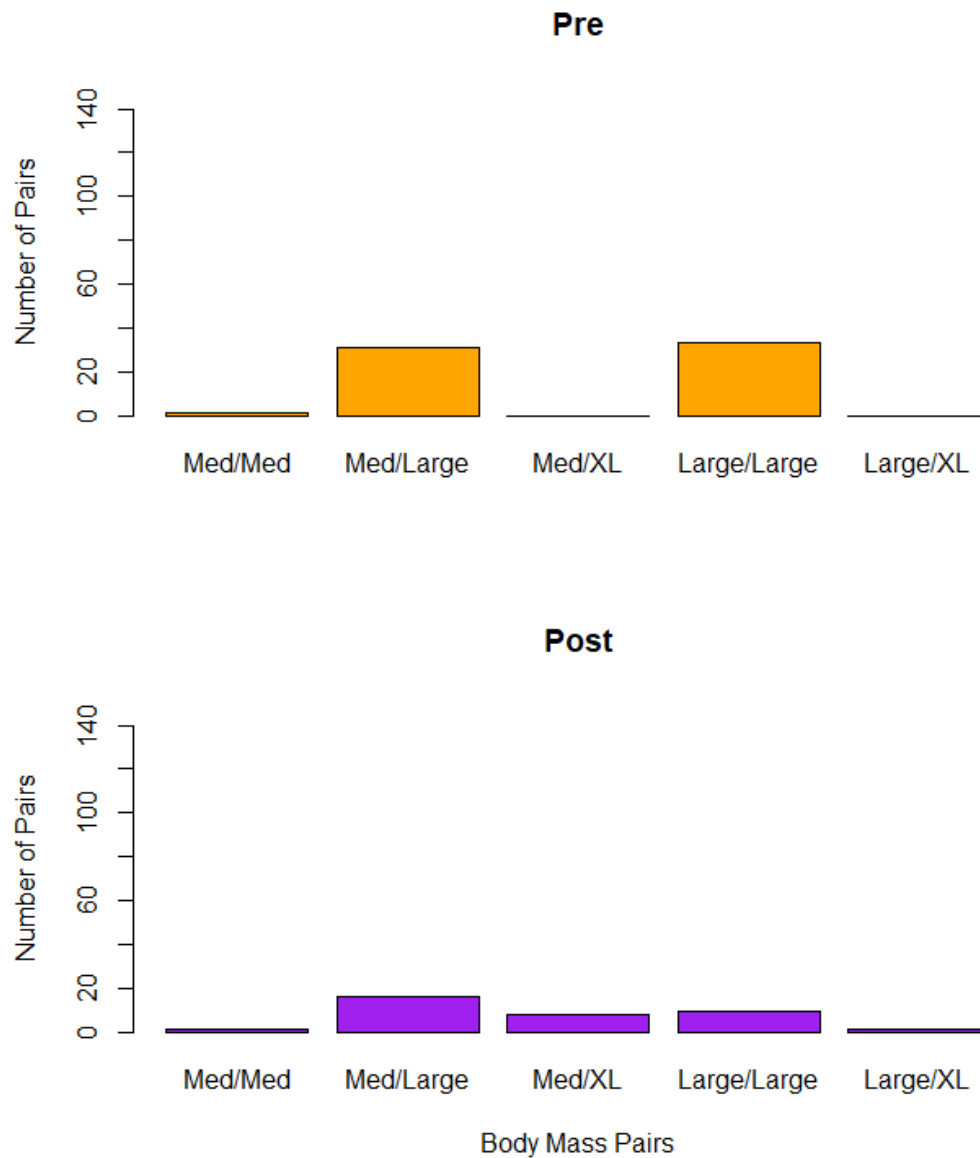
Figure S6. **Barplot of body mass category pairs between all significantly segregating NA-NA pairs**. Pre represents the pre-glaciation period of the late Pliocene. Post represents the post-glaciation period of the early Pleistocene.
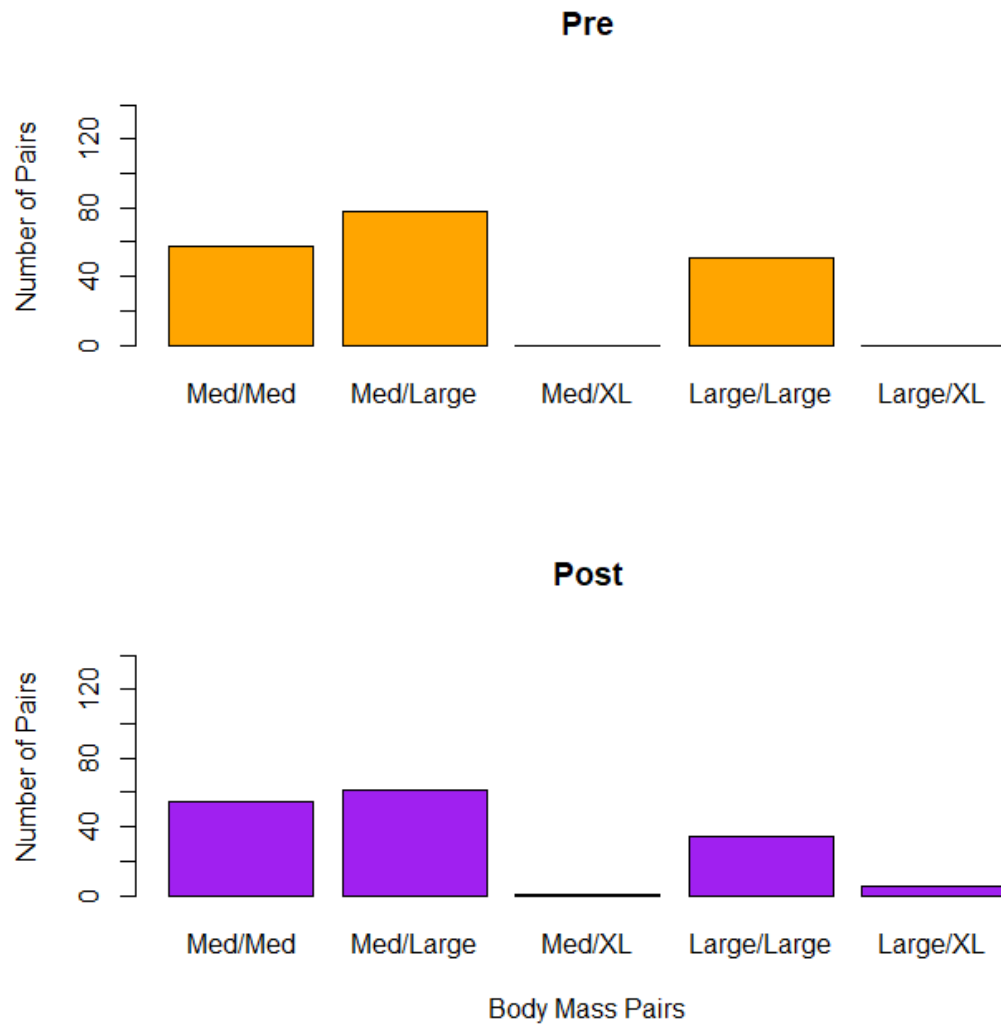
Figure S7. **Barplot of body mass category pairs between all significantly aggregating NA-NA pairs**. Pre represents the pre-glaciation period of the late Pliocene. Post represents the post-glaciation period of the early Pleistocene.
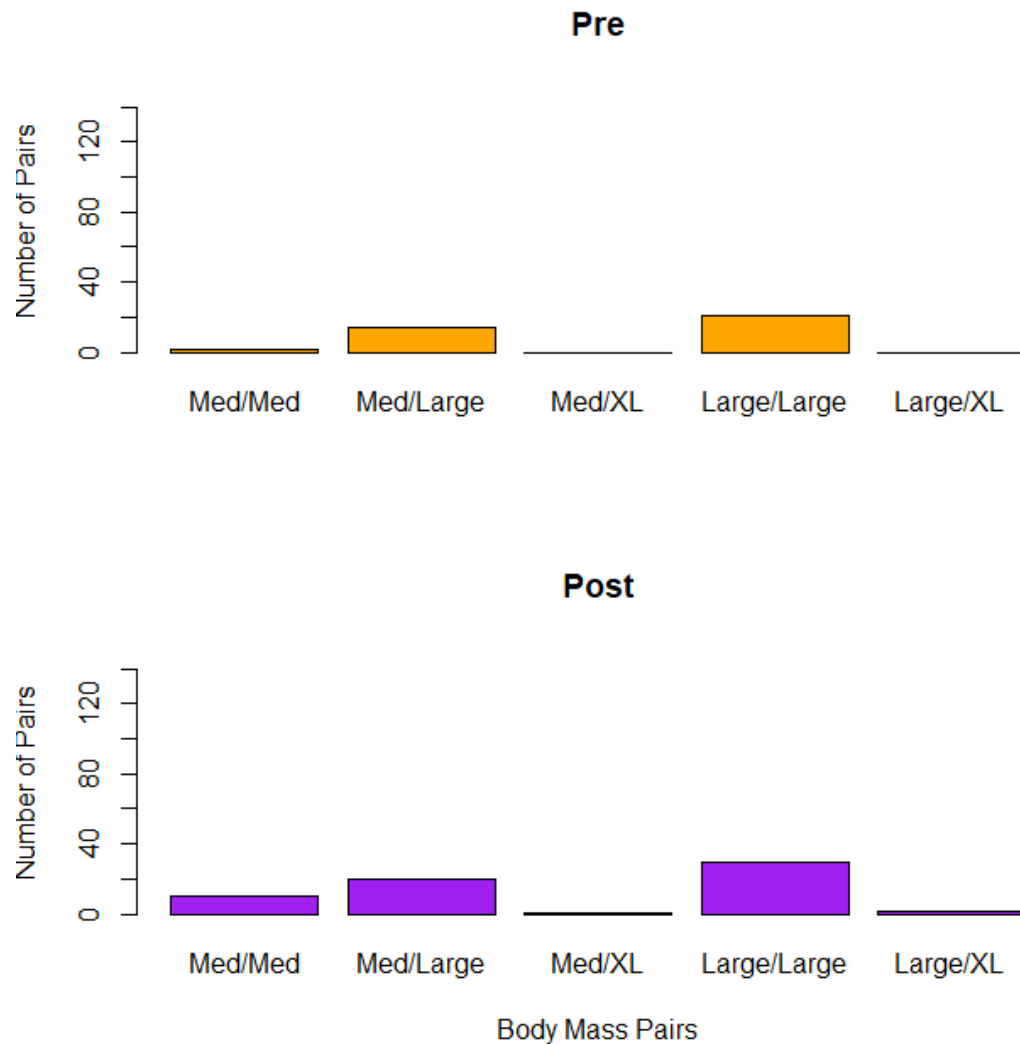
Figure S8. **Barplot of body mass category pairs between all significantly aggregating and segregating pairs NA-SA pairs**. Pre represents the pre-glaciation period of the late Pliocene. Post represents the post-glaciation period of the early Pleistocene.
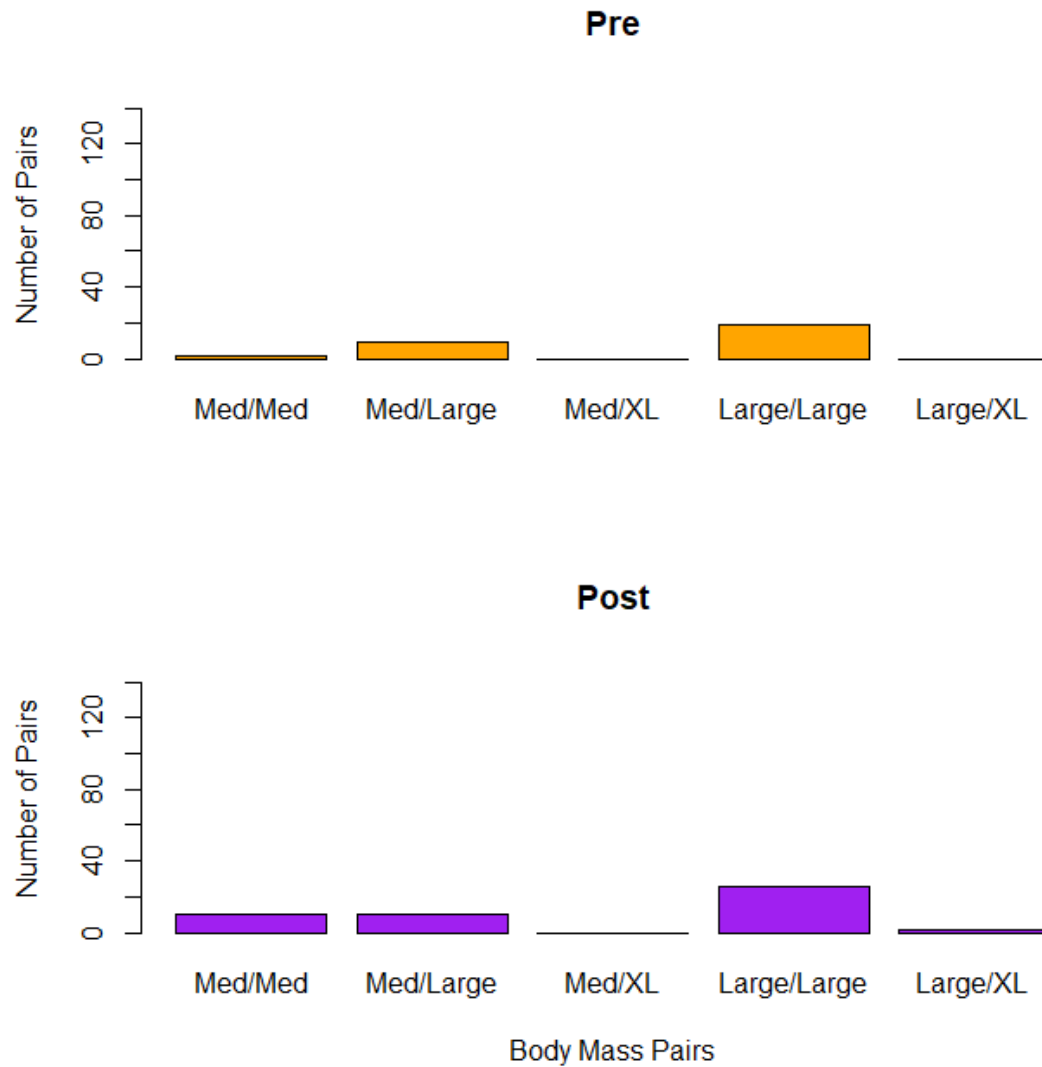
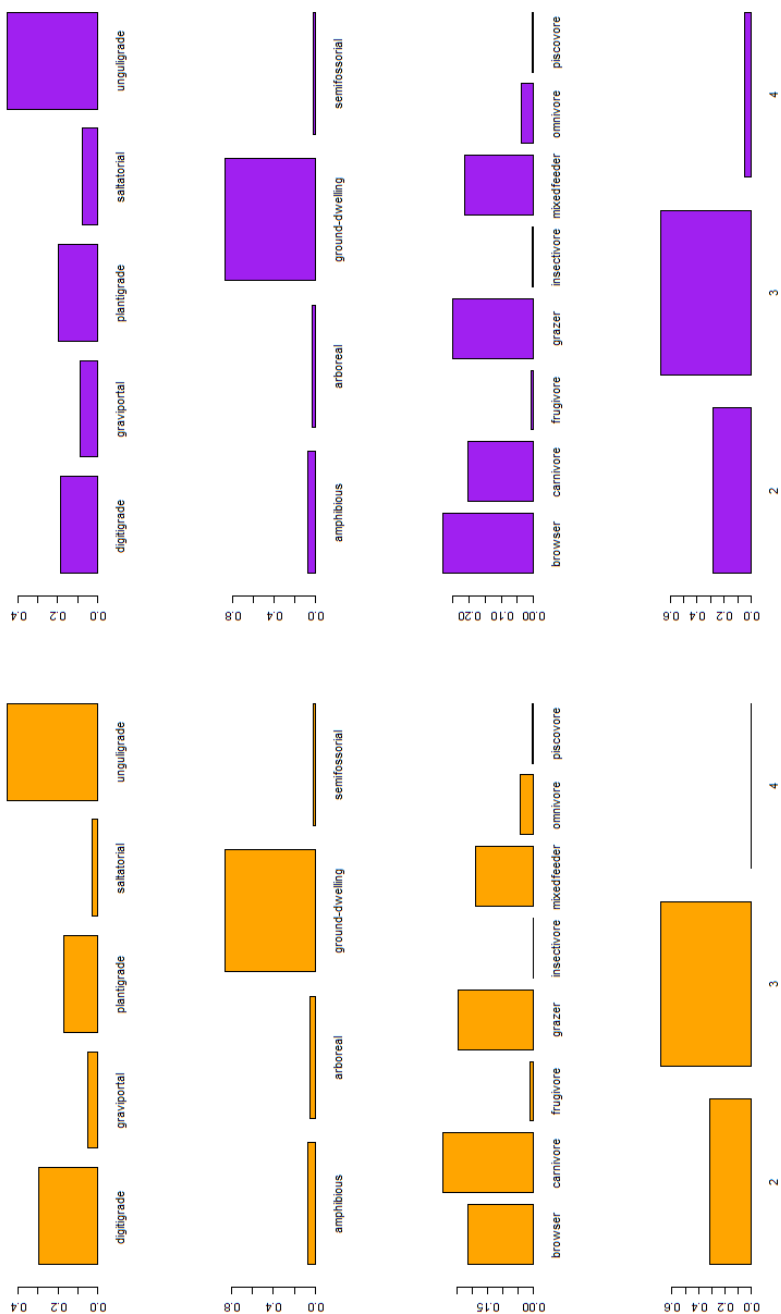Figure S9. **Barplot of body mass category pairs between all significantly aggregating NA-SA pairs.** Pre represents the pre-glaciation period of the late Pliocene. Post represents the post-glaciation period of the early Pleistocene.
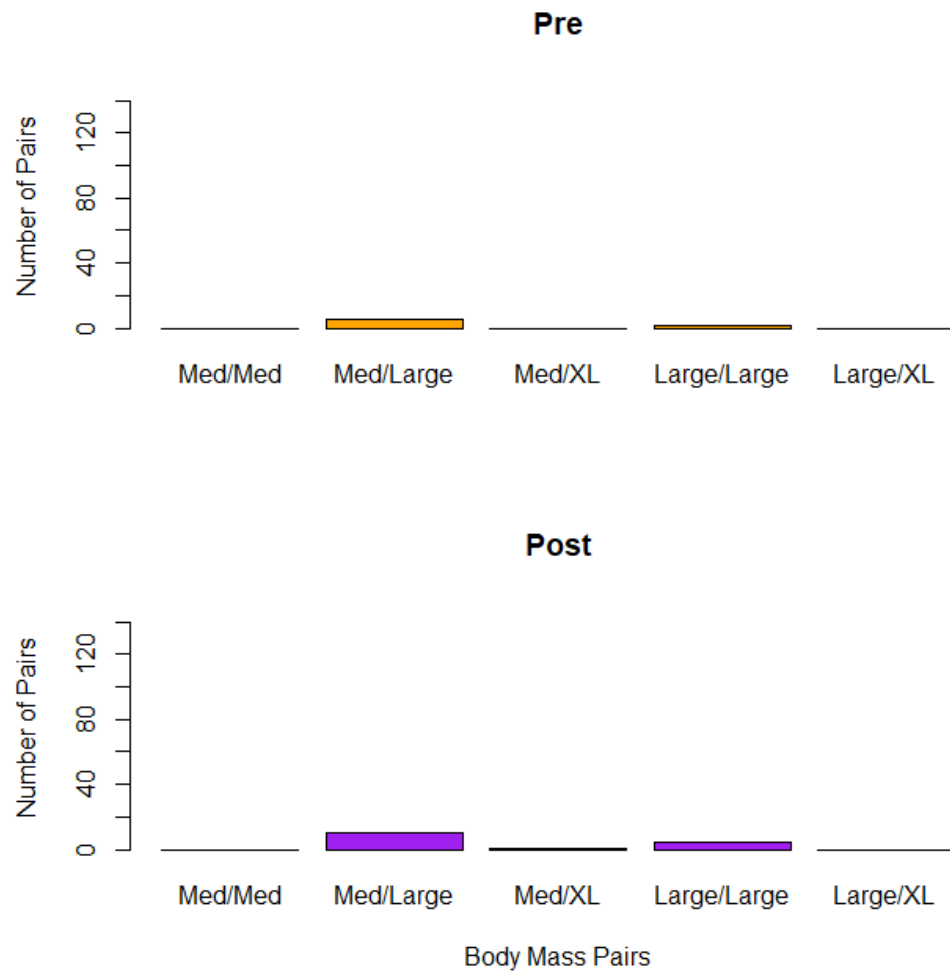
Figure S10. **Barplot of body mass category pairs between all significantly segregating NA-SA pairs**. Pre represents the pre-glaciation period of the late Pliocene. Post represents the post-glaciation period of the early Pleistocene.

Appendix A

Chapter 1 Supplementary Materials Section

Taxonomy and Traits

There were 264 paleocommunities compiled for this study that were downloaded from published databases (Alroy 1998, Smith et al. 2018, Paleobiology Database; paleobiodb.org/). The most updated taxonomic name for each species was collected from the PBDB. The estimated date ranges for each paleocommunity based on geologic location were modified to the best of our ability to reduce age uncertainties using the primary literature (Datafile1: Locality Dating). Our 264 paleocommunities had an average age range of 1.539 million years. Our database includes 2,462 mammal species. A combination of databases and primary literature were used to identify species traits: locomotion, diet, life habit and body mass (table S1, DataFile2: Mammal Traits). Locomotion is identified by the limb morphology of the mammal species. Life habit is described as the most common lifestyle the mammal has within a habitat. Diet is based on the most common food source of the species. Diet categories were restricted to those we could most accurately be distinguished in the fossil record. Some diet categories used in our databases were combined to limit diet uncertainties in earlier or rarer species (table S1); granivores were combined with frugivores and piscivores were considered carnivores. Species traits that were unable to be found in primary sources were filled using that of the lowest taxonomic rank available. When body mass was not available, body mass was averaged at the lowest available taxonomic level (genus, family, order).

A complete list of taxa and trait data can be found in DataFile2 as well as reference information for each trait.

Occurrences and Chronostratigraphy

We use fossil occurrence data on 34165 North American occurrences of terrestrial mammal species from 7271 localities spanning from the Campanian to the Holocene that were downloaded from the Paleobiology Database (PBDB) on 2021-08-25. We refined the upper and lower bounds of site ages provided by PBDB in several ways. First, we used an updated time scale (particularly for North American Land Mammal Ages) based on Gradstein et al (2020). Second, those localities assigned to a particular faunal zone receive the upper and lower bounds for that zone rather than for the time interval. We base zone ages on either Gradstein et al. (2020), or (for older zonation schemes) published correlations between alternative zonation schemes and those used in Gradstein et al. (2020). The compete compilation is available at https://github.com/PeterJWagner3/Supplementary/tree/main/RData_Databases. Finally, we used still more refined dates from radiometric dates or from ordinations such as Appearance Event Ordination (Alroy 1994) when available.

We assigned sites and finds to 1 million-year (1-myr) duration bins. The upper and lower bounds of many sites often span more than one million years. Even those sites with a possible age range of less than one million years would span two bins: e.g., a site places in the *Wa6* zone is between 53.25 and 52.95 million years old. Thus, sites were given a probability of being in each bin. A site from the *Wa6* zone thus would have a probability of 0.833 of being in the 54-53 Ma bin and a probability of 0.167 of being in

the 53-52 Ma bin. We calculate the probability of a species being present in any 1-myr

bin as one minus the product of the probability that each site including the species is

absent from that bin. For example, if a species is known from 6 sites from the *Wa6* zone,

then P[present 54-53 Ma] = $1-(1–0.833)^6=0.9998$, and P[present 53-52

Ma=$1-(1-0.167)^6=0.665$. P[present]=1.0 for any 1 myr bin only if the upper bound of one

or more sites belongs to that bin or an older one, and the lower bound to one or more sites

belongs to that one or a younger bin. For example, a species known from *Wa3* (55.0-54.5

Ma) and *Wa7* (53.25-52.95 Ma) must be present in the both the 55-54 Ma bin and the 54-

53 Ma bin. For our analyses, we assumed that a species was present in a bin if P[present]

> 0.5. Thus, species known from very few and/or poorly constrained sites wind up

excluded from our analyses. However, 3544 of the 3964 species in the PBDB are placed

in at least one bin with a probability > 0.5.

Statistics

We used the methods found in Villéger et al. 2008 and the function dbfd from the

R package "FD" to calculate functional diversity. We calculated three components of

functional diversity; functional evenness, functional richness, and functional divergence

(for description see table S2). These three indices were chosen because they are

independent from one another. To calculate functional diversity, we created a trait matrix

that included species names and four traits (i.e., locomotion, body mass, life habit, diet).

The trait matrix is converted into a distance matrix using Gower's dissimilarity method

(Petchey and Gaston 2002). We used the Gowers dissimilarity distance method due to

the use of categorical data. A PCoA is run on the distance matrix to ordinate species in

multidimensional space by returning PCoA coordinated for each species. Our data is non-Euclidean, so we applied the square root correction. Five axes were used to calculate the convex hull volume for each paleocommunity. We have a 0.71 reduced quality measure of functional space with five axes. All analyses were computed using R software (R Development Core Team 2019).

To identify significant shifts in functional diversity we ran a breakpoint analysis on each functional diversity index. We used the R package "breakpoint" to estimate the location of breakpoints for each FD index. These estimates were then plugged into R package "segmented" to determine the exact location of breakpoints and the appropriate number of breakpoints occurring in each FD index. AICc values were used to determine the best number of breakpoints for each functional diversity index (table S3-S5). To evaluate the potential relationship between global climate and mammalian functional diversity, delta-^{18}O were gathered from the most recent global temperature reconstruction found in Westerhold et al. 2020. The delta-^{18}O values were averaged for each paleocommunity based on the age range of that locality. For example, if a locality has an estimated age between 50 and 48 million years, all delta-^{18}O values within those two million years were averaged. Delta-^{18}O does not have a significant effect on FRic or FDiv (Fig. 4). FEve has a weak, positive relationship with delta-^{18}O primarily driven by Pleistocene paleocommunities that had high FEve values and high delta-^{18}O values (Fig.4).

We calculated functional diversity of the North American continental mammal fauna in the 1 Myr-bins as described above. This helps us to infer processes acting on the

continental fauna and influencing the way mammals filtering into communities. These species were then matched with the mammal trait data. Functional diversity was calculated using bins as sites. The square-root correction was used for our non-Euclidean data and five axes were used to calculate functional richness to correspond with the methods for our community-level functional diversity calculations. The quality of the reduced multidimensional space to calculate functional richness was 0.720325. The square-root correction was used for our non-Euclidean data and five axes were used to calculate functional richness to correspond with the methods for our community-level functional diversity calculations. The quality of the reduced multidimensional space to calculate functional richness was 0.7235852.

To demonstrate functional changes in multidimensional space of the North American mammal fauna, we plotted species in 1-million-year time bins using each species PCoA axes calculated from the dbfd function in the "FD" package for ordination. We used the stat_density_2d function from the R package "ggplot2" to create a visual tool. The graph shows changes in the density of species found in functional space and how it changes through time (Figs 4, S12).

We calculated the proportion of archaic orders verses modern orders in paleocommunities and ran a regression on the proportion of archaic orders and each functional diversity index to determine if archaic mammals assembled differently than modern orders. If they did assemble differently than modern orders, we would expect to see a shift in mammal paleocommunity structure during the period of time when they go extinct about 29 Ma. The regressions were only run with paleocommunities older than 29

million years old to only include the period before archaic orders went extinct. We see no significant relationship between the proportion of archaic orders and functional diversity indices (Fig. 4). The regressions do show a pattern of low functional diversity and paleocommunities with high proportions of archaic orders stemming from Paleocene paleocommunities prior to the major Paleocene-Eocene immigration events of new orders of mammals into North America.

Origination and extinction rates

We estimate extinction and origination rates using sampling+survivorship (sampling+reverse-survivorship or nascence for origination) analyses (Foote 2001b, 2003, Alroy 2008). We use a modification of prior methods presented in Congreve et al. (2021). The procedure is the same for both origination (λ) and extinction rates (μ), save that we estimate extinction based on taxa sampled in younger intervals and origination based on taxa sampled in older intervals. The likelihood of any given λ over time t is $L[\lambda t|S_{9\&10},S_{10}]$ where S_{10} is the number of species in Bin 10 and $S_{9\&10}$ is the number of species in Bins 9 & 10. If we observe $S_{10}=100$ species in Bin 10, $s_o=65$ of those 100 species in Bin 9, and another $s_R=10$ of the remaining ($S_{10}-s_o$)=35 species in Bin 8, then $S_{9\&10}$ is at least 75. However, it might be as high as 100 if we "simply" failed to sample all 25 of those species (Sepkoski 1975, Foote and Raup 1996). The likelihood of λ now is weighted by the binomial probability of $S_{9\&10}$ given S_{10} and some sampling rate ψ (Foote 1997, 2001a). The sampling rate ψ makes its own predictions about the number of sampled species: $P[1+ \text{finds} | \psi,t]=1-e^{-\psi t}$. The likelihood of any hypothesized richness, $S_{9\&10}=(s_o+s_R)\ldots S_{10}$, then is the binomial probability $P[s_o | S_{9\cdot10}, 1-e^{-\psi t}]$. Now:

$$L[\lambda, t | s_o, s_R, S_{10}] = \sum_{S_{9\&10} = (S_o + S_R)}^{S_{10}} P[s_o | \psi, S_{9\&10}, t] \times L[\lambda, t | S_{9\&10}, S_{10}] \quad \text{[eq. 1]}.$$

In the example above, the likelihood of λ becomes the probability of 25 species evolving

from a pool of 75 species given λ × the probability of sampling 65 of 75 species given ψ

+ the probability of 24 species evolving from a pool of 76 species × the probability of

sampling 65 of 76 species given ψ + etc. + the probability of 0 species evolving from a

pool of 100 species × the probability of sampling 65 of 100 species given ψ. This

marginalizes the unknown $S_{9\&10}$ by considering all possible values of S_H.

The approach outlined above accounts for both imperfect sampling and variable sampling

over time. The latter is considerable, as shown by the variation in sites per 1 myr bin

(Supplementary Figure 1). However, within any one bin, the sampling rate (ψ) is never

homogeneous among taxa: even when preservation potential of individuals is

comparable, occupancy distributions among taxa typically are exponential (Liow 2013,

Foote 2016); this in turn generates exponential distributions of sampling rates among

contemporaneous species in which the *mean* sampling rate is greater than the median

(Wagner and Marcot 2013). We can use quantiles from a sampling distribution to

marginalize this uncertainty when assessing the likelihood of λ:

$$L[\lambda, t | s_o, s_R, S_{10}] = \sum_{q=1}^{Q} \sum_{S_{9\&10} = (S_o + S_R)}^{S_{10}} \frac{P[s_o | \psi_q, S_{9\&10}, t] \times L[\lambda, t | S_{9\&10}, S_{10}]}{Q} \quad \text{[eq. 2]}.$$

Here, we used 4 quartiles and thus average the likelihood of λ over $Q=4$ possible

sampling rates. We estimate the distribution of sampling rates for each 1 myr bin

following the approach set out by Wagner and Marcot (2013). As in prior studies,

lognormal distributions typically do much better than do either exponential distributions or the null invariant model. We therefore use lognormal distributions for each 1 Myr-bin. Origination and extinction rate likelihoods for each bin reflect the probability of all possible survivors from the prior bin (origination) or to the next subsequent bin (extinction) multiplied by the probability of sampling the observed number of species given the possible richness and the best lognormal distribution of sampling rates. Thus, in our final analyses, the likelihood of λ is the probability of 25 species evolving from a pool of 75 species given $\lambda \times$ the average probability of sampling 65 of 75 species given ψ_1, ψ_2, ψ_3 & ψ_4 + the probability of 24 species evolving from a pool of 76 species $\times$ the average probability of sampling 65 of 76 species given ψ_1, ψ_2, ψ_3 & ψ_4 + etc. + the probability of 0 species evolving from a pool of 100 species $\times$ the average probability of sampling 65 of 100 species given ψ_1, ψ_2, ψ_3 & ψ_4, with ψ_1, ψ_2, ψ_3 & ψ_4 coming from the best model describing the distribution of species with 1, 2, 3, etc. finds in each bin.

Controlling for Biases in the Fossil Record and Sensitivity Analyses

To control for taphonomic biases in the data, we required the communities to have a minimum of 15 species and three clades; rodents, ungulates and carnivores. These clades are representative of trophic levels and varying body sizes. Before the appearance of order Rodentia other orders filling the same niche were accepted. Coastal communities and marine mammals were excluded from this study as well as order Chiroptera due to poor preservation.

There is a bias in the fossil record against small-bodied mammals in that they are less likely to preserve and are more common in the most recent fossil localities. Many

studies exclude mammals under 1kg to remove this issue. However, including small-bodied mammals is essential in gaining an accurate understanding of paleocommunity functional diversity. To test for a bias in our data, we found the bottom quartile of body mass in our data and plotted it against time. No relationship was found between time and the number of small-bodied mammals (fig. S9). No size bias was found against small-bodied mammals in our data, so we included the full range of mammalian body sizes. We included body mass for each species as a trait to calculate functional diversity.

However, there were not body mass estimates available for every species in the database. For these species, they were given a body mass average using a higher taxonomic rank (e.g. genus, family). The same approach was taken for mammals that were not identified to species or genus. For example, if the mammal was identified as Ursus sp., all available Ursus species body masses were averaged and used as Ursus sp.'s body mass estimate. We wanted to be sure that having averaged body masses in our database did not alter our results, so we removed all averaged species and recalculated functional diversity. The overall pattern of all three functional diversity indices remained the same, suggesting that the averaged body masses did not determine our results (fig. S5).

We also ran regressions for each functional diversity index against species richness to determine if changes in species richness over the Cenozoic were driving our results. We found a strong, positive relationship existed between species richness and the functional richness of paleocommunities with more than 30 species. To assess the impact the species richness to functional richness relationship had on our results, we removed all

paleocommunities with 30 species or more from the analysis, thus removing the influence of species richness from our results. Removing paleocommunities with more than 23 species did not change the overall pattern of functional richness across the Cenozoic (fig. S2-4). Based on the results of our sensitivity analyses, we determine that our results are real and not driven by a bias in the fossil record.

Major Ecological and Environmental Events of the Cenozoic

The fossil record allows examination of functional diversity of mammal communities over long periods of time prior to large-scale impacts by humans and can shed light on the stability of communities in the face of major ecological and evolutionary transitions. The Cenozoic (66-0 Ma) was marked by a variety of climatic, environmental, and ecological changes (Retallack 2007; Zachos et al. 2008; Westerhold et al. 2020) beginning with the diversification of mammals triggered by the extinction of non-avian dinosaurs. An overall cooling trend through the Cenozoic resulted in a transition from high latitude subtropical forests at the Paleocene-Eocene boundary (~56 ma) to cyclical glaciation periods by the Early-Middle Pleistocene (EMPT, ~800 ka). Periods of rapid global warming allowed high latitude migrations of mammals into North America by continental land bridges. The largest of these immigration events occurred during the Paleocene-Eocene Thermal Maximum (PETM, ~55.5 Ma), a short-term climate excursion caused by a large input of CO_2 into the atmosphere (Wing et al. 2005). Three new orders of ground-dwelling and arboreal mammals (Artiodactyla, Perissodactlya, and Primates) immigrated into North America from Asia and Europe during this time (Smith et al. 2006). One of the most exceptional examples of mammal

community reorganization was in response to the Early Eocene Climatic Optimum (EECO; 53.3 - 49.1 Ma) (Inglis et al. 2020). Wet, subtropical conditions created a diverse floral community driving increased diversification in several mammalian groups. Mammal alpha diversity doubled in the early part of the EECO. However, these paleocommunities were short-lived. The Bridgerian Crash (50-47 ma) followed the end of the EECO and ~40% of that alpha diversity was lost (Woodburne 2009). The Bridgerian Crash (50-47 ma), a time of cooler temperatures, greater seasonality, and aridity, had high faunal turnover rates. North America saw a decline in generic diversity and a reorganization of mammal communities during this period (Woodburne et al. 2009). The drying and cooling climate created a transition to more open habitats. In turn, diversity of archaic mammals declined with the loss of arboreal and medium-sized species, while cursoriality increased (Smits 2015 PNAS). Archaic orders of mammals were extinct from paleocommunities by the middle Oligocene (~30 ma; Fig. S4). Grasslands began to expand with the diversification of grasses by the onset of the Oligocene (34 ma, Strömberg 2005). North America was dominated by grasslands by the middle to late Miocene (Strömberg 2011). During this time ungulates radiated, reaching their highest diversity between 16-14 ma (Janis et al. 2002). By 2.7 mya the onset of glacial cycles in North America began (Brierley and Fedorov 2010, Bacon et al. 2016). The environment was cold and dry, with extensive ice sheets and boreal forests. In line with Bergmann's Rule, large size was favored, and many mammal orders reached their maximum size (Saarinen et al. 2014).

Appendix B

Chapter 2 Supplementary Materials Section

Methods

There were 264 paleocommunities compiled for this study that were downloaded from published databases (Alroy 1998, Smith et al. 2018, Paleobiology Database; paleobiodb.org/). The most updated taxonomic name for each species was collected from the PBDB. The estimated date ranges for each paleocommunity based on geologic location were modified to the best of our ability to reduce age uncertainties using the primary literature (Datafile1: Locality Dating). Our 264 paleocommunities had an average age range of 1.539 million years. Our database includes 2,462 mammal species. A combination of databases and primary literature were used to identify species traits: locomotion, diet, life habit and body mass (Table S1, DataFile2: Mammal Traits). Locomotion is identified by the limb morphology of the mammal species. Life habit is described as the most common lifestyle the mammal has within a habitat. Diet is based on the most common food source of the species. Diet categories were restricted to those we could most accurately be distinguished in the fossil record. Some diet categories used in our databases were combined to limit diet uncertainties in earlier or rarer species (Table S1); granivores were combined with frugivores and piscivores were considered carnivores. Species traits that were unable to be found in primary sources were filled using that of the lowest taxonomic rank available. When body mass was not available, body mass was averaged at the lowest available taxonomic level (genus, family, order).

A complete list of taxa and trait data can be found in DataFile2 as well as reference information for each trait.

Sensitivity Analyses

To ensure that uncertainty in traits for occurrences not identified to species was not driving our results, functional and taxonomic beta diversity were run a second time, excluding all occurrences not identified to species (Figure S2). When rerunning functional and taxonomic beta diversity excluding all specimens not identified to species, one paleocommunity, East Lake, had to be excluded from the analysis. The functional.beta.pair function in package "betapart" can only calculate functional beta diversity if a paleocommunity contains at least five species. East Lake only contained three species when genus level occurrences were removed.